The Hong Kong Polytechnic University

Department of Building Services Engineering

A Study on Thermal Environmental Control, Indoor Air Quality and Energy Efficiency Using Task\ambient Air Conditioning (TAC) Systems in Sleeping Environments in the Subtropics

Mao Ning

A thesis submitted in partial fulfillment of the requirements

for the Degree of Doctor of Philosophy

July 2014

CERTIFICATE OF ORIGINALITY

I hereby declare that this thesis is my own work and that, to the best of my knowledge and belief, it reproduces no material previously published or written, nor material that has been accepted for the award of any other degree or diploma, except where due acknowledgement has been made in the text.

Mao Ning

Department of Building Services Engineering

The Hong Kong Polytechnic University

Hong Kong SAR, China

July, 2014

Abstract

A human being spends approximately one-third of his / her life in sleep. Sleep is not simply a state of rest, but has its own specific functions to help people overcome tiredness. Recently, the influence of indoor thermal environment and air quality in a bedroom on the quality of sleep has been gradually understood. On the other hand, the use of air conditioning in bedrooms significantly contributes to the increased energy use in buildings. Therefore, it becomes highly necessary to study the air conditioning systems applied to sleeping environments where an appropriate indoor thermal environment and suitable air quality should be maintained at a low energy use. A programed research work on applying task\ambient air conditioning (TAC) to a sleeping environment has been therefore carried out and is presented in this thesis.

The first part of the programmed research work reported in this thesis is an experimental study on the thermal, ventilation and energy saving performances of using a ductless bed-based TAC system in an experimental bedroom, as compared to that of using a full volume air conditioning (FAC) system. The experimental results demonstrated that using the ductless bed-based TAC system could lead to better ventilation effectiveness and energy saving performance, but a poor thermal performance in terms of a higher draft risk, than using the FAC system. To reduce the draft risk, while still maintaining an acceptable energy saving performance, it was possible to select a proper supply air temperature and air flow rate as well as a proper supply vane angle.

In the second part of the programmed research work, an experimental and numerical study on the influence of return air inlet locations on the performance of the TAC system was carried out. In this study, two settings for the TAC system were designed. For Setting 1, the same TAC system as that in the first part of research work was used. For Setting 2, the TAC system was modified by adding a return air plenum with an inlet placed under the bed. The operating performances of the bed-based TAC system at the above two settings in terms of thermal environmental control and energy saving were experimentally evaluated. A computational fluid dynamics (CFD) method for evaluating air flow and temperature fields in the experimental bedroom was then developed and validated using the experimental results. Using the validated CFD method, the air flow and temperature fields were obtained, which helped explain the differences in the operating performances of the bed-based TAC system at the two settings. Both the experimental and numerical study results suggested that the bed-based TAC system at Setting 2 performed better in controlling thermal environment in an occupied zone but with a relatively poorer energy saving performance, as compared to that at Setting 1.

Considering that the position of a supply outlet in an air conditioning (A/C) system would significantly influence its operating performances in terms of thermal control, ventilation effectiveness and energy saving, in the third part of the programmed research work, a study on performance evaluations of an A/C system installed in the experimental bedroom with its supply outlet positioned at five different heights was carried out. The study included a numerical simulation using a CFD method and performance evaluation based on the CFD simulation results. The detailed distributions of air flow, temperature and CO_2 concentration inside the bedroom were simulated using the CFD method when the A/C system was operated at different supply air temperatures, supply air flow rates and fresh air flow rates, with its supply outlet placed at 5 different heights (5 height settings). Based on the simulation results, the operating performances in the three aspects of ventilation effectiveness, thermal control and energy saving for the A/C system operated at different conditions, were then obtained and analyzed. In view of the inadequacy of using separately each of the three performance evaluating indexes, an evaluating tool called TOPSIS (Technique for Order Preference by Similarity to an Ideal Solution) was employed to evaluate the overall performance of the A/C system at various operating conditions, through integrating the indexes for ventilation effectiveness, thermal control and energy saving. The study results indicated that the best overall performance was achieved at a supply air temperature of 23 °C, a supply air flow rate of 50 l/s and a fresh air flow rate of 13 l/s when the supply outlet was placed at 1.1 m above floor level (H1100 setting). Among the five height settings, the A/C system performed the best at H800 setting.

In the last part of the programmed research work, an optimization study for the operating parameters (supply air temperature, supply air flow rate and supply air humidity) of the ductless bed-based TAC system installed in the experimental bedroom was carried out, in order to obtain a thermally neutral sleeping environment at minimum energy use, taking into account the total insulation values of beddings and bed. A CFD method was firstly applied to calculating the PMV (Predicted Mean Valve) and EUC (energy utilization coefficient) values for 16 simulation cases. Based on the simulation results, the DOE (design of experiment) method was applied to identifying operating parameters, individually or combined, which would significantly affect thermal neutrality and energy use, and linear regression models for PMV and EUC using the identified parameters were respectively established. Thereafter, the linear regression models were used to obtain the optimum operating parameters of the bed-based TAC system, so that a thermally neutral sleeping environment can be maintained at a minimum energy use.

Publications Arising from the Thesis

I. Journal Papers

- **Mao Ning**, Pan Dongmei, Deng Shiming and Chan Mingyin, Thermal, ventilation and energy saving performance evaluations of a ductless bed-based task/ambient air conditioning (TAC) system. *Energy and Buildings*, 66 (2013) 297-305 (Based on Chapter 5).

- **Mao Ning**, Pan Dongmei, Chan Mingyin and Deng Shiming, Experimental and numerical studies on the performance evaluation of a bed-based task\ambient air conditioning (TAC) system, *Applied Energy*, 136 (2014) 956-967 (Based on Chapter 6).

- **Mao Ning**, Pan Dongmei, Chan Mingyin and Deng Shiming, Performance evaluation of an air conditioning system with different heights of supply outlet applied to a sleeping environment. *Energy and Buildings*, 77 (2014) 281-291 (Based on Chapter 7).

- **Mao Ning**, Pan Dongmei, Chan Mingyin and Deng Shiming, Operating parameter optimization of a bed-based task\ambient air conditioning (TAC) system for a thermally neutral environment with minimum energy use, *Indoor* *and Built Environment*, Submitted, 2014 (Based on Chapter 8).

II. Conference Papers

- **Mao Ning**, Pan Dongmei, Chan Mingyin, Deng Shiming and Song Mengjie. Numerical study on the effects of the height of supply air outlet on air flow, CO_2 transport and thermal comfort in a bedroom. ICAE2013-41, *International Conference on Applied Energy*, Taipei, Taiwan. May 30- June 2, 2014.

- **Mao Ning**, Pan Dongmei, Chan Mingyin and Deng Shiming. Performance evaluation of bed-based task/ambient air conditioning (TAC) systems, ICAE2014-459, *International Conference on Applied Energy*, Pretoria, South Africa. July 1-4, 2013.

Acknowledgements

I must express my grateful thanks to my Chief Supervisor, Dr. Chan Mingyin, Assistant Professor, and my Co-Supervisor, Prof. Deng Shiming, Professor and Associate Head, of the Department of Building Services Engineering (BSE), The Hong Kong Polytechnic University, for their readily available supervision, valuable suggestions, patient guidance, continuous help and encouragement throughout the course of the work.

My special thanks go to The Hong Kong Polytechnic University for financially supporting my study. I would like to thank Dr. Pan Dongmei for her guidance during my study. I would like to also thank Dr. Xu Xiangguo, Dr. Xia Liang, Dr. Pan Yan, Mr. Song Mengjie and Mr. Li Zhao for their assistance in my experimental work. In addition, I wish to express my gratitude to the technicians in the Heating, Ventilation and Air Conditioning Laboratory of the BSE Department for their supports during my experimental work.

Finally, I would like to express my deepest gratitude to my parents and all other family members. I could not have completed my work without their loves, encouragement and continuous supports.

Table of contents

List of Figures

Chapter 6

Chapter 7

Chapter 8

Appendix A

List of Tables

Nomenclature

Variable	Description	Unit
A_D	Surface area	m^2
C	CO_2 concentration at a measurement position	ppm
C	Convective heat loss	W/m^2
C_e	CO_2 concentration in exhaust air	ppm
C_{oz}	Mean CO_2 concentration in the occupied zone	ppm
C_r	CO_2 concentration in return air	ppm
C_{res}	Sensible loss due to respiration	W/m^2
C_s	CO_2 concentration in supply air	ppm
D_{im}	Mass diffusion coefficient	m^2/s
$D_{T,i}$	Thermal diffusion coefficient	m^2/s
E	Total energy	J
E_{res}	Latent heat loss due to respiration	W/m^2
E_{sk}	Evaporative heat loss from skin	W/m^2
f_{cl}	Clothing area factor	-
$\vec{g}$	Gravitational acceleration	m/s^2
h	Enthalpy	J
h'	Overall sensible heat transfer coefficient: overall equivalent uniform conductance between body (including clothing) and environment	$W/(m^2K)$

h_c	Convective heat transfer coefficient at surface	W/(m^{2}K)
h_j	Enthalpy of specie j	J
i_m	Total vapor permeation efficiency	-
J_i	Diffusion flux of species *i*	kg/(m^{2}s)
k_{eff}	Effective conductivity	W/m·k
k_{eff}	Effective conductivity	W/m·k
L	Thermal load on the body	W/m^2
L_R	Lewis ratio	K/kPa
M	Metabolic heat production	W/m^2
P	Pressure	Pa
p_a	Water vapor pressure in ambient air	kPa
$P_{sk,s}$	Water vapor pressure in saturated air at t_{sk}	kPa
Q_f	Fresh air flow rate	l/s
Q_s	Supply air flow rate	l/s
R	Radiative heat loss	W/m^2
r_b	Thermal resistance of a bedding	m^{2}K/W
$R_{e,cl}$	Evaporative resistance of clothing	m^{2}K/W
RQ	Respiratory quotient	-
RH_s	Relative humidity in supply air	-
R_t	Total equivalent uniform thermal resistance between body and environment including clothing and boundary resistance	m^{2}K/W
Sc_t	Turbulent Schmidt number	-
S_i	Rate of creation by addition of species $_i$	kg/(m^{3}s)

T	Air temperature	K
t	Air temperature at a measurement position	ºC
t_a	Ambient air temperature	ºC
t_{cl}	Clothing surface temperature	ºC
t_o	Operative temperature	ºC
t_{oz}	Average air temperature in an occupied zone	ºC
$\overline{t_r}$	Mean radiant temperature	ºC
t_s	Supply air temperature	ºC
t_{sk}	Mean skin temperature	ºC
T_u	Turbulence intensity	-
t_{uz}	Average air temperature in an unoccupied zone	ºC
U	Nondimensionalized velocity	-
v	Air velocity at measurement position	m/s
V	Air velocity	m/s
V_{O2}	Volumetric rate of O_2	l/s
w	Skin wetness	-
Y_i	Mass fraction of the species i	-

Greek symbols

μ_{eff}	Effective dynamic viscosity	Pa·s

$\bar{\bar{\tau}}_{eff}$	Deviatoric stress tensor	Pa
μ_t	Turbulent viscosity	Pa·s
ρ	Air density	kg/m^3
$\bar{\bar{\tau}}$	Stress tensor	Pa
μ_t	Turbulent viscosity	Pa·s
α	Sensitivity coefficient for evaluating PMV	-

Abbreviation

ADPI	Air diffusion performance index	-
CFD	Computational fluid dynamics	-
CN	Nondimensionalized CO_2 concentration	-
DOE	Design of experiment	-
DR	Draft risk	-
DR	Draft risk	-
EDT	Effective draft temperature	ºC
EUC	Energy utilization coefficient	-
EUC	Energy utilization coefficient	-
EUC	Energy utilization coefficient	-
FAC	Full volume air conditioning	-
PMV	Predicted mean vote	-
RAC	Room air conditioners	-

RH	Relative humidity	-
TAC	Task\ambient air conditioning	-
TEM	Nondimensionalized temperature	-
VE	Ventilation effectiveness	-

Subscripts

a	Ambient
b	Bedding
c	Convective
cl	Clothing
e	Exhaust
f	Fresh air
oz	Occupied zone
r	Return
res	Respiration
s	Supply
sk	Skin
uz	Unoccupied zone

Chapter 1

Introduction

Sleep plays an important role in the daily life of a human being. On one hand, approximate 1/3 of human life is spent in sleep. On the other hand, sleep is not simply a state of rest, but has its own specific functions, such as helping people overcome tiredness and benefiting the performance of daytime activities. It has been commonly acknowledged that the quality of sleep is mainly determined by the mental-physical factors of a sleeping person and the environmental factors in a bedroom. These environmental factors, among others, include thermal environment and indoor air quality, which are usually provided and maintained by building Heating, Ventilation and Air Conditioning (HVAC) systems. However, the use of building HVAC systems significantly contributes to the increased energy use in buildings. To reduce the building energy use, novel HVAC systems such as TAC systems have been developed and extensively studied. Nonetheless, these studies focused on the performances of TAC systems mainly in workplaces, but not in sleeping environments. Therefore, further studies on applying TAC systems to sleeping environments with respects to their performances of thermal environment control, indoor air quality and energy use need to be carried out, and a programmed research work has been carried out and is presented in this Thesis.

The thesis begins with an extensive literature review where firstly the previous work related to indoor thermal comfort, indoor air quality and energy use in sleeping environments, is reviewed to better understand the effects of thermal environment and air quality in a sleeping place on the quality of sleep, and the issues related to energy use of air conditioning in buildings, with an emphasis on energy use in residential buildings. Secondly, a review on the types, the advantages and the ranges of operating parameters of TAC systems and their related studies is presented. Finally, the issues related to applying numerical approaches to studying the thermal environment around a human body and indoor air quality are also reviewed. Through the literature review, the expected targets of further investigations in maintaining appropriate sleeping thermal environments and suitable air quality in bedrooms at a low energy use have been identified.

The research proposal covering the aims and objectives, the title of the programmed research work, the research methodologies is presented in Chapter 3.

Chapter 4 describes an experimental setup to facilitate carrying out the programmed research work reported in this thesis. A brief description of an experimental DX A/C station consisting of a DX/AC plant and an environmental chamber is firstly given. This is followed by detailing the experimental setup having two system arrangements: FAC system arrangement and a ductless bed-based TAC system arrangement, placed in an experimental bedroom. Finally, the measurement methods used are discussed.

Chapter 5 presents the first part of the programmed research work of an experimental study, using the experimental setup, on thermal, ventilation and energy saving performances of using a ductless bed-based TAC system in the experimental bedroom, as compared to that of using a FAC system. The experimental results demonstrated that using the ductless bed-based TAC system could lead to a better ventilation performance and energy saving performance, but a poor thermal performance in terms of a higher draft risk than using the FAC system. To reduce the draft risk, while still maintaining an acceptable energy saving performance, it was possible to select a proper supply air temperature and air flow rate as well as a proper supply vane angle.

Chapter 6 reports the second part of the programmed research work of a study on the influence of return air inlet locations on the performance of a bed-based TAC system. In this study, two settings for the TAC system were designed. For Setting 1, the same TAC system as that in the first part of research work was used. For Setting 2, the TAC system was modified by adding a return air plenum with an inlet placed under the bed. The operating performances of the bed-based TAC system at the above two settings in terms of thermal environmental control and energy saving were experimentally evaluated using the experimental setup. A CFD method for evaluating air flow and temperature fields in the experimental bedroom was then developed and validated using the experimental results. Using the validated CFD method, the air flow and temperature fields were obtained, which helped explain the differences in the operating performances of the bed-based TAC system at the two settings. Both the experimental and numerical study results suggested that the bed-based TAC system at Setting 2 performed better in controlling thermal environment in an occupied zone but with a relatively poorer energy saving performance, as compared to that in Setting 1.

Considering the position of a supply outlet in an air conditioning (A/C) system would significantly influence its operating performances in terms of thermal environmental control, ventilation effectiveness and energy saving, in Chapter 7, the third part of the programmed research work on performance evaluations of an A/C system installed in the experimental bedroom with its supply outlet positioned at five different heights is reported. It includes a numerical simulation using a CFD method and performance evaluation based on the CFD simulation results. The detailed distributions of air flow, temperature and CO_2 concentration inside the experimental bedroom were simulated using the CFD method when the A/C system was operated at different supply air temperatures, supply air flow rates and fresh air flow rates, with its supply outlet placed at 5 different heights (5 Height Settings). Based on the simulation results, the operating performance in the three aspects of thermal environmental control, ventilation effectiveness and energy saving for the A/C system operated at different conditions, were then obtained and analyzed. In view of the inadequacy of using separately each of the three performance evaluating indexes, an evaluating tool called TOPSIS was employed to evaluate the overall performance of the A/C system at various operating conditions, through integrating the indexes for ventilation effectiveness, thermal environmental control and energy saving. The study results indicated that the best overall performance was achieved at a supply air temperature of 23 °C, a supply air flow rate of 50 l/s and a fresh air flow rate of 13 l/s when the supply outlet was placed at 1.1 m above floor level (H1100 Setting). Among the five height settings, the A/C system performed the best at H800 Setting.

In Chapter 8, taking into account the total insulation value of beddings and bed, an optimization study of the operating parameters (supply air temperature, supply air flow rate and supply air humidity) of the bed-based TAC system at which a thermally neutral environment can be maintained with a minimum energy use is presented, as the last part of the programmed research work. A CFD method was firstly applied to calculating the PMV and EUC values for 16 simulation cases. Based on the simulation results, the DOE method was applied to identifying operating parameters, individually or combined, which would significantly affect thermal neutrality and energy use, and linear regression models for PMV and EUC using the identified parameters were established, respectively. Thereafter, the linear regression models were used to obtain the optimum operating parameters of the bed-based TAC system, so that a thermally neutral sleeping environment can be maintained at a minimum energy use. The study results suggested that for a bed-based TAC system, at a specified total insulation value of beddings and bed, increases in supply air flow rate, supply air RH and supply air temperature would lead to a lower energy use while still maintaining a thermal comfortable level. Under a given total insulation value of beddings and bed, jointly using the DOE method and CFD method can help find the optimum operating parameters of the bed-based TAC system, at which a thermally neutral sleeping environment was maintained at minimum energy use.

The conclusions of the thesis and the proposed future work are presented in the final Chapter.

Chapter 2

Literature review

2.1 Introduction

Sleep plays an extraordinarily important role in the daily life of a human being. On one hand, approximate 1/3 of human life is spent in sleep as revealed in a survey that the mean sleep duration of American people is 6.9 hours per night in weekdays and about 7.5 hours in weekends [Sleep in America Polls 2002]. On the other hand, sleep is not simply a state of rest, but has its own specific functions [Hobson 1995], such as helping people overcome tiredness and benefiting the performance of daytime activities [Engle-Friedman 2003]. For decades, numerous medical researchers have investigated various factors that affected the quality of sleep [Sayar 2002, Cuellar et al. 2006]. It was commonly acknowledged that the quality of sleep was mainly determined by mental-physical factors of a sleeping person and environmental factors in a bedroom. These environmental factors, among others, include thermal environment and indoor air quality. Different levels of indoor temperature influence sleep duration, number of awakenings and thermal comfort of a sleeping person. Furthermore, according to American Conference of Governmental Industrial

Hygienists (ACGIH) and Occupational Safety and Health Administration (OSHA), indoor CO_2 concentration level at below 5000 ppm is safe and a high level of CO_2 concentration may cause rapid heart beating, mental depression, unconsciousness and even death [Nelson 2000, Priestly 2003], affecting people's health. In addition, a suitable indoor air humidity level is also important since this directly affects occupants' thermal comfort and indoor air quality.

The purpose of providing air conditioning in buildings is to maintain appropriate indoor thermal comfort and an acceptable indoor air quality (IAQ) for occupants at both daytime and nighttime. Over the past years, different A/C systems have been developed for achieving improved indoor thermal comfort and IAQ, these including dedicated outdoor air systems (DOAS), independent control of temperature and humidity system (ICTHS), cold ceiling and displacement ventilation systems (CC/DV), personalized ventilation systems (PV), under-floor air distribution (UFAD) systems and task\ambient air conditioning (TAC) systems, etc.

In the tropical or sub-tropical regions where summers are hot and humid and may last for over 7 months in a year, room air conditioners (RACs) are widely used in residential buildings at nighttime to maintain thermally comfortable sleeping environments. This has been demonstrated in a survey on the situations of sleeping thermal environment and the use of air conditioning in bedrooms in residential buildings in Hong Kong [Lin and Deng 2006]. The survey results revealed that up to 68% of the respondents would leave their RACs on during sleep.

However, the wide spread use of air conditioning at both daytime and nighttime contributed to increased energy use in buildings. For example in Hong Kong, residential A/C consumed 155 GWh of electricity in 1971, or 14.6% of the total residential electricity use. In 2011, residential A/C electricity consumption was increased to 4983 GWh, or 45% of the total residential electricity [Hong Kong Energy Statistics 2012]. Consequently, it becomes increasingly necessary to develop novel air conditioning systems, so as to reduce energy consumption for A/C while still maintaining a suitable level of indoor thermal comfort and indoor air quality.

Therefore, task\ambient air conditioning (TAC) has been developed, which is defined as a space conditioning system that allows thermal conditions in small, localized zones to be individually controlled by occupants [Bauman and Arens 1996]. For the last two decades, there has been an increasing interest in using TAC. TAC systems used in offices at daytime have been investigated in a large number of previous studies and many benefits associated with using TAC systems revealed: enhancing thermal comfort, improving indoor air quality and reducing energy consumption, etc. By allowing personal control over local thermal environment using TAC, the thermal comfort of occupants can be greatly improved. In addition, the use of TAC can help improve indoor air quality in an occupied zone, since fresh air can be directly delivered to occupants to remove contaminants from the occupied zone efficiently. Unlike daytime activities such as working in a workplace, sleeping is confined to a relatively small space and a sleeping person is naturally immobile. Therefore, TAC systems should be best applied to sleeping environments.

However, the current practices in TAC systems are mainly concerned with the situations in which people are awake in workplaces, such as offices [Shute 1995, Spoormaker 1990, Bauman 1999]. These may however not be directly applicable to TAC systems for sleeping environments. Furthermore, current research on TAC systems for sleeping environments in the subtropics is mainly concerned with thermal environment control in sleeping environment and the related issues of energy saving [Pan et al. 2012]. IAQ control in sleeping environment using TAC systems has not yet been taken considered in previous studies. Therefore, it becomes necessary to study thermal environmental control, indoor air quality and energy efficiency when using TAC systems in sleeping environments in the subtropics.

In this Chapter, the fundamentals related to sleep and the environmental factors that may affect the quality of sleep are firstly reviewed. Secondly, a review on the previous studies on thermal comfort, IAQ and the issues of energy use by building A/C installations are discussed and reported. This is followed by reporting a review on the types, the advantages and the ranges of operating parameters of TAC systems and their related studies for daytime applications. Fourthly, a review on numerically studying the thermal environment and IAQ in buildings using CFD technique is reported. Finally, a conclusion where future required research work is identified is given.

2.2 Sleep

2.2.1 Definition of sleep

Sleep is a variable but specific brain activity. It is a highly organized, complex behavior characterized by a relative disengagement from the outer world [Teofilo 2005]. Under normal conditions, sleep is associated with little muscular activity with a stereotypic posture, and reduced response to environmental stimuli [Teofilo 2005]. Normal human sleep comprises two distinct states known as non-rapid eye movement (NREM) sleep and rapid eye movement (REM) sleep. The former accounts for 75 - 80% of sleep time, and appears as wakefulness-maintaining mechanisms. NREM sleep is further divided into four stages based on the pattern of the brainwaves. Stage 1 of NREM sleep is a transitional phase between full wakefulness and sleep. It can also emerge briefly during transitions from sleep to wake or after brief body movements. Stage 2 of NREM sleep is marked by the appearance of EEG (Electroencephalography) spindles, which is the first bona fide sleep stage, on which adults spend 50-60% of sleep time. Stages 3 and 4 of NREM sleep are frequently combined and called delta sleep, deep sleep, or slow wave sleep. The latter represents however active form of sleep and is characterized by intermixed cerebral activity associated with striated muscle atonia and rapid eye movements [Rechtschaffen and Kales 1968].

2.2.2 Functions of sleep

Sleep plays an extraordinarily important role in the daily life of a human being. On one hand, approximate 1/3 of human life is spent in sleep as revealed in a survey that the mean sleep duration of American people is 6.9 hours per night in weekdays and 7.5 hours in weekends [Sleep in America Polls 2002]. On the other hand, sleep is not simply a state of rest, but has its own specific functions [Hobson 1995], such as helping people overcome tiredness and benefiting the performance of daytime activities [Engle-Friedman 2003].

Sleep appears to have beneficial effects on human body and general health. Sleep may influence mortality and morbidity, and the endocrine and immune systems [Akerstedt and Nilsson 2003]. Prolonged sleep deprivation in rodents, drosophila and possibly humans is fatal, which would support a general life sustaining function for sleep [Shaw et al. 2002, Cortelli et al. 1999].

Sleep has profound effects on mental performance, which suggests that sleep in some general way facilitates normal neuronal function. For example, strong evidences indicate that sleep affects learning and synaptic plasticity [Benington and Frank 2003, Stickgold et al. 2001].

2.2.3 Factors influencing the quality of sleep

It has been commonly acknowledged that the quality of sleep was mainly determined by mental-physical factors of a sleeping person and environmental factors. The latter includes lighting, noise, thermal environment and air quality in a bedroom. For decades, studies have been gradually carried out to investigate the thermal environment and indoor air quality that may affect the quality of sleep [Sayar et al. 2002, Cuellar et al. 2006].

2.2.3.1 Thermal environment

Previous experimental results have demonstrated that when the thermal environment in a bedroom deviated greatly from the so-called “thermal comfort zone”, sleep quality can be disturbed or even deteriorated as soon as the thermoregulatory responses were present.

Kendel and Schmidt-Kessen [1973] studied the effect of high air temperatures on sleep duration. It was shown that a higher temperature would lead to an increase in the number and duration of awakenings after sleep onset. Karacan et al. [1978]

reported that at a microclimate air temperature of 39 ºC inside a blanket heated by a circulating fluid at a temperature of 49 ºC, the total sleeping time was decreased. H´enane et al. [1977] found out that increasing air temperature to 35-39 ºC did not greatly change sleep pattern, but the awakening periods were increased. Karacan et al. [1978] demonstrated that exposure to a high air temperature decreased the number of REM sleep episodes of a sleeping person, whereas the mean duration and the mean length of REM sleep-intervals remained unchanged [Parmeggiani and Velluti 2005]. Buguet et al. [1979] pointed out that for subjects sleeping in tents in the Arctic winter, sleep was shortened and frequently interrupted by awakenings and body movements. Comparing the influence of high (34-37 ºC) and low (21 ºC) ambient temperatures on sleep, Haskell et al. [1981] pointed out that the durations of wakefulness of Stage 1 sleep were increased in cold exposure whereas that of Stage 2 sleep was decreased. It was concluded that a low ambient temperature was more disruptive to sleep.

In addition to air temperature in sleeping environment, other thermal environmental factors such as indoor air velocity and humidity level would also impact the quality of sleep. In the study carried out by Tsuzuki et al. [2008], 17 male subjects wearing short pajamas were asked to separately sleep on a bed covered with a cotton blanket under different testing conditions. The experimental results suggested that having an appropriate air velocity inside a sleeping environment helped reduce the duration of wakefulness through decreasing the skin temperature, rectal temperatures, and furthermore the body mass loss if in a warm humid condition. Okamoto-Mizuno et al. [1999] found that a high humidity exposure for a sleeping person at a high air temperature during nighttime increased the thermal load to suppress a decrease in rectal temperature, and thus increased wakefulness.

2.2.3.2 Indoor air quality

It has been suggested that CO_2 may be disruptive to normal sleep. Early anecdotal evidence of this was presented by Schaefer [1958] during a 3-6 day sojourn in an atmosphere containing 3% CO_2. During the first 24 hours, general excitement and agitation resulted in a decreased ability to fall asleep. As alveolar PCO_2 (partial pressure of CO_2) increased, arousal from sleep eventually occurred due to the hypercapnic distress. Hedemark and Kronenberg [1982] investigated arousal responses to CO_2 rebreathing during sleep. It was found that the range of P_ACO_2 (partial pressure of CO_2 in alveolar) (49.2 ± 0.4 torr) resulted in arousal in all subjects. A similar study was conducted by Berthon-Jones and Sullivan [1984] who noted that arousal occurring at increased P_ACO_2 as sleep progressed from Stage 2 (58.6 ± 0.9 torr) to Stage 4 (63.8 ± 0.8 torr) for male subjects. CO_2 was revealed to alter normal thermoregulatory responses to cold temperatures. In general, a higher CO_2 concentration in bedrooms would cause arousal which indirectly affects the quality of sleep.

2.3 Thermal comfort

2.3.1 Definition of thermal comfort

Thermal comfort is the condition of mind that expresses satisfaction with a thermal environment [ASHRAE Standard 55-2013]. This definition leaves open on what is meant by “condition of mind” or “satisfaction”, but it correctly emphasizes that judgment of comfort is a cognitive process involving many inputs influenced by physical, physiological, psychological and other processes. There are two personal and four environmental variables that influence the thermal comfort of an occupant [Fanger 1970]: activity level and clothing of the occupant; air temperature, mean radiant temperature, air relative humidity and air velocity.

Extensive studies on indoor thermal comfort for occupants have been carried out [Fanger 1970, de Dear and Brager 1998, Gagge et al. 1986, Nakano et al. 2002, Schiller 1990 and Newsham 1997], with most of them focusing on daytime occupancy. A Comfort Model for daytime occupancy has also been developed by Fanger [1970]. Nevertheless, limited studies on thermal comfort in sleeping environments using experimental, theoretical and numerical methods [Karacan et al. 1978, Lin and Deng 2008a, Lin and Deng 2008b, Pan et al. 2011 and Pan et al. 2012] have also been carried out, and are summarized as follows.

2.3.2 Thermal comfort in sleeping environments

2.3.2.1 Experimental study

Numerous medical researchers have investigated the influence of thermal parameters in a sleeping environment on the quality of sleep. Different researchers carrying out experimental studies on the effects of high and low ambient temperatures on human sleep stages adopted different thermal neutral temperatures in sleep in the range of 20 to 32ºC [Karacan et al. 1978, Haskell et al. 1981, Candas et al. 1982, Macpherson 1973, Sewitch et al. 1986, Di Nisi et al. 1989 and Dewasmes 2000]. Table 2.1 details different thermal neutral temperatures used in various studies related to sleep. It can be seen that there is a fairly great range of thermal neutral temperatures, indicating that a well-agreed single thermal neutral temperature has not yet been established. In most of the research studies related to sleep, thermal neutral temperatures were different due to different experimental conditions. This indicates there is a need to find a method to determine the thermal neutral temperature at a standard experimental condition.

Table 2.1 Different thermal neutral temperatures adopted in studies related to sleep

Literature	Thermal neutral temperature (ºC)	Condition of test subjects	Remark
Macpherson 1973	29-32	Naked	Air temperature
Karacan et al. 1978	22.2	Covered	Air temperature
Haskell et al. 1981	29	Naked	Air temperature
Candas et al. 1982	32	Naked	Operative temperature
Palca 1986	29	Naked	Air temperature
Sewitch et al. 1986	20-22	Covered	Air temperature
Di Nisi et al. 1989	30	Naked	Operative temperature
Dewasmes et al. 2000	28	Naked	Air temperature

2.3.2.2 Theoretical study

By modifying the thermal comfort model developed by Fanger [1970] for daytime occupancy, Lin and Deng [2008a] developed a thermal comfort model for sleeping environments. The heat balance between a human body and its sleeping thermal environment was described as:

$$40 = \frac{34.6 - t_o}{R_t} + \frac{0.06 i_m L_R (p_{sk,s} - p_a)}{R_t} + 0.056(34 - t_a) + 0.692(5.87 - p_a) \qquad (2.1)$$

Where R_t, the total thermal resistance, is affected by beddings, sleepwear, bed and mattress, percentage coverage of body surface area by bedding and bed, air velocity, direction of airflow and sleeping posture, etc. [Lin and Deng 2008a].

By solving Equation (2.1), a comfort equation for sleeping environments which combined both environmental and personal variables was derived:

$$\begin{aligned} 40 = \frac{1}{R_t}\left[\left(34.6 - \frac{4.7\bar{t}_r + h_c t_a}{4.7 + h_c}\right) + 0.3762(5.52 - p_a)\right] \\ + 0.056(34 - t_a) + 0.0692(5.87 - p_a) \end{aligned} \qquad (2.2)$$

There are five variables, R_t, $\bar{t}_r$, t_a, p_a and h_c in Equation (2.2). The convective heat transfer coefficient, h_c, is the function of air velocity, v; therefore, similar to daytime occupancy, four variables (i.e., $\bar{t}_r$, t_a, p_a, and v) are thermal environmental variables that determine a thermally neutral sleeping environment under a given bedding system.

By solving Comfort Equation (2.2) at various combinations of variables, comfort charts were established.

Fig. 2.1 illustrates the comfort lines showing the combinations of operative temperature, wet bulb temperature and the total insulation value of beddings and bed, under which thermal neutrality can be achieved. It can be seen that the influence of relative humidity on the thermal comfort of a sleeping person was relatively small. A change from absolutely dry air (RH = 0%) to saturated air (RH = 100%) can be compensated by only a 0.95 ~ 1.63 ºC (at the range of 2.4 ~ 0.8 clo total insulation values) decrease in operative temperature. The higher the total insulation value, the less the decrease in operative temperature. For example, when the total insulation value was 1.0 clo, a 1.5 ºC reduction in operative temperature would adequately compensate the change of relative humidity from 0% to 100%, compared to 1.1 ºC reduction in operative temperature at the total insulation of 2.0 clo.

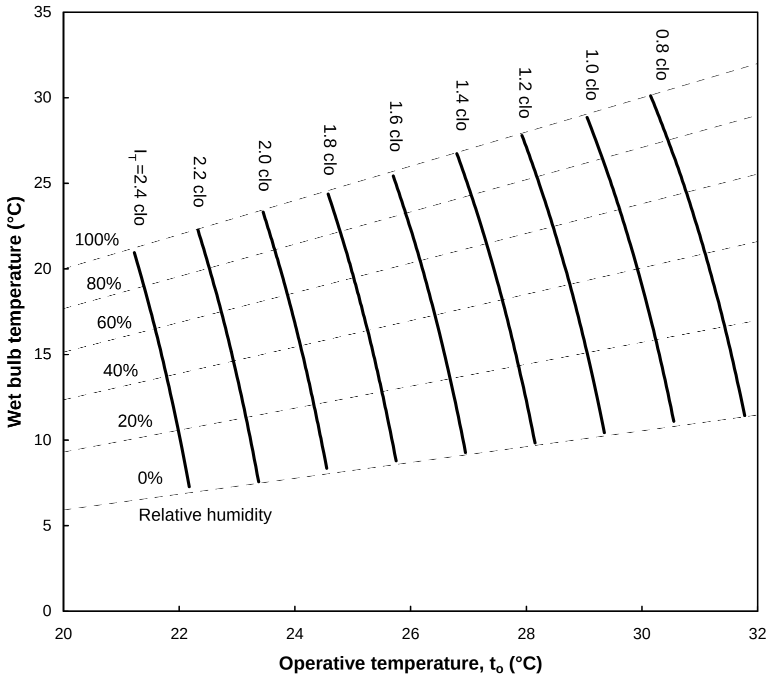

Fig. 2.1 Comfort lines (operative temperature vs. wet bulb temperature) with an indoor air velocity of not greater than 0.15 m/s [Lin and Deng 2008a]

On the other hand, the total insulation value provided by a bedding system significantly influenced the operative temperature for sleeping persons. This was clearly illustrated in Fig. 2.2, which shows the relationships between the operative temperature and the total thermal insulation of a bedding system under different indoor relative humidity levels. It can be seen from Fig. 2.2 that a linear relationship between the operative temperature and the total insulation value is demonstrated.

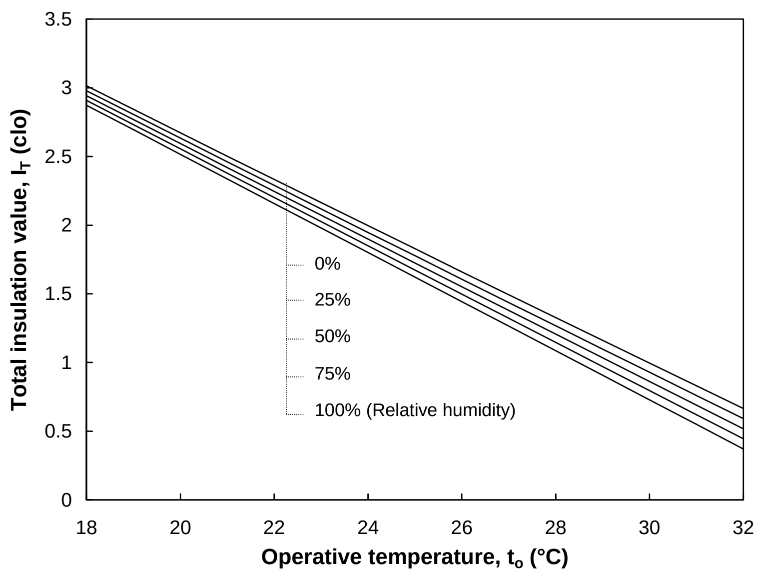

Fig. 2.2 Relationship between operative temperature and the total insulation value with an indoor air velocity of not greater than 0.15 m/s [Lin and Deng 2008a]

2.3.2.3 Numerical study

Based on the theoretical study of thermal comfort in sleeping environments, numerical studies were carried out to determine the thermal neutral temperatures in a conditioned bedroom [Pan et al. 2011]. The obtained thermal neutral temperatures at the three different beddings, with different percentage coverages of body surface area by beddings, are shown in Fig. 2.3. It was shown that the thermal resistance of beddings could significantly affect the thermal neutral temperature of a sleeping person, i.e., the higher the thermal resistance of beddings, the lower the thermal neutral temperature. The study results obtained at different supply air velocities suggested that supply air velocity did not significantly affect the thermal neutral temperature when people were covered with three different beddings at 100% coverage.

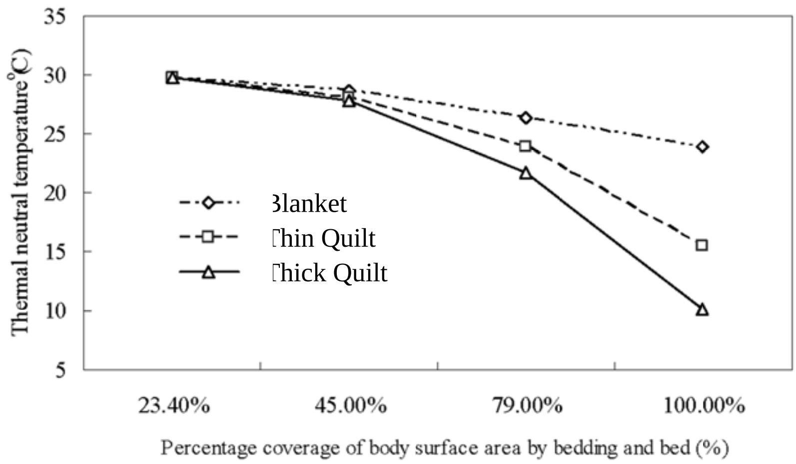

(a) at a supply air velocity of 0.12 m/s

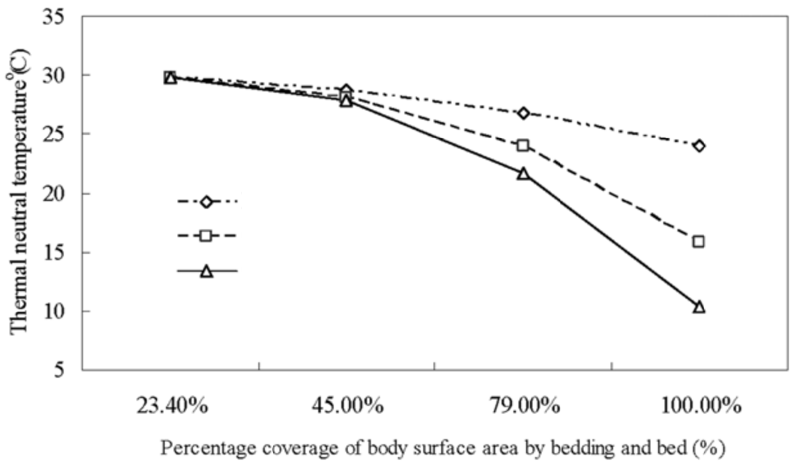

(b) at a supply air velocity of 0.24 m/s

Fig. 2.3 The relationship between thermal neutral temperature and percentage coverage of body surface area by bedding and bed at the three different beddings [Pan et al. 2011]

2.4 Indoor air quality

In a typical air-conditioned indoor environment, CO_2 concentration may be selected as a surrogate indicator in assessing indoor air quality and ventilation efficiency [ASHRAE 62.1-2013, Persily 1997, Hui et al. 2007]. Various studies concerning indoor CO_2 level have been carried out [ASHRAE 62.1-2013, Möhle et al. 2003], covering the health effects of elevated CO_2 concentrations [Hoskins 2003], the impact of CO_2 concentration on the occupants' perceptions of an indoor environment [Persily 1997], the relationship between CO_2 concentrations and other contaminants [Hui 2007], and the relationship between CO_2 level and outdoor air ventilation rate, etc. [Möhle et al. 2003, Hoskins 2003].

2.4.1 Health effects of CO_2 level

CO_2 can have a negative health effect if it is inhaled. Inhaling CO_2 may cause rapid breathing, rapid heart beating, headache, sweating, shortness of breath, dizziness, mental depression, visual disturbances, shaking, unconsciousness and death to an extreme. Table 2.2 summarizes the acute health effects following exposure to high levels of concentration of CO_2. Exposure of humans to CO_2 concentrations ranging from 17% to 30% within 1 minute leads to loss of controlled and purposeful activity, unconsciousness, coma, convulsions and death [OSHA 1978, CCOHS 1990, Dalgaard et al. 1972, CATAMA 1953, Lambertsen 1971]. Exposure to concentrations from greater than 10% to 15% CO_2 leads to dizziness, drowsiness, severe muscle twitching, and unconsciousness within a minute to several minutes [Wong 1992, CATAMA 1953, Sechzer et al. 1960]. Exposure to 7% to 10% CO_2 can produce unconsciousness or near unconsciousness within a few minutes [Schulte 1964, CATAMA 1953, Dripps and Comroe 1947]. Acute exposures to 6% CO_2 affected vision by decreasing visual intensity discrimination in 1 to 2 minutes [Gellhorn 1936] and resulted in a 3% to 8% decrease in hearing. Exposure to a concentration of 6% CO_2 can produce hearing and visual disturbances within 1 to 2 minutes [Gellhorn 1936]. After several hours' exposure to atmospheres containing 2% CO_2, headache and dyspnea can occur with mild exertion [Schulte 1964]. A concentration of 3% CO_2 would produce headache, diffuse sweating and dyspnea at complete rest after an exposure period of several hours [Schulte 1964]. Exposure to 4 to 5% CO_2 for 15 to 32 minutes can produce headache and dizziness, increased blood pressure and uncomfortable dyspnea within a few minutes [Schulte 1964 and Patterson et al. 1955].

Table 2.2 Acute health effects of high levels of concentrations of CO_2

CO_2 concentration (%)	Exposure time	Effects
17-30	Within 1 minute	Loss of controlled and purposeful activity, unconsciousness, convulsions, coma, death
>10-15	1 minute to several minutes	Dizziness, drowsiness, severe muscle twitching, unconsciousness
7-10	Few minutes 1.5 minutes to 1 hour	Unconsciousness, near unconsciousness Headache, increased heart rate, shortness of breath, dizziness, sweating, rapid breathing
6	1 - 2 minutes 16 minutes Several hours	Hearing and visual disturbances Headache, dyspnea
4-5	Within a few minutes	Headache, dizziness, increased blood pressure, uncomfortable dyspnea
3	1 hour	Mild headache, sweating, and dyspnea at rest
2	Several hours	Headache, dyspnea upon mild exertion

(1% = 10000 ppm)

A high CO_2 concentration level could result in uncomfortability or even serious health problems as stated above. Therefore, safe CO_2 levels were recommended. A previous research showed that CO_2 concentrations in office buildings typically ranged between 350 and 2500 ppm [Seppänen et al. 1999]. ASHRAE recommended the approximate steady state indoor concentration of 870 ppm, based on the assumptions that outdoor CO_2 is 350 ppm and indoor CO_2 generation rate is 0.31 L/min per person [ASHRAE Standard 62.1-2013]. According to ACGIH [1991] and OSHA [1978], an indoor CO_2 concentration level below 5000 ppm is safe.

2.4.2 Generation of CO_2 in buildings

The primary indoor source of CO_2 in buildings is the respiration of building occupants. People generate CO_2 and consume oxygen, at a rate that depends primarily on their body size and their level of physical activity. The relationship between activity level and rates of CO_2 generation and oxygen consumption is included in ASHRAE Handbook [2013]. The rate of oxygen consumption, V_{O2}, in l/s, of a person is given by the following equation:

$$V_{O2} = \frac{0.00276 A_D M}{(0.23 RQ + 0.77)} \tag{2.3}$$

where *RQ* is the respiratory quotient, i.e., the relative volumetric rates of CO_2 produced to oxygen consumed. M is the level of physical activity, or the metabolic rate per unit of surface area of a human body, in mets (1 met = 58.2 W/m^2). A_D is the surface area in m^2.

Figure 2.4 shows the oxygen consumption rate and CO_2 generation rate as a function of physical activity for an average sized adult with a surface area of 1.8 m^2 at a *RQ* level of 0.83 [Emmerich and Persily 2001]. For a sleeping person, the metabolic rate is at 0.7 met. Therefore, according to ASHRAE Standard 62.1-2013, a sleeping person produces 0.003 l/s of CO_2.

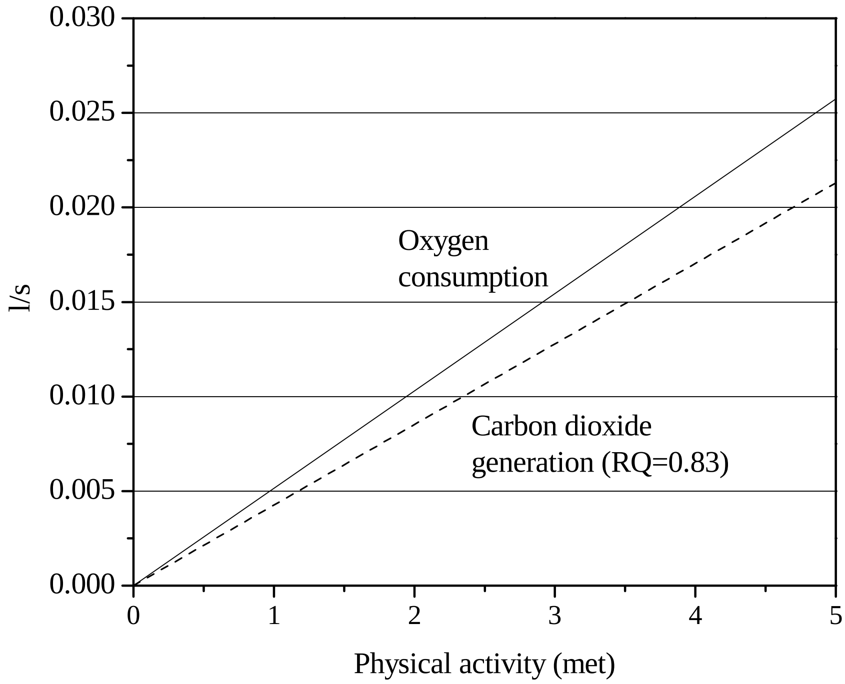

Fig. 2.4 CO_2 generation and O_2 consumption as a function of physical activity (for an average size adult) [Emmerich and Persily 2001]

2.5 Energy use in buildings

With a fast economic growth and an increase in living standard, air conditioning has been increasingly applied to various buildings. This has led to a significant increase in energy consumption. For example, Fig. 2.5 shows the monthly electricity consumption in the commercial and residential sectors from 1979 to 2006 in Hong

Kong [Lam et al. 2008]. A continuous increasing trend in monthly electricity use from 1979 to 2006 is demonstrated. According to the Hong Kong Energy Statistics Annual Report [1979-2006], an average annual growth rate of 5.9% was recorded in the residential sector from 2099 GWh in 1979 to 9841 GWh in 2006.

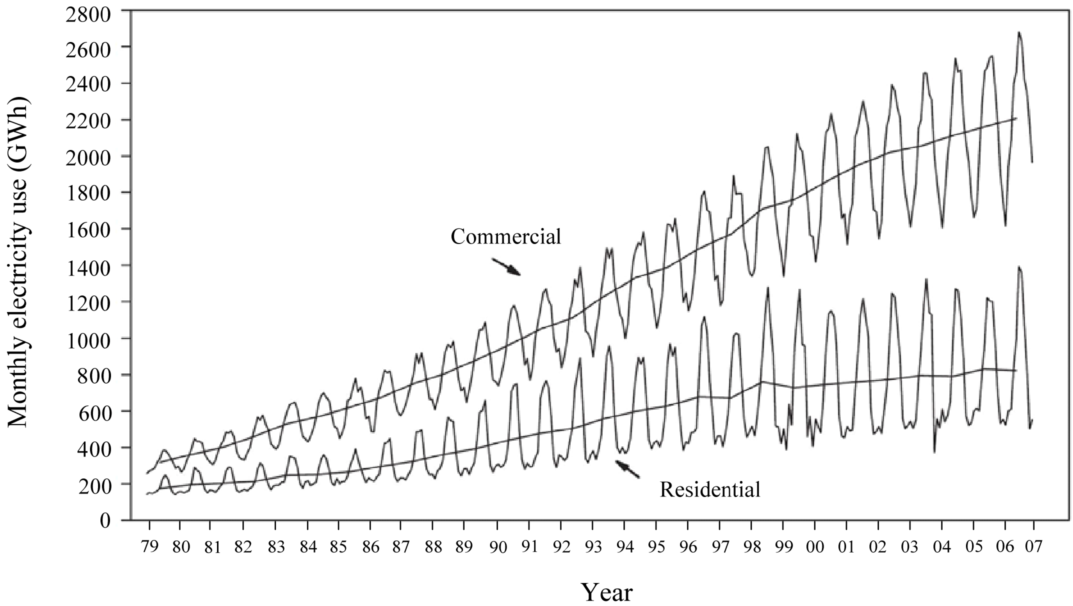

Fig. 2.5 Monthly electricity consumption in the commercial and residential sectors from 1979 to 2006 in Hong Kong [Lam et al. 2008]

In this section, the energy use for air conditioning in residential buildings in Hong Kong is used as an illustrative example for discussing energy use in buildings.

2.5.1 Energy use of air conditioning in residential buildings in Hong Kong

Due to Hong Kong's unique climates, air conditioners are widely used to maintain a thermally comfort environment in residential buildings. 95% of Hong Kong households own at least one air-conditioner, and air-conditioners are operated mostly from April to October [Tso and Yau 2003]. A survey carried out by Wan and Yik [2004] suggested that the air-conditioners for bedrooms are mainly operated at night, starting after 20:00 hr. The operating patterns for the air-conditioners in those surveyed households during weekdays are shown in Table 2.3 [Wan and Yik 2004].

Table 2.3 Operating patterns of air-conditioners in residential buildings in Hong Kong [Wan and Yik 2004]

Percentage of air-conditioners operated	Living room	Bed room
80%	18:00-22:00	23:00-05:00
20%	13:00-22:00	20:00-07:00

According to Hong Kong Energy End-use Data [2013], air conditioning in residential buildings is responsible for 23% of the total residential energy use in 2013, as shown in Fig. 2.6. In addition, electrical energy consumption patterns are different remarkably in summer and winter seasons. During the summer months, air-conditioning contributes to 59% of the total residential energy consumption and leads to the increased of the monthly electricity use, as shown in Fig. 2.5 [Tso and Yau 2003].

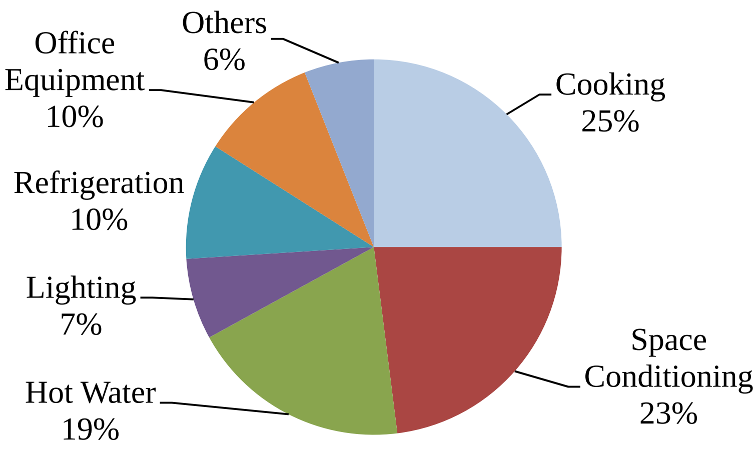

Fig. 2.6 Energy end-use in residential buildings [Hong Kong Energy End-use Data 2013]

2.5.2 Cooling loads in residential buildings in Hong Kong

With regards to space cooling loads residential air conditioners have to deal with, the heat gain from envelope is an important contributor. In a residential building in the subtropical Hong Kong, envelope heat gains accounted for more than 70% of the total cooling load for a bedroom, as shown in Fig. 2.7 [Lin and Deng 2004]. At nighttime, the metabolic rate of a sleeping person is low, therefore, the heat gain from the envelope dominates the total cooling load in a bedroom.

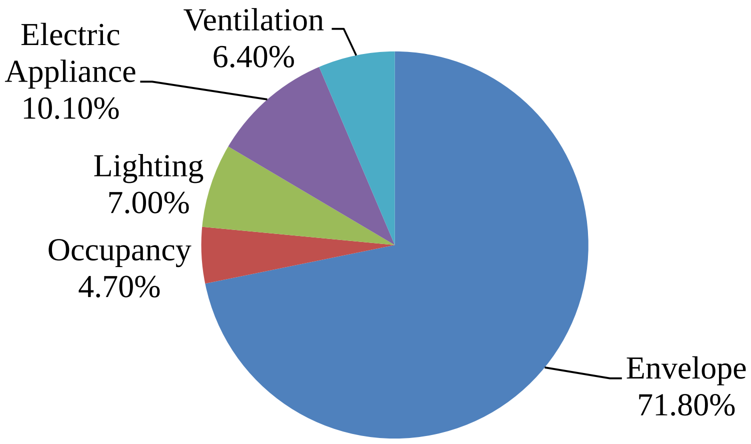

Fig. 2.7 Percentage breakdown of the total cooling load for the bedroom facing west at the A/C starting time [Lin and Deng 2004]

Furthermore, the total cooling loads in bedrooms in Hong Kong vary significantly overnight, as illustrated in Fig. 2.8 which shows the hourly profiles of the total cooling load in bedrooms facing four orientations (i.e., East, South, West and North) in the summer design day in Hong Kong. It can be observed that all the total cooling loads peaked at 22:00 when A/C started, decreased rather quickly over the next 2 hours, and then decreased relatively slowly between 0:00 and 6:00. After 6:00, these loads were slightly increased due to increased space heat gains from outdoor air temperature going up slightly from its lowest value at that time, and from lights and electric appliances if turned on.

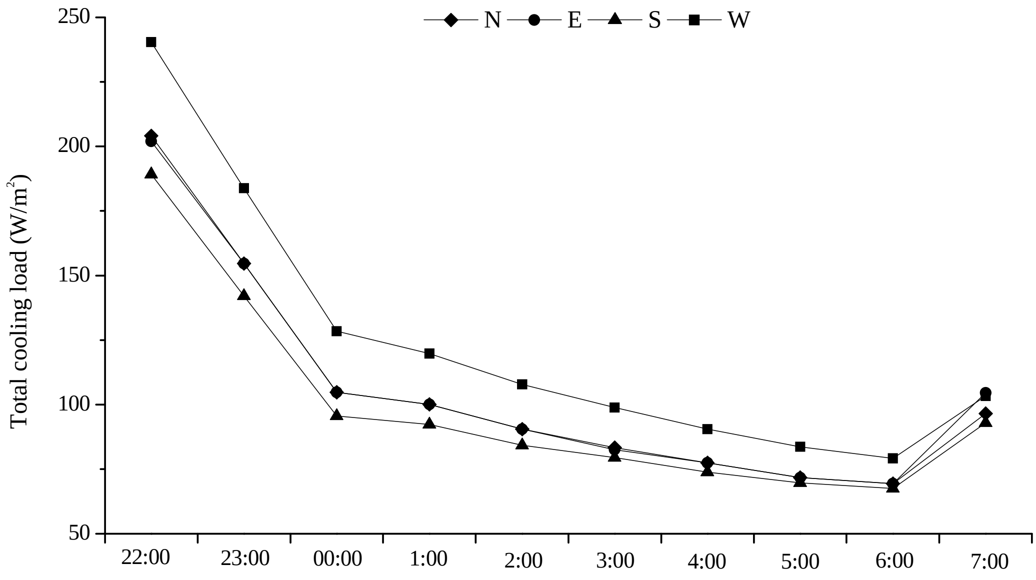

Fig. 2.8 Hourly profiles of the total cooling load for bedrooms facing four different orientations in the summer design day in Hong Kong [Lin and Deng 2004]

2.6 Task\ambient air conditioning (TAC) systems

TAC systems have attracted increasingly research attention, due to their excellent performances in local thermal environmental control and energy saving. A TAC system permits the thermal conditions in a small, localized zone to be individually controlled by its occupants, while allowing thermal environmental conditions outside the zone to freely fluctuate [Bauman and Arens 1996]. Typically, occupants could control the speed and direction, and in some cases the temperature of supply air to the zone. A TAC system is therefore designed to provide individual control and accommodate individual preferences over thermal environment, and to offer the potentials for improved productivity and energy saving for air conditioning.

2.6.1 TAC systems applied to workplaces at daytime

2.6.1.1 Types of TAC systems

There are mainly three types of TAC systems applied to workplaces and other leisure places at daytime according to their installation positions: floor based, workstation based and ceiling based.

(1) Floor based TAC systems

Floor based TAC systems are the mostly utilized. They were extensively used in South Africa, Europe [Spoormaker 1990, Sodec and Craig 1991], the United States [Shute 1992, Shute 1995] and Japan [Matsunawa 1995, Tanabe 1995]. For a floor based TAC system, its supply outlets were incorporated into a raised access floor. Supply air was either drawn from a low-pressure under-floor plenum by local variable or constant-speed fans, or forced through a pressurized under-floor plenum by a central air handler, and delivered to a space through floor-level supply outlets. Fig. 2.9 shows a floor based TAC system with a TAM (task air modules) [Bauman et al. 1995]. A floor based TAM can provide the required air-volume and allow occupants to control the direction of supply air.

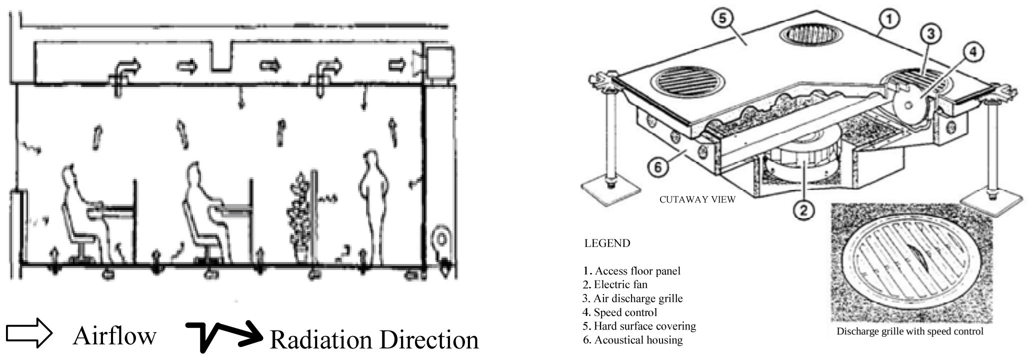

Fig. 2.9 A floor based TAC system with Task Air Modules [Bauman et al. 1995]

(2) Workstation based TAC systems

i) Desk integrated

For a desk integrated TAC system, its air supply outlet was installed somewhere in a desk. Various desktop supply outlets have been developed and used, such as desktop level grills at the back of a desk surface [Argon 1994], free-standing directable supply nozzles at the back of a work surface [Sodec 1984, Arens et al. 1991, Bauman et al. 1993] and a linear grill at a desk's front edge directly facing a seated occupant [Argon 1994, Wyon 1995]. A sketch of a typical desktop integrated TAC system with a PEM (Personal Environmental Module) installed [Bauman et al. 1998] on a desktop is shown in Fig. 2.10(a). Moreover, a portable fan-filter unit placed next to a desk to supply air with a flexible duct to an outlet placed underneath the desk [Faulkner et al. 1999] is shown in Fig. 2.10(b). Fig. 2.10(c) shows two other types of desk integrated TAC systems. For the first one, the position and angle of diffuser through flexible duct may be adjusted, and for the other, a PEM consisting of mixing box and diffusers was placed on the desk [Amai et al. 2007].

ii) Partition integrated

A partition integrated TAC system [Argon 1994, Matsunawa et al. 1995, Pan et al. 2005] can be applied to a partitioned workstation and was convenient to be linked to a raised access floor. Supply air was delivered through a passageway that was integrated into the partition design to controllable supply diffusers located just above desk level, or to the diffusers on top of the partitions (for ambient environmental control). Fig. 2.11(a) shows a terminal unit of a partition integrated TAC system

[Argon 1994]. Fig. 2.11(b) shows a partition integrated TAC system which was designed with a head-ventilation device to cool the head of an occupant by air motion [Zhang et al. 2010]. Moreover, a number of partition integrated TAC systems installed in Japanese buildings were investigated by the Society of Heating, Air-conditioning and Sanitary Engineers of Japan [Imagawa and Mimma 1991, Matsunawa et al. 1995].

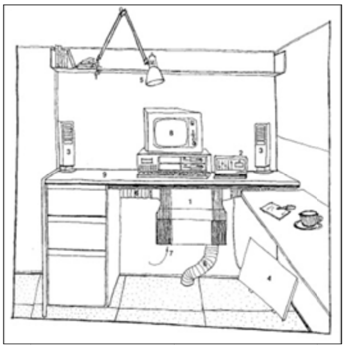

(a) A desktop integrated TAC system
[Bauman et al. 1998]

(b) A desk-mounted TAC system
[Faulkner et al. 1999]

(c) Other types of desk integrated TAC system [Amai et al. 2007]

Fig. 2.10 Desk integrated TAC systems

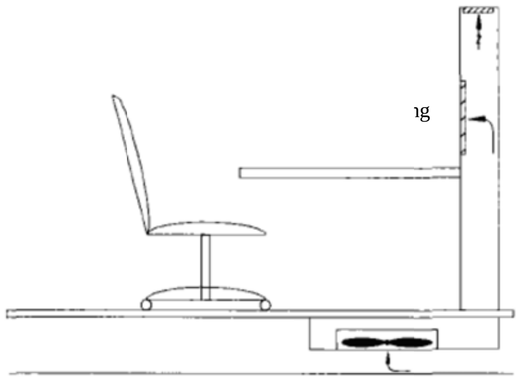

(a) A terminal unit of a partition integrated TAC system [Argon 1994]

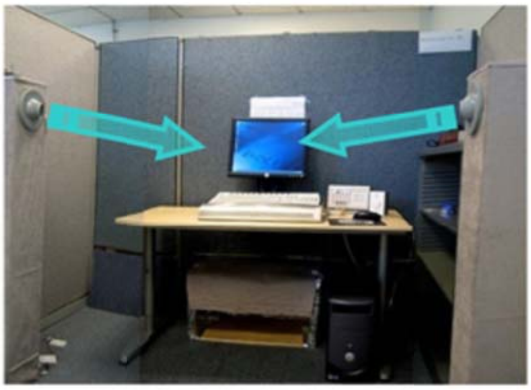

(b) A partition integrated TAC system with head ventilation devices

[Zhang et al. 2010]

Fig. 2.11 Partition integrated TAC systems

(3) Ceiling based TAC systems

Ceiling based TAC systems [Tamblyn 1995, Yang et al. 2008, 2009 and 2010] were mostly seen in retrofit projects, where installing raised floor was difficult due to limited floor-to-slab height. Similar to that in a conventional air conditioning system, the supply air outlets of ceiling based TAC systems were above a work space. Fig. 2.12 shows a typical ceiling based TAC system [Tamblyn 1995]. A remote controller was essential for this type of TAC systems to be practically operatable.

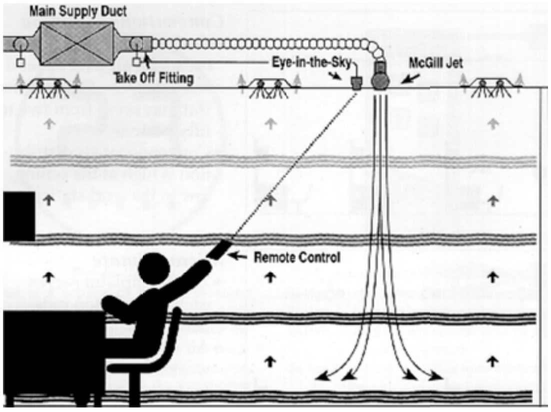

Fig. 2.12 A ceiling based TAC system [Tamblyn 1995]

2.6.1.2 The benefits of using TAC systems

Studies have been carried out to investigate the operational performances of TAC systems used for daytime activities, through field measurement and laboratory experiments. Results from these studies demonstrated that the use of TAC systems can help improve thermal comfort and indoor air quality, and reduce energy consumption [Bauman et al. 1993, Shute 1995, Faulkner et al. 1995, Pan et al. 2005, Tham et al. 2004, Amai et al. 2007].

By allowing individual occupants to control their thermal environments, their individual thermal comfort preferences can be accommodated. It was demonstrated by laboratory tests that a TAC system with fan-driven supply outlets provided personal control of the occupant’s microclimate over a sizable range up to 7 ºC for desktop outlets and up to 5 ºC for floor based outlets [Tsuzuki et al. 1999]. Amai et al. [2007] carried out an experimental study on four types of TAC systems installed in a climate chamber. It was found out that using TAC systems achieved better thermal comfort. A personal environmental module based TAC system was flexible and easy to control, therefore offered a significant potential to improve thermal comfort in workspaces [Cho et al. 2001]. Bauman et al. [1998] conducted a series of experiments on the responses of occupants to different air conditioning systems, and the results showed a large increase in mean ratings of satisfaction for all three factors: temperature, temperature control and air movement when using TAC.

Through delivering fresh air near the occupants, good ventilation effectiveness and indoor air quality at breathing level can be achieved [Nielsen 1996]. Studies have shown that a desk-mounted TAC system can significantly improve ventilation effectiveness [Faulkner et al. 2002, Melikov et al. 2002]. Shute et al. [1995] studied the air quality in a room using a floor based TAC system and found out that the suspended substance concentrations was obviously lower when compared to using a conventional air conditioning system. Spoormaker et al. [1995] studied indoor pollutants concentrations in a building using a floor based TAC system, and the results indicated that the index of each pollutant was much lower than that specified in relevant standards.

The use of TAC systems also helped achieve energy saving. This was because when a full volume air conditioning (FAC) system was used, a comfortable indoor environment for everywhere in a room may be maintained. However, when a TAC system was used, only a comfortable indoor environment within an occupied zone would be maintained, but air temperatures outside the occupied zone were allowed to fluctuate to even out of comfort limits. As compared to the use of FAC systems, the use of TAC systems can result in energy saving since air conditioning in an unoccupied zone was unnecessary. Pan et al. [2005] experimentally compared the performance of a personalized air-conditioning system, which was called an innovative partition-type fan-coil unit (PFCU), with that of a central A/C system, in terms of thermal comfort achieved and cooling energy consumed. The experimental results showed that the use of the personalized system can shorten the duration required in achieving the same level of thermal comfort, and save up to 45% of energy use.

2.6.1.3 Ranges for operating parameter of TAC systems

The suitable ranges of operating parameters used in various TAC systems have been studied and are listed in Table 2.4. These included supply air temperature, supply air velocity, supply air direction, thermal load level, etc. For a floor-based TAC system, Bauman et al. [1995] recommended that local supply air temperatures should be maintained at above 17 °C to avoid uncomfortable cold draft for the occupants nearby. A floor supply module should be installed 1-1.5m away from a workstation to avoid draft. For a desk based TAC system, using larger nozzles to deliver a fixed amount of air at a lower velocity helped reduce the potential of draft discomfort while still maintaining an acceptable ventilation performance at a moderate to high air supply flow rate [Bauman et al. 1993, Faulkner et al. 1999]. Moreover, Gong et al. [2006] suggested that when a task\ambient supply outlet was 15 cm away from an occupant, a supply velocity of 0.3 to 0.45 m/s was suitable at a supply air temperature of 21 °C, while a supply velocity of 0.3 to 0.9 m/s was better at a supply temperature of 23.5 °C. Therefore, by suitably controlling its supply air velocity, air temperature, and supply air direction, a TAC system can be operated to maintain acceptable thermal comfort and avoid draft in an occupied zone.

Table 2.4 Operating parameters of different types of TAC systems

Literatures	Types	Supply temperature (°C)	Supply flow rate (L/s)	Supply direction	Thermal load level (W/m^2)
Bauman et al. 1991	Floor based	18	16-33	Toward, inward and combined	35-55
Bauman et al. 1995	Floor based	16 - 21.6	16-47	Toward and inward	25-50
Faulkner et al. 1995	Floor based	15.9 - 22.9	27-82	Toward, inward	17.8-43.5
Mutsunawa et al. 1995	Floor based	18 - 20	74-83	-	31-40
Bauman et al. 1993	Workstation based (desktop integrated)	16.6 - 20.8	14-50	Toward and straight	24-51
Faulkner et al. 1993	Workstation based (desktop integrated)	19	7-26.1	Vertical, horizontal, toward and parallel	-
Faulkner et al. 1999	Workstation based (desktop integrated)	18.4 - 26.1	7-38	Vertical, horizontal, toward and parallel	-
Mutsunawa et al. 1995	Workstation based (partition integrated)	18 - 20	74-83	-	31-40
Jeong et al. 2006	Workstation based (partition integrated)	22 - 27	20	-	-

2.6.2 TAC systems applied to sleeping environments at nighttime

Limited studies have been carried out on TAC systems applied to sleeping environments. Pan et al. [2012] developed a novel bed-based TAC system installed in an experimental bedroom, as shown in Fig. 2.13. Two supply air plenums were symmetrically placed on both sides of a mattress bed to ensure a uniform supply air distribution. Flexible air ducts were used to link the bed-based TAC system to both supply inlet and return outlet. The experimental results and related analysis indicated a better performance of the bed-based TAC system in thermal control and energy saving. Moreover, it was pointed out that using a bed-based TAC system was suitable when operated at a supply air temperature of 20 - 22 °C and a supply flow rate of 50 l/s using a thin quilt, or 24 °C and 50 l/s using a blanket.

However, there existed a number of noticeable inadequacies when using the novel bed-based TAC system developed. Firstly, there were a bulky supply air plenum and flexible air ducts, shown in Fig. 2.13, causing inconvenience to users. Secondly, the experimental bedroom was treated as having no envelope heat gain by assuming all heat gains coming from an internal source. However, the cooling load due to envelope heat gain may actually account for over 70% of the total space cooling load at nighttime [Lin and Deng 2004]. Thirdly, indoor air quality and humidity distribution profiles in the experimental bedroom when using the novel bed-based TAC system were not investigated. Therefore, the bed-based TAC system should be modified and studied to make it more applicable for practical.

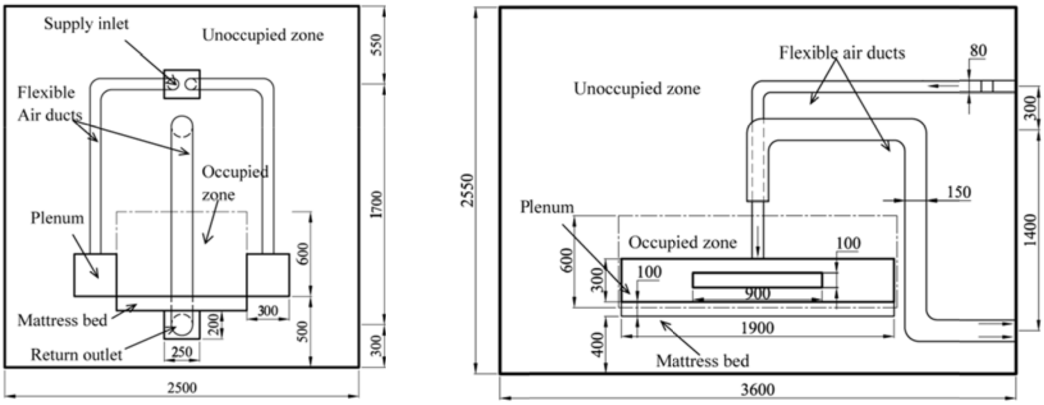

Fig. 2.13 The schematics of a novel bed-based TAC system [Pan et al. 2012]

2.7 The use of CFD method to study indoor thermal environments

With the rapid advancements in computing capacity and speed, computational fluid dynamics (CFD) has been widely used in many subject areas, including aerospace, food processing, buildings and environmental science. Among many other applications, the use of CFD techniques has become a powerful tool in building HVAC related studies for predicting indoor air flow, indoor air temperatures and IAQ, etc. [Nielsen 1974, Liddament 1991, Jones and Whittle 1992, Moser 1992, Chen 1996, Ladeinde and Nearon 1997, Emmerich et al. 1997, Spengler and Chen 2000, Chen and Zhai 2004, Stamou and Katsiris 2006, Zhai 2006, Zhang et al. 2007, Murakami et al. 1995].

2.7.1 Governing equations

The flow field was calculated by three-dimensional and steady-state Reynolds averaged Navier-Stokes (RANS) equations, combined with continuity and energy equations. The governing equations are as follows:

Continuity equation:

$$\frac{\partial \rho}{\partial t} + \nabla \cdot (\rho \vec{v}) = 0 \qquad (2.4)$$

Momentum equation:

$$\frac{\partial}{\partial t}(\rho \vec{v}) + \nabla \cdot (\rho \vec{v}\vec{v}) = -\nabla P + \nabla \cdot (\overline{\overline{\tau}}) + \rho \vec{g} \qquad (2.5)$$

Where p is the static pressure, $\overline{\overline{\tau}}$ the stress tensor and $\rho\vec{g}$ the gravitational body force.

Energy equation:

$$\frac{\partial}{\partial t}(\rho E)+\nabla\cdot(\vec{v}(\rho E+p))=\nabla\cdot(\rho k_{eff}\nabla T-\sum_j h_j\vec{J_j}+(\overline{\overline{\tau}}_{eff}\cdot\vec{v})) \tag{2.6}$$

Where k_{eff} is the effective conductivity, and $\vec{J_j}$ the diffusion flux of species j. E is expressed as follows:

$$E=\sum_j Y_j h_j-\frac{p}{\rho}+\frac{v^2}{2} \tag{2.7}$$

To predict CO_2 and moisture transfer inside a room, a species transport model can be used. The conservation equation for the species transport is given in the following general form:

$$\nabla\cdot(\rho\vec{v}Y_i)=\nabla[(\rho D_{i,m}+\frac{\mu_t}{Sc_t})\nabla Y_i]+S_i \tag{2.8}$$

Where Y_i is the local mass fraction of the i^{th} species, $D_{i,m}$ the mass diffusion coefficient for species i in the mixture, Sc_t the turbulent Schmidt number and S_i any defined source term.

2.7.2 Turbulence models and applications

Generally, the use of CFD predicts turbulent flows through three approaches: Direct Numerical Simulation (DNS), Large Eddy Simulation (LES), and Reynolds-Averaged Navier-Stokes (RANS) equation simulation with turbulence models, as shown in Table 2.5.

Airflow inside buildings is characterized by a display of various flow elements. For example, air movement at a supply opening and an exhaust can be described as jet flow and potential flow, respectively, and the airflow in a room may be divided into natural convection, forced convection, or mixed convection according to its driving force. However, certain turbulence models are only good at dealing with certain flow elements. It has been almost impossible so far to identify a single model that can be used to evaluate all room air flow patterns economically and accurately. The choice of a turbulence model is a compromise which depends on such considerations as: the physics encompassed in the flow, the established practice for a specific class of problems, the level of accuracy required, the available computational resources, and the amount of time available for simulation, etc.

Table 2.5 Turbulence models for predicting airflows in enclosed environments

<table>
<tr><th colspan="3">Turbulence model classification</th><th>Primary turbulence models used
in indoor air simulations</th></tr>
<tr><td colspan="3">DNS</td><td>Orszag 1970</td></tr>
<tr><td colspan="3">LES</td><td>LES-Sm (Smagorinsky 1963)
LES-Dyn (Germano et al. 1991; Lilly 1992)
LES-Filter (Zhang and Chen 2000, 2005)</td></tr>
<tr><td rowspan="7">RANS</td><td rowspan="6">EVM</td><td>Zero-eqn</td><td>0-eq. (Chen and Xu, 1998)</td></tr>
<tr><td rowspan="3">Two-eqn</td><td>Standard k-ε (Launder and Spalding 1974)
RNG k- ε (Yakhot and Orszag 1986)
Realizable k- ε (Shih et al. 1995)</td></tr>
<tr><td>LRN-LS (Launder and Sharma1974)
LRN-JL (Jones and Launder 1973)
LRN-LB (Lam and Bremhorst 1981)</td></tr>
<tr><td>LRN k-ω (Wilcox 1994)
SST k-ω (Menter 1994)</td></tr>
<tr><td rowspan="2">Multi-eqn</td><td>v2f-dav (Davidson et al. 2003)</td></tr>
<tr><td>v2f-lau (Laurence et al. 2004)</td></tr>
<tr><td colspan="2">RSM</td><td>RSM-IP (Gibson and Launder 1978)
RSM-EASM (Gatski and Speziale 1993)</td></tr>
</table>

Up to the present moment, k-ε models are still the most commonly used in practical engineering applications. A standard k-ε model is only applicable to fully turbulent flow. In the region near a solid surface, this model should be applied in conjunction with wall functions considering the dominant effects of viscosity, and the simulation accuracy would be greatly impacted by the location of the first grid close to the wall boundaries [Niu and Kooi 1992]. In the simulations of airflow around a human body, the most frequently used turbulence models are the RNG k-ε model and the low Reynolds number k-ε model. Murakami et al. [1995] pointed out that since no wall functions were applicable for the standard k-ε turbulence model to simulate the airflow around thermal manikins, the low Reynolds number k-ε model with locally-fine grids at the human body surface was the only way to calculate the convective heat transfer. However in the simulations using the low Reynolds number k-ε model and an accurate geometric model of a human body, it was difficult to achieve convergence due to the extremely fine grids near the human body [Voigt 2001].

All these three types of k-ε models mentioned above had their shortcomings. For example, the turbulence energy was over-predicted by a standard k-ε model [Wringt and Eason 1999, Kim and Chen 1989]. Very fine grids should be used near a wall and computational stability was probably a problem if a low Reynolds number k-ε model was employed. A RNG k-ε model was still required to be used in conjunction with wall functions.

A further turbulence model, the k-ω model [Wilcox 1988, Menter 1994], has also received increasing attentions in many industrial applications since last decade. To overcome the weakness of the *k-ω* model's robustness in predicting wake region and free shear flows, a shear stress transport (SST) *k-ω* model was developed by Menter [1994] through integrating both the *k-ε* and the *k-ω* models. Arun and Tulapurkara [2005] computed the turbulent flow inside an enclosure with a central partition using three advanced turbulence models: RNG *k-ε* model, Reynolds stress model and SST *k–ω* model. It was found out that the SST *k-ω* model can capture complex flow features such as the movement of vortices downstream of the partition, flow in reverse direction in the top portion of the enclosure, and the exit of flow with swirl. Stamou and Katsiris [2006] used the SST *k-ω* model, the standard *k-ε* model, the RNG *k-ε* model and a laminar flow model to predict air velocity and temperature distributions in a model office room with a task ventilation system. By comparing with experimental data, it was concluded that the three turbulent models predicted satisfactorily the main qualitative features of the flow and the SST *k-ω* model performed slightly better than the other two. Kuznik et al. [2007] also evaluated the Realizable *k-ε* model, the RNG *k-ε* model, the standard *k-ω* model and the SST *k-ω* model by comparing their predictions with experimentally measured air temperature and velocity in a mechanically ventilated room with a strong jet inflow. It was found that the *k-ω* models presented a new potential to model airflows in enclosed environments with good accuracy and numerical stability. Most previous studies indicated that the SST k-ω model [Menter 1994] had a better overall performance than the standard k-ε and the RNG k-ε models.

2.7.3 Mesh generation

The correctness and accuracy of a simulation result depends very much on grid quality. The accuracy is influenced by a number of grid factors, such as grid topology, grid shape, grid size and the consistency of grids with geometry, etc.

There are four methods to discretize a space: cartesian co-ordinates, cylinder co-ordinates, body-fitted co-ordinates and unstructured grids. In the simulation of airflow around complicated geometries such as those of a human body, body-fitted co-ordinates and unstructured grids are often used to represent the complex boundaries. Body-fitted co-ordinates are suitable for internal or external flows with smoothly varying irregular boundaries. Unstructured grids are more flexible in grid distribution than body-fitted coordinates.

A ventilated space is usually divided into 2 parts: a cuboid enclosing an occupant and the rest of the space. The cuboid is built with unstructured grids due to complex geometries of a thermal manikin while the rest of space is discretized with structured grids [Gao and Niu 2005a] due to its simple geometry and higher quality of structured grids.

2.7.4 Related numerical studies on the thermal environment around a human body

In order to correctly evaluate thermal comfort of an individual, the thermal environment around a human body should be known. To facilitate carrying out the related studies, thermal manikins have been used for many years [Holmér 2004].

A review on certain important issues related to CFD study on the thermal environment around a human body was reported by Gao and Niu [2005a], including geometric complexity, boundary conditions and related simulation results obtained. Firstly, thermal manikins may differ in size, posture and the level of geometric complexity. The level of geometric complexity of thermal manikins depended on the purpose of study. The geometries of a thermal manikin can be often obtained from computer aided design, but a digital thermal manikin having a complicated geometry may be obtained using laser scanning technique [SØrensen and Voigt 2003, Gao and Niu 2004, Gao et al. 2006]. The use of thermal manikins with simple geometry required fewer computational resources and less time for modelling and grid generation. However, using a detailed representation of a human body can help better reflect the reality to produce more accurate simulation results. Secondly, two methods were usually used to describe the boundary condition of a human body: a fixed surface temperature and a fixed surface heat flux. Usually, the surface temperature of a human body was set between 31 °C [Murakami et al. 1997] and 33.7 °C [SØrensen and Voigt 2003]. The convective heat flux was set between 20 W/m^2 [Hayashi et al. 2002a] and 25 W/m^2 [Brohus and Nielsen 1996]. Lastly, radiative and convective heat transfers from a human body were numerically investigated, and the study results have been used to assess the thermal comfort of a human being [Murakami et al. 2000, Silva and Coelho 2002, Yang et al. 2002, SØrensen and Voigt 2003, Gao and Niu 2004, Gao et al. 2006].

2.7.5 Related numerical studies on indoor air quality

There has been growing concerns on IAQ for decades. A survey showed that people in Hong Kong spent about 85% of their time indoors [Chau et al. 2002]. Therefore, a large number of numerical studies were carried out on IAQ in buildings, where different air conditioning systems, such as displacement ventilation systems, mixing ventilation systems, floor based TAC systems and desk based systems were installed.

Lau and Chen [2007] studied the indoor environment inside a high-cooling load workshop with a floor displacement ventilation system. The CO_2 concentration distributions inside the workshop were studied using SF6 (sulfur hexafluoride) as a tracer gas. The impacts of several system parameters, such as air change rate, number of diffusers, diffuser location, occupant location, furniture arrangement, partition location and arrangement of exhausts, on IAQ were investigated based on thermal comfort level and indoor air quality. Noh et al. [2007] performed an experimental and numerical study on CO_2 concentration levels in a lecture room equipped with a mixing ventilation system. It was found out that when the ventilation rate was greater than 800 m^3/h, the CO_2 concentration level is satisfactory. Lin et al. [2005] conducted a numerical research on the CO_2 concentration distributions and mean age of air in an office room and compared the performances between using displacement and mixing ventilations. Gao and Niu [2005b] conducted a numerical study on the performances of a personal ventilation (PV) system. It was found out that a better air quality in the breathing zone can be expected due to more fresh air entering this zone. Zheng et al. [2009] carried out a numerical research on CO_2 concentration distributions in a modern office equipped with a TAC system. The research showed that CO_2 concentrations around occupants were much lower than other regions with a high ventilation effectiveness.

2.8 Conclusions

Currently, air conditioning is mainly concerned with the situations in which people are awake in workplaces or other leisure places, such as shopping malls and restaurants. However, in tropical and sub-tropical regions, due to their climatic condition, air conditioning is required not only in daytime at a workplace, but also at nighttime in a sleeping environment, such as bedrooms in residential buildings and guest rooms in hotels. Therefore, it has become highly necessary to study the thermal environment in an air conditioned sleeping space in order to provide people with a thermally comfortable sleeping environment.

Previous medical research work on the factors affecting the quality of sleep has been undertaken, as reported in Section 2.2. It has been commonly acknowledged that the quality of sleep is mainly determined by the mental-physical factors of a sleeping person, but may also be significantly affected by the environmental factors in a bedroom such as thermal environment and indoor air quality, among others, like noise and lights. Therefore, a limited number of previous studies on surveying sleeping thermal environments and bedroom air conditioning, studying the thermal comfort, developing an appropriate thermal comfort model and determining the thermally neutral environment for sleeping environments have been carried out, as shown in Section 2.3. In Section 2.4, the health impacts and generation of indoor CO_2, which can be used as a surrogate indicator of IAQ, are reviewed. Therefore, to contribute to achieving quality sleep, appropriate thermal environment and indoor air quality in a bedroom should be provided and maintained by using air conditioning technology.

In addition, the increased use of building air conditioning contributes to increased energy uses in buildings, as reported in Section 2.5 using energy use in Hong Kong as an example. Therefore, in the tropical or sub-tropical regions, for residential buildings or any other buildings such as hotels and hospitals where sleeping environments are present, air conditioning is used at not only daytime but also nighttime for maintaining thermally comfortable sleeping environments. This consequently contributes to the increased A/C energy uses in buildings. Therefore, it is necessary to develop / study novel A/C systems applicable to sleeping environments at reduced building A/C energy consumptions.

Because of their excellent performance in local thermal environmental control and energy saving, TAC systems have attracted increasingly research attention. Different types of TAC systems applied at daytime and their benefits and operating characteristics are reviewed in Section 2.6.1. Limited previous studies on TAC systems applied to sleeping environments are also reviewed in Section 2.6.2. It is noted that the current applications of TAC systems are mainly for daytime activities, such as in workstations, but less for nighttime applications such as bedrooms in residences or other sleeping environments. On the other hand, there are a number of noticeable inadequacies for the existing TAC systems applied to sleeping environments. Consequently, studies should be carried out to develop novel TAC systems applied to sleeping environments, and the performances of the TAC systems in terms of ventilation should be evaluated.

Furthermore, numerical studies have been carried out to investigate the micro-climate around a human body and CO_2 transport inside a room, as presented in Section 2.7. These studies have provided useful references for further related numerical studies. Consequently, it is possible to study numerically the developed novel TAC systems applied to a sleeping environment in terms of thermal environment control, ventilation effectiveness and energy use.

The extensive literature review presented in this Chapter has identified a number of areas where further in-depth research work to maintain an appropriate sleeping thermal environment at an acceptable indoor air quality and a reduced energy consumption is urgently required. These are the expected targets of investigation to be reported in this Thesis.

Chapter 3

Proposition

3.1 Background

It is evident from the Literature Review presented in Chapter 2 that the environmental factors including thermal environment and indoor air quality in a bedroom would significantly affect the quality of sleep. On the other hand, the current studies on thermal environmental control and indoor air quality in buildings using air conditioning are mainly concerned with situations in which people are awake in workplaces or other leisure places, such as shopping malls and restaurants. Furthermore, currently, the use of TAC systems is also mainly for workspaces at daytime. Consequently, relevant further studies focusing on evaluating operating performances of TAC systems used in sleeping environments should be carried out.

To contribute to sleep quality, in the tropics and sub-tropics, the use of air conditioning in bedrooms to maintain an appropriate thermal environment and an acceptable indoor air quality is necessary. However, this would lead to the increased energy use in buildings. Since the use of TAC systems results in a better performance in thermal environment control, ventilation effectiveness and energy use, and a sleeper is normally immobile and confined to a small space, it is expected that applying TAC systems to sleeping environments would help achieve better thermal environment control and ventilation effectiveness at reduced energy use.

Given that different operating performances may be resulted in for a TAC system operated at different system configurations, it is therefore necessary to study the operating performances of a TAC system applied to a sleeping environment at different system configurations, such as different return air inlet locations, and different heights of a supply outlet.

Furthermore, the operating parameters of a TAC system applied to a sleeping environment and the total insulation value of beddings and bed may significantly affect a thermally neutral environment in a bedroom. Consequently, it becomes necessary to identify optimized operating parameters of the TAC system to achieve a thermally neutral sleeping environment under different total insulation values of beddings and bed at minimum energy use.

3.2 Project title

A programmed research work on applying TAC to sleeping environments in the subtropics has been therefore carried out and is reported in this thesis. There are four parts in the programmed research work: 1) experimentally studying the thermal environmental control, ventilation effectiveness and energy saving performances of using a ductless bed-based TAC system, as compared with that of a FAC system installed in an experimental bedroom; 2) experimentally studying the influence of different return air inlet locations on the performance of the ductless bed-based TAC system; 3) numerically evaluating performances of an A/C system installed in the experimental bedroom with its supply outlet positioned at five different heights through integrating the performance indexes separately for thermal environmental control, ventilation effectiveness and energy saving; 4) carrying out an optimization study to identify the operating parameters (supply air temperature, supply air flow rate and supply air humidity) of the ductless bed-based TAC system installed in the experimental bedroom in order to obtain a thermally neutral sleeping environment under different total insulation values of beddings and bed at minimum energy use. The proposed programmed research work is therefore entitled “A study on thermal environmental control, indoor air quality and energy efficiency using task\ambient air conditioning (TAC) systems in sleeping environments in the subtropics".

3.3 Aims and objectives

The aims and objectives of the programmed research work are as follows:

1) To experimentally investigate the operating performances of a TAC system in terms of thermal environmental control, indoor air quality and energy saving, and compare the influences of different return inlet locations of the TAC system on its operating performances;

2) To apply CFD methods to numerically studying the air velocity, air temperature, air humidity and CO_2 concentration distributions in a sleeping environment, and to experimentally validate the CFD methods;

3) To carry out an overall performance evaluations for the TAC system by integrating three performance indexes for thermal environmental control, ventilation effectiveness and energy saving;

4) To carry out an optimization study for the operating parameters of the TAC system so as to obtain a thermally neutral sleeping environment under different total insulation values of beddings and bed at minimum energy use.

3.4 Research methodologies

Experimental, numerical and other system optimization methods including TOPSIS and DOE methods were be employed in this programed research work. Firstly, experimental methods were used to study the operating performances of a ductless bed-based TAC system in an experimental bedroom, as compared to that of using a FAC system in the first part of the programmed research work. Air temperatures, air velocities, air humidities and CO_2 concentrations in the experimental bedroom, surface temperatures of an external wall and window of the experimental bedroom and heat flux of a thermal manikin were measured. The thermal environmental control performance for the TAC system in terms of draft risk (DR) and air relative humidity, the ventilation performance in terms of ventilation effectiveness (VE) and energy saving performance in terms of energy utilization coefficient (EUC) were evaluated and compared between the two systems.

Secondly, experimental and numerical methods were applied to studying the influence of return air inlet locations on the performance of the ductless bed-based TAC system. Two settings for the ductless bed-based TAC system were designed. The operating performances of the ductless bed-based TAC system at the two settings in terms of thermal environmental control and energy saving were firstly experimentally evaluated. Afterwards, a CFD method for evaluating air flow and temperature fields in the experimental bedroom was developed and validated using the experimental results.

Thirdly, the TOPSIS method and numerical approach were used to study the performance of an A/C system installed in the experimental bedroom with its supply outlet positioned at five different heights. A numerical study was carried out using CFD to study the air flow and temperature fields and CO_2 distributions inside the bedroom. Based on the simulation results, the operating performance in the three aspects of thermal environmental control, ventilation effectiveness and energy saving for the A/C system operated at different conditions, were then obtained and analyzed. The TOPSIS method was employed to evaluate the overall performance of the A/C system at various operating conditions, through integrating the three individual indexes for thermal environmental control, ventilation effectiveness and energy saving.

Fourthly, the DOE method and numerical approach were employed to carry out an optimization study for the operating parameters (supply air temperature, supply air flow rate and supply air humidity) of the ductless bed-based TAC system in order to obtain a thermally neutral sleeping environment under different total insulation values of beddings and bed at minimum energy use. A CFD method was applied to calculating the PMV (Predicted Mean Valve) and EUC (energy utilization coefficient) values for 16 simulation cases. Based on the simulation results, the DOE (design of experiment) method was applied to identifying operating parameters, individually or combined, which would significantly affect thermal neutrality and energy use, and linear regression models for PMV and EUC using the identified parameters were established, respectively. Thereafter, the linear regression models were used to obtain the optimum operating parameters of the bed-based TAC system, so that a thermally neutral sleeping environment can be maintained at a minimum energy use.

Chapter 4

Experimental setup

4.1 Introduction

All the experimental work reported in Chapters 5, 6, 7 and 8 of this thesis was carried out using an experimental setup established inside an existing experimental direct expansion (DX) A/C station, which is available in the HVAC Laboratory of Department of Building Services Engineering, The Hong Kong Polytechnic University. The station includes a DX A/C plant and an environmental chamber, as schematically shown in Fig. 4.1. The primary purpose of having the experimental station is to facilitate carrying out the research work related to DX A/C technology.

This Chapter firstly presents a brief description of the DX A/C plant and the environmental chamber. This is followed by detailing the experimental setup with respects to system arrangement and settings used in the programmed research work. Finally, measurement methods used are presented.

4.2 DX A/C plant

The major components in the DX A/C plant include a variable-speed rotor compressor, an EEV (electronic expansion valve), a high-efficiency tube-louver-finned DX evaporator, an air-cooled tube-plate-finned condenser, and supply air fan, as well as the associated supply air ductwork. The DX A/C plant is responsible for maintaining the air temperature and humidity inside the chamber at normal air conditioning operations. Inside the chamber, there are sensible heat and moisture load generating units (LGU). Their heat and moisture generation rates can be varied either manually or automatically with a pre-set pattern through operator's programming.

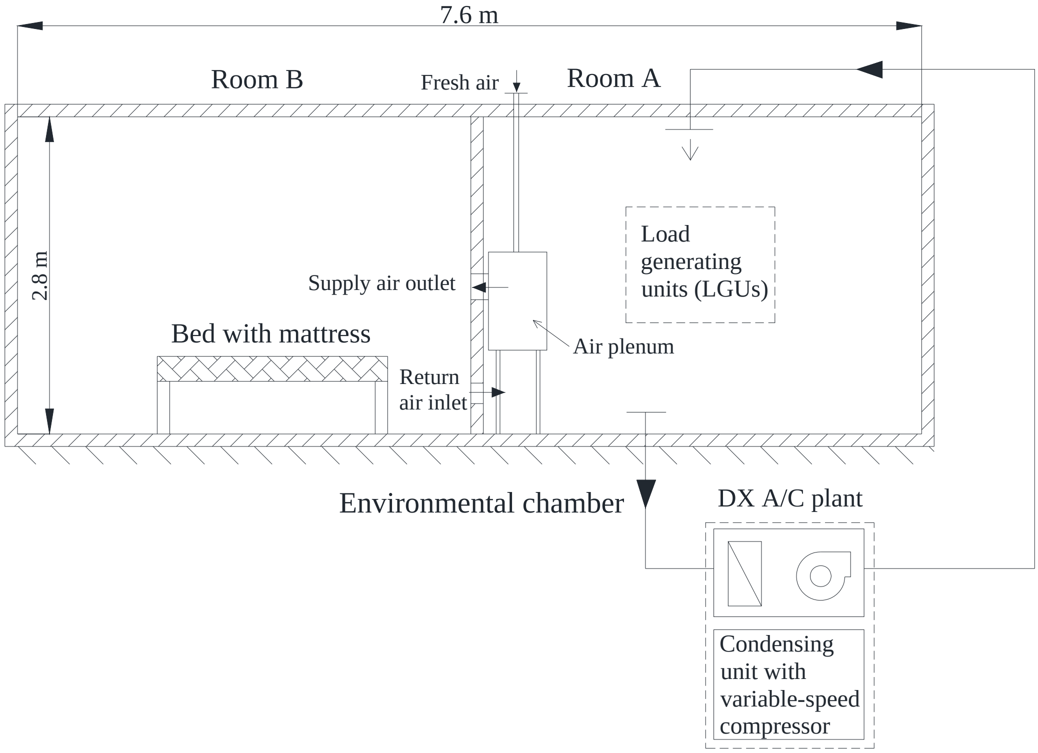

Fig. 4.1 An experimental DX A/C station

4.3 Environmental chamber

The environmental chamber measuring at 7.6 m (L)×3.8 m (W) ×2.8 m (H) was divided into two adjacent rooms for simulating different thermal environments: Room A and

Room B, as shown in Figs. 4.1 and 4.2. Room B was further separated into a larger space and a smaller space by a simulated external wall which was made of wooden board and glass. The larger space was used as an experimental bedroom, measuring at 3.62 m×2.6 m×2.53 m. The smaller space was used as a simulated outdoor environment, where two electrical heaters were placed. The sizes and thermal conductivities of the wooden board and glass are given in Table 4.1. In Room A, air temperature and humidity can be precisely controlled jointly by the DX A/C plant and LGUs. Therefore, conditioned air at a required air temperature, relative humidity and air flow rate can be supplied from Room A to the experimental bedroom through a plenum and a supply air outlet, as shown in Fig. 4.1.

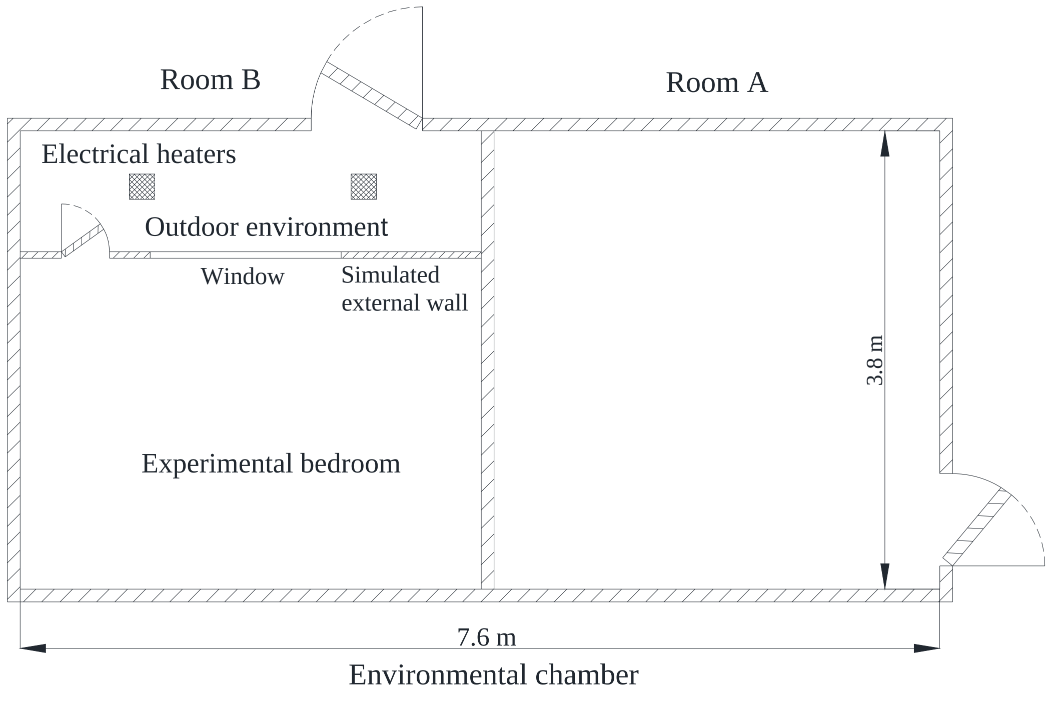

Fig. 4.2 An environmental chamber

Table 4.1 Sizes and properties of the materials used in the simulated external wall

Material	Thermal conductivity (W/K m)	Area (m^2)	Thickness (mm)
Wooden board	0.2	7.66	18
Glass	0.9	1.50	6

4.4 Experimental setup

The experimental bedroom, the simulated outdoor environment, air plenum placed in Room A with a supply outlet, and a return air inlet to Room A formed the base of the experimental setup. An experimental bed with a mattress on it was placed inside the experimental bedroom, as shown in Fig. 4.1. When carrying out experiments, conditioned air was supplied from Room A to the experimental bedroom, and fresh air from the outside of the DX A/C station to the experimental bedroom.

A thermal manikin, consisting of 16 different body parts as shown in Table 4.2, was built and placed on the bed, to assemble a sleeping person. Electric resistance wires were used as heating elements and placed on the outer surface of the thermal manikin. Based on ASHRAE Standard 55, and a previous related experimental study [Lin and Deng 2008], heating flux values at different parts of the thermal manikin were determined, as shown also in Table 4.2, making a total heating power input of 52.02 W, which remained unchanged in all experiments. To simulate the exhale of CO_2 from the sleeping person to the experimental bedroom, a plastic pipe of 4 mm diameter was installed near the mouth of the thermal manikin. According to ASHRAE Standard [ASHRAE Standard 55-2013], a sleeping person gives out 0.17 L/min of CO_2. However, this flow rate was too small to easily lead to measurement error. Therefore, CO_2 flow rate was set at 1 L/min, since the study objective here was to compare the ventilation effectiveness at different experimental conditions.

Table 4.2 Details of the 16 body parts of the thermal manikin

Part No.	Part name	Areas (m2)	Heating flux (W/m2)	Heating power (W)
1	Head	0.084	43.57	3.66
2	Neck	0.033	16.97	0.56
3	Trunk	0.304	26.71	8.12
4	Left upper arm	0.064	37.97	2.43
5	Right upper arm	0.064	38.75	2.48
6	Left forearm	0.038	41.05	1.56
7	Right forearm	0.038	39.47	1.50
8	Left hand	0.019	24.21	0.46
9	Right hand	0.019	24.21	0.46
10	Left thigh	0.142	39.15	5.56
11	Right thigh	0.142	40.00	5.68
12	Left low leg	0.123	54.96	6.76
13	Right low leg	0.123	56.42	6.94
14	Left foot	0.026	35.00	0.91
15	Right foot	0.026	35.00	0.91
16	Pygal	0.114	35.35	4.03
Total	-	1.36	-	52.02

There were two system arrangements for the experimental setup: a FAC system arrangement and a ductless bed-based TAC system arrangement. For the former, the supply air outlet (0.57×0.21 m) was placed at 2.0 m above the floor level, and the return air inlet (0.37×0.16 m) at 0.32 m above the floor level, as shown in both Fig. 4.3 and Fig. 4.6. For the latter, there were two settings to study the system performances at different return air paths. In Setting 1, a supply air outlet was placed at 1.1 m above the floor level, and return air inlet at also 0.32 m above the floor level, as shown in both Fig. 4.4 and Fig. 4.7. In Setting 2, as shown in Fig. 4.5 and Fig. 4.8, the TAC system in Setting 1 was modified by adding a return air plenum with an inlet placed under the bed. In this programmed research work, a cuboid (1.84×0.92×0.6 m) immediately above the bed with mattress was designated as an occupied zone for the purpose of parameter measurements and results analysis, and the rest of the experimental bedroom as an unoccupied zone, as shown in Figs. 4.6 and 4.7.

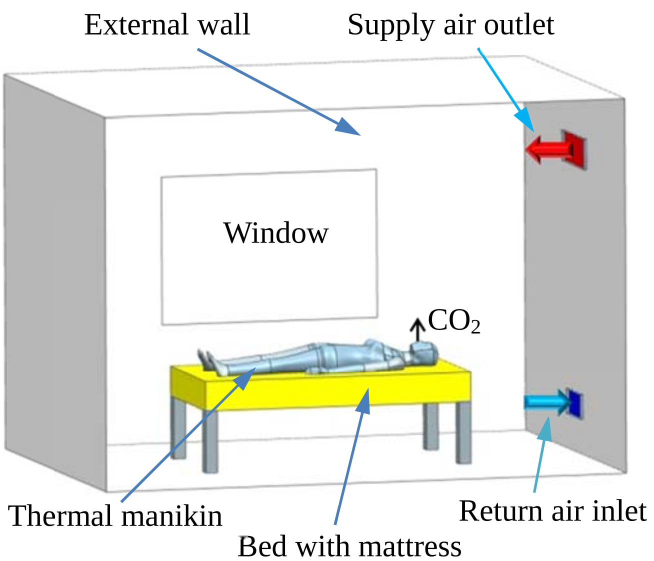

Fig. 4.3 Overview of the FAC system arrangement

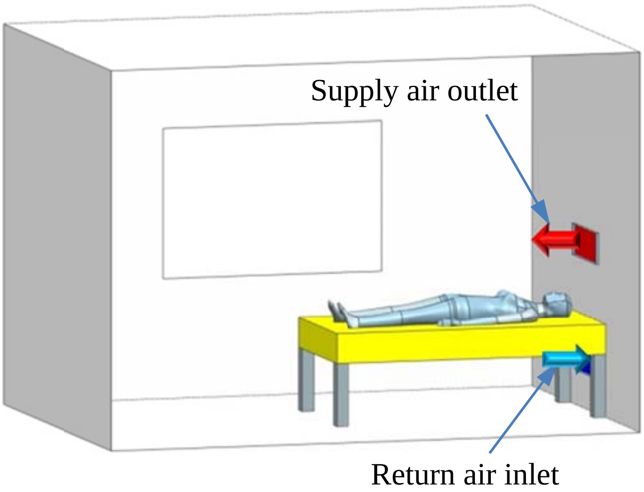

Fig. 4.4 Overview of the ductless bed-based TAC system arrangement (Setting 1)

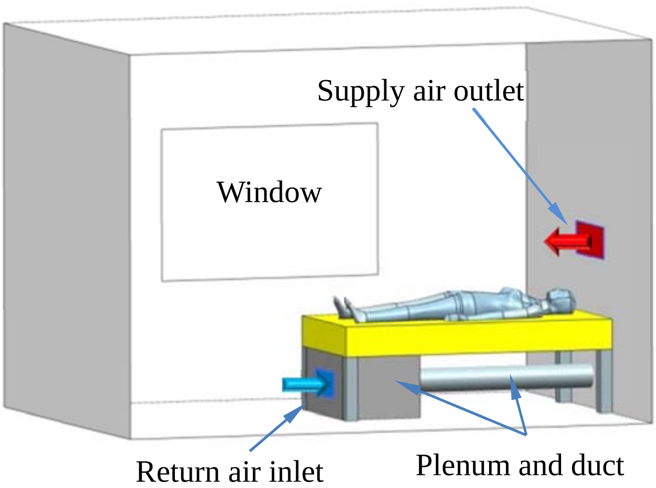

Fig. 4.5 Overview of the modified TAC system arrangement (Setting 2)

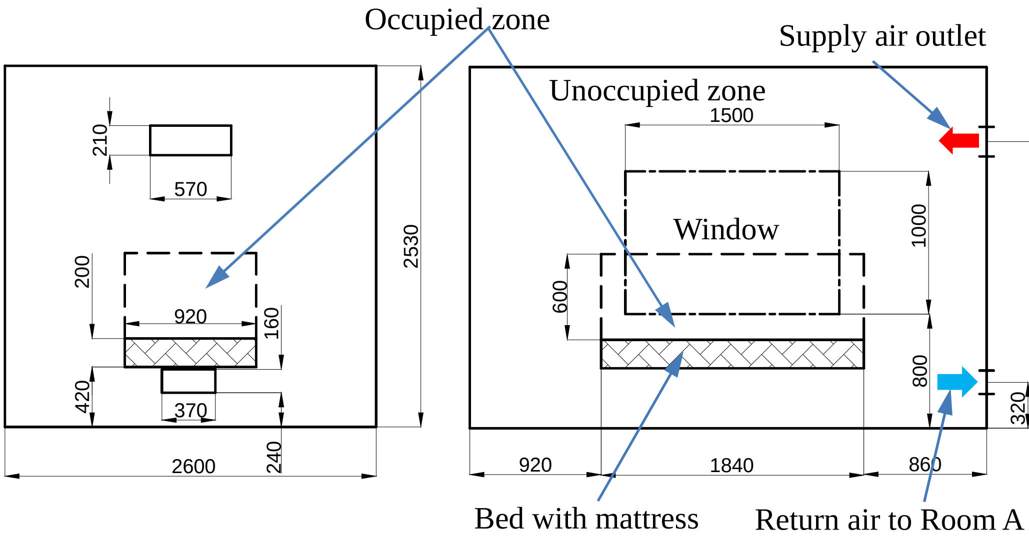

Fig. 4.6 Sectional views of the FAC system arrangement

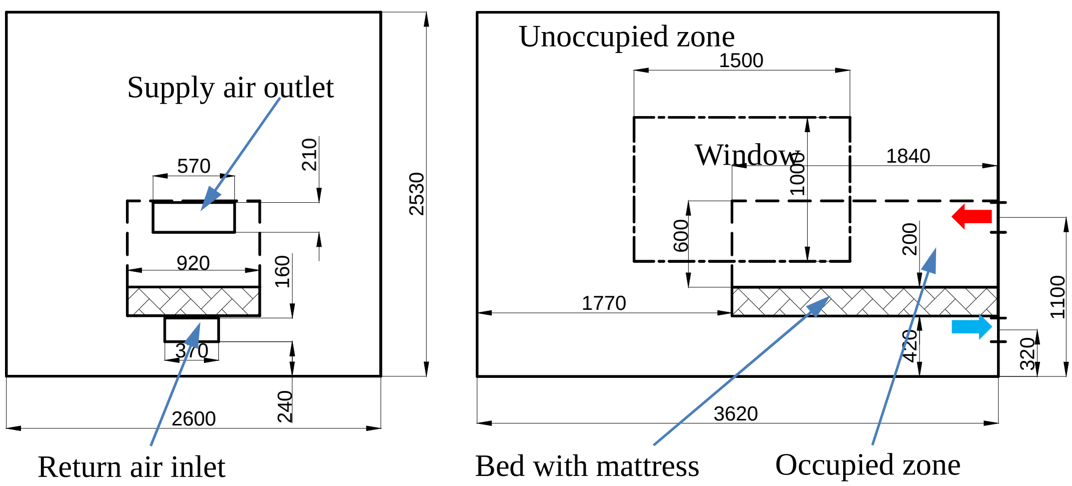

Fig. 4.7 Sectional views of the ductless bed-based TAC system arrangement (Setting 1)

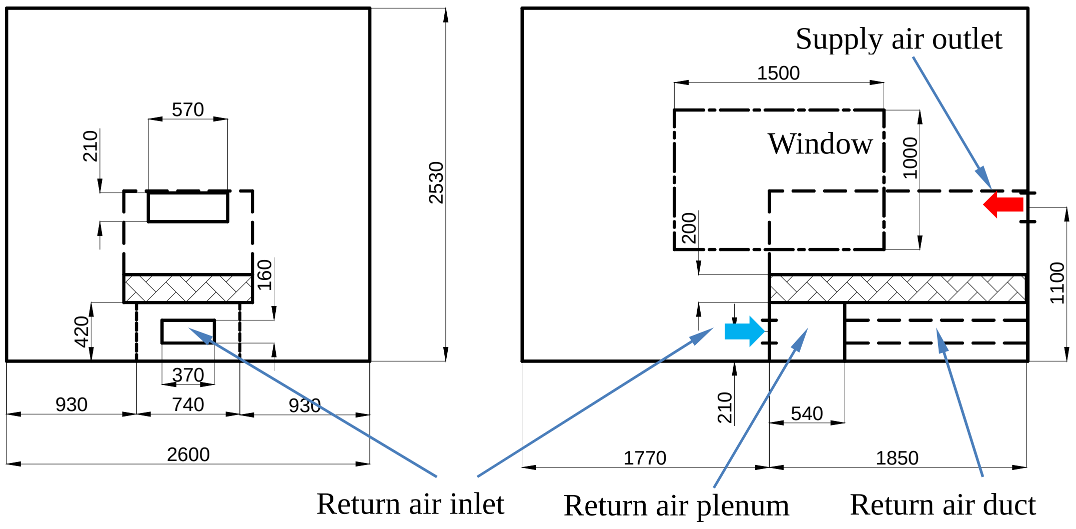

Fig. 4.8 Sectional views of the modified TAC system arrangement (Setting 2)

4.5 Measurement methods

4.5.1 Measurement positions

For the FAC system arrangement, eight measurement locations in the unoccupied zone and six in the occupied zone were identified, as shown in Fig. 4.9(a). However, for the TAC system arrangement, the measurement location, H, was removed, but all other locations were retained, as shown in Fig. 4.9(b). Inside the unoccupied zone, air dry-bulb temperature, wet-bulb temperature and air velocity were measured at four heights, 0.1 m, 0.6 m, 1.1 m and 1.7 m above floor level, at each of these locations [ISO Standard 7730]. The measured air temperatures in eight locations at the FAC system arrangement or seven locations at the TAC system arrangement, totally 32 or 28 measured values, were averaged to be the mean air temperature in the unoccupied zone, respectively. Inside the occupied zone, the above parameters and CO_2 concentration were measured at 0.8 m and 1.0 m above floor level in each of the six locations, totally 12 positions, as shown in Fig. 4.9. The measured air temperatures in the 12 positions in the occupied zone at both the FAC system arrangement and the TAC system arrangement were averaged to be the mean air temperature in the occupied zone, respectively. Furthermore, inside the occupied zone, air relative humidities at 0.8 m above floor level in each of the six locations were obtained based on the measured dry-bulb temperatures and wet-bulb temperatures there [ASHRAE Handbooks 2009]. They were averaged to obtain a mean value of relative humidity in the occupied zone.

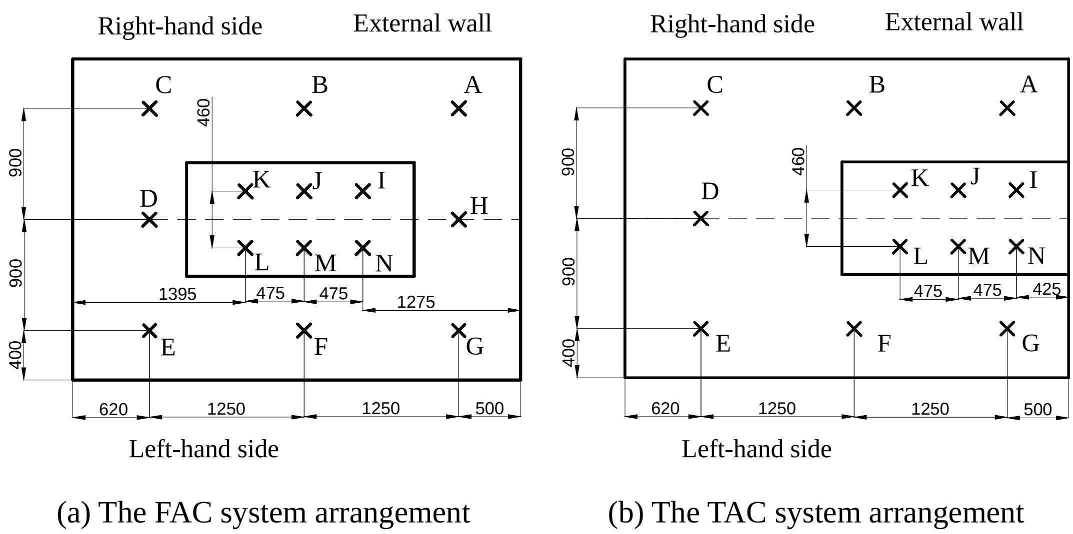

Fig. 4.9 Measurement locations inside the experimental bedroom at two system arrangements

4.5.2 Measuring instrumentation

Air temperatures were measured using K-type thermal couples, and air velocities an air velocity transducer having an accuracy of ±4% (0.05 to 0.5 m/s). The CO_2 flow rate was controlled and adjusted by an acrylic block flow meter with an accuracy of ±3% of full scale, and CO_2 concentrations were measured using a carbon dioxide monitor with an accuracy of ±5% of reading. The supply air flow rate was measured using a FlowHood and an Airdata Multimeter ADM-870 with an accuracy of ±3% of full scale. The power supply to the electrical heaters was measured by a Single-Phase Power Quality Analyser with an accuracy of ±1%.

4.6 Conclusions

An experimental setup was established in an existing experimental DX A/C station to facilitate carrying out all the experimental work involved in the programmed research work. There were two system arrangements, an FAC system arrangement and a TAC system arrangement. For the latter, there were two settings. An experimental bedroom was established as part of the setup, and an occupied zone and an unoccupied zone were designated. A thermal manikin was used to assemble a sleeping person.

The availability of such an experimental setup is expected to be extremely useful in investigating the operating performances of a TAC system installed in a bedroom in terms of thermal environment control, ventilation effectiveness and energy saving.

Numerical studies using CFD methods on indoor thermal environment and indoor air quality may thus be validated using the experimental data obtained, and the validated CFD methods can be used for further analysis of indoor thermal environment (air temperature and flow field) and indoor air quality.

Photos showing the experimental setup are in Appendix A.

Chapter 5

Thermal, ventilation and energy saving performance evaluations of a ductless bed-based TAC system

5.1 Introduction

Currently, air conditioning is used to provide people with thermally comfortable indoor environments not only in workplaces and other leisure places at daytime, but also in sleeping environments such as bedrooms in residential buildings, guest rooms in hotel buildings and hospital wards at night-time, as presented in Chapter 2.

In order to reduce energy use for building air conditioning, novel air conditioning systems including TAC systems have been developed. TAC systems used in workplaces in daytime have been investigated in a large number of previous studies and many benefits associated with using TAC systems revealed: enhancing thermal comfort, improving indoor air quality and reducing energy consumption, etc., as presented in Chapter 2. On the other hand, unlike daytime activities such as working in a workplace, sleeping is confined to a relatively small space and a sleeping person is naturally immobile. Therefore, TAC systems should be best applied to sleeping environments. Pan et al. [2012] carried out an experimental study on evaluating the thermal and energy saving performances of a novel bed-based TAC system installed in an experimental bedroom. The experimental results and related analysis demonstrated that the use of the novel bed-based TAC system can help achieve energy saving, compared with the use of a full volume air conditioning (FAC) system. However, there existed a number of noticeable inadequacies for the novel bed-based TAC system developed. Firstly, there were a bulky supply air plenum and flexible air ducts, as shown in Fig. 5.1, causing inconvenience to users. Secondly, the experimental bedroom was treated as having no envelope heat gain by assuming all heat gains coming from an internal source. However, the cooling load due to envelope heat gain may actually account for over 70% of the total space cooling load at nighttime [Lin and Deng 2004]. Thirdly, indoor air quality and humidity distribution profiles in the experimental bedroom when using the novel bed-based TAC system were not investigated. However, indoor air quality and humidity would also impact significantly the sleeping quality of a human being. Furthermore, a suitable indoor air humidity level is also important since this directly affects occupants' thermal comfort and indoor air quality.

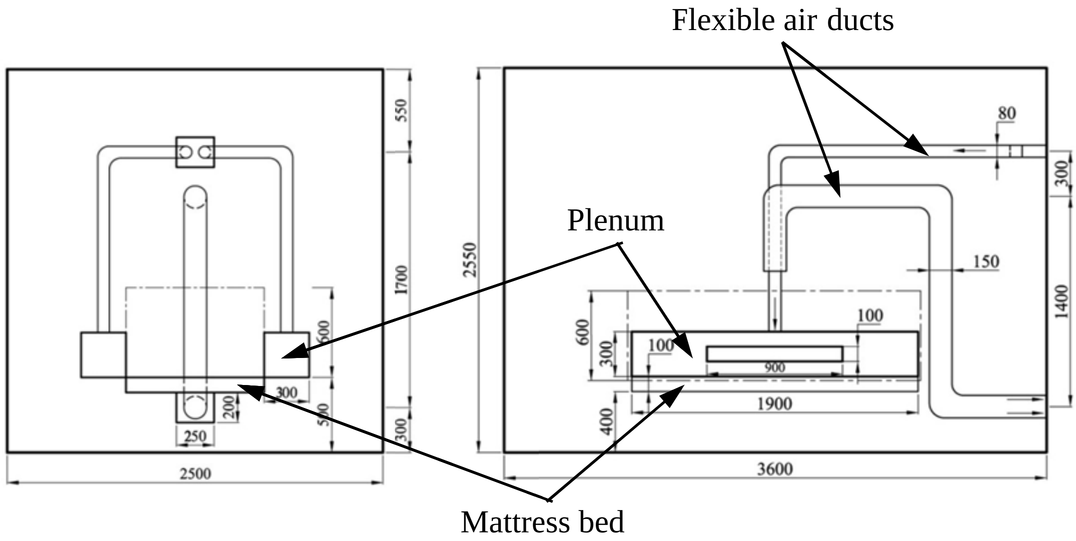

Fig. 5.1 Sectional view of the novel bed-based TAC system in a previous study [Pan et al. 2012]

To address the above-mentioned inadequacies [Pan et al. 2012], a number of modifications were therefore introduced as follows:

Firstly, a ductless bed-based TAC system arrangement was designed. It only consisted of a supply air outlet, a return air inlet and a bed with mattress, without flexible air ducts and the bulky supply plenums, as shown in Figs. 4.4 and 4.7 in Chapter 4. Therefore, a TAC system became more flexible for integration with the design of a bed and was more user friendly. Secondly, the envelope heat gain was considered. Two electrical heaters were used to generate a simulated envelope heat gain of 504 W, which was determined based on the area of the experimental bedroom

[Lin and Deng 2004], as shown in Fig. 4.2 in Chapter 4. Thirdly, indoor air quality and humidity distribution profiles were evaluated.

Therefore, the performances of the ductless bed-based TAC system arrangement in terms of thermal control, ventilation effectiveness and energy saving were experimentally evaluated, as the first part of the programmed research work, and are presented in this Chapter. The evaluation was based on the performance comparison between the ductless bed-based TAC system arrangement, as shown in Figs. 4.4 and 4.7 in Chapter 4, and an ordinary FAC system arrangement, as shown in Figs. 4.3 and 4.6 in Chapter 4. The experimental setup and measurement methods are respectively presented in Sections 4.4 and 4.5 in Chapter 4. In this Chapter, firstly, experimental conditions are reported. Secondly, the experimental results of performance evaluation are presented and analyzed. Finally, discussions on further improving the operational performance of the ductless bed-based TAC system arrangement are given.

5.2 Experimentation

5.2.1 Experimental setup and measurement methods

All experimental work reported in this Chapter was carried out using the experimental setup which is described in Sections 4.3 and 4.4, and is shown in Figs. 4.1 and 4.2 in Chapter 4. The measurement methods for the two system arrangements are also detailed in Section 4.5 in Chapter 4.

5.2.2 Experimental conditions

In the previous related experimental study on the novel-bed based TAC system [Pan et al. 2012] where no external envelope heat gain was present, a supply air temperature between 20 °C and 24 °C was used. However, in the current study, an envelope heat gain of 504 W was present, therefore, a lower supply air temperature between 17 °C and 23 °C was used. Consequently, the supply air flow rates were determined at 170 l/s, 140 l/s and 110 l/s at the FAC system arrangement, and at 110 l/s, 80 l/s and 50 l/s at the TAC system arrangement.

Table 5.1 summarizes various groups of experimental conditions. There were totally six experimental groups for different purposes. The purposes for Group 1 experiments were to compare thermal performance, ventilation and energy saving performances between the TAC system arrangement and the FAC system arrangement. In addition, the purposes of Groups 2 and 3 experiments were to investigate the effects of different supply air temperatures and supply air flow rates on draft risk at the TAC system arrangement. Moreover, in Group 4 experiments, the effects of different fresh air flow rates on ventilation performance at the TAC system arrangement were compared. In Group 5 experiments, the effects of different supply vane angles, as shown in Fig. 5.2, on draft risk and energy saving performance at the TAC system arrangement were compared. Finally, in Group 6 experiments, the effects of envelope heat gain on energy saving performance at the TAC system arrangement were also studied.

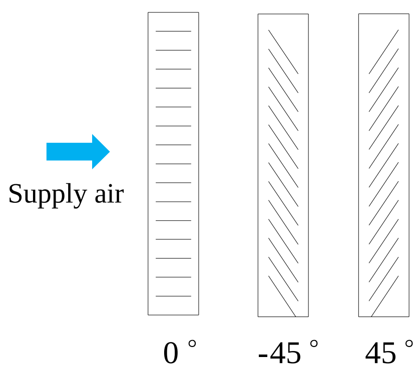

Fig. 5.2 Three different supply vane angles used

Table 5.1 Experimental conditions

Group	Series No.	Supply air temperature, t_s (°C)	Supply air flow rate, Q_s (L/s)		Fresh air flow rate, Q_f (L/s)	Supply vane angle (°)	Envelope heat gain (W)	Results shown in
			FAC	TAC				
1	1.1	19	110	110	6.5	0	504	Figs. 5.3, 5.6, 5.7, 5.9 and 5.10
	1.2	21	110	110	6.5	0	504	
2	2.1	19	-	50	6.5	0	504	Fig. 5.4
	2.2	21	-	50	6.5	0	504	
	2.3	23	-	50	6.5	0	504	
3	3.1	21	-	50	6.5	0	504	Fig. 5.5
	3.2	21	-	80	6.5	0	504	
	3.3	21	-	110	6.5	0	504	
4	4.1	19	-	80	6.5	0	504	Fig. 5.8
	4.2	19	-	80	15	0	504	
5	5.1	21	-	80	6.5	0	504	Figs. 5.11 and 5.12
	5.2	21	-	80	6.5	-45	504	
	5.3	21	-	80	6.5	+45	504	
6	6.1	19	-	80	6.5	0	504	-
	6.2	19	-	80	6.5	0	0	

5.3 Results analysis

In this Section, firstly, the measured thermal performances in the experimental bedroom at the two different system arrangements, which related to the thermal comfort of a sleeping person in terms of Draft Risk (DR) and Relative Humidity (RH) in the occupied zone will be presented. Secondly, the measured ventilation performance, in terms of ventilation effectiveness at the two system arrangements was compared and is presented. Furthermore, the measured energy saving performances in terms of cooling performance and Energy Utilization Coefficient (EUC) at the two system arrangements was compared and is reported. Finally, an improvement method of varying the supply vane angle was proposed to reduce the draft risk in the occupied zone at the TAC system arrangement.

5.3.1 Measured thermal performances

Two parameters, draft risk (DR) and relative humidity, were selected to assess the thermal performances, in the occupied zone, between using FAC and TAC.

5.3.1.1 Draft risk (DR)

Draft is an unwanted local cooling for a human body caused by air movement. Draft risk (DR) is a draft rating index used to predict the percentage of occupants feeling draft:

$$DR=(34-t)(v-0.05)^{0.62}(0.37vT_u+3.14) \tag{5.1}$$

(For $v \leq 0.05$ m/s, use v=0.05m/s; For DR>100%, use DR=100%) [ASHRAE Standard 55-2013, ISO Standard 7730]

Where T_u is the turbulence intensity, which can be estimated to be 40% for mixing ventilation systems, such as underfloor air distribution (UFAD) systems, and TAC systems. It is suggested that the value of DR in each measurement position should not be greater than a permissible value of 20% [ASHRAE Standard 55-2013].

The evaluated values of DR in each measurement position in the occupied zone at the two system arrangements are shown in Fig. 5.3. It can be seen that at the FAC system arrangement, the values of DR in all measurement positions were lower than 20%, while those at the TAC system arrangement in most of the measurement positions were higher than 20%. This indicated that using the ductless bed-based TAC system could lead to more serious draft risk than using the FAC system.

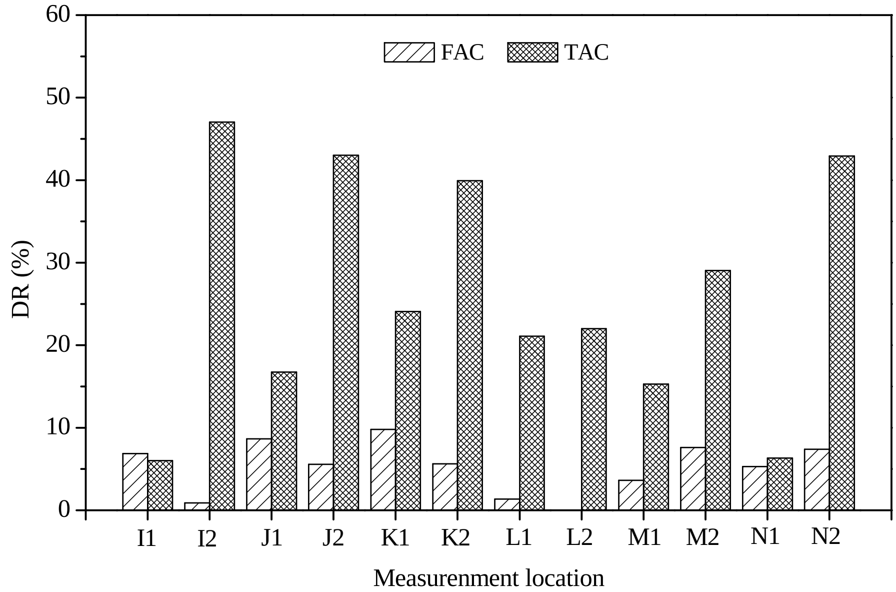

Fig. 5.3 Values of DR at each measurement position in the occupied zone at the two different system arrangements (t_s =21 °C, Q_s =110 l/s)

(I1 represents 0.8 m above the floor level, and I2 1.0 m, at measurement position I)

From the averaged DR values at different supply air temperatures and flow rates at the TAC system arrangement, shown in Figs. 5.4 and Fig. 5.5, respectively, it can be seen that the averaged values of DR decreased with an increase in supply air temperature or a decrease in supply air flow rate. It is therefore recommended that when using the ductless bed-based TAC system, much attention should be paid to selecting appropriate supply air temperature and flow rate to reduce the risk of draft.

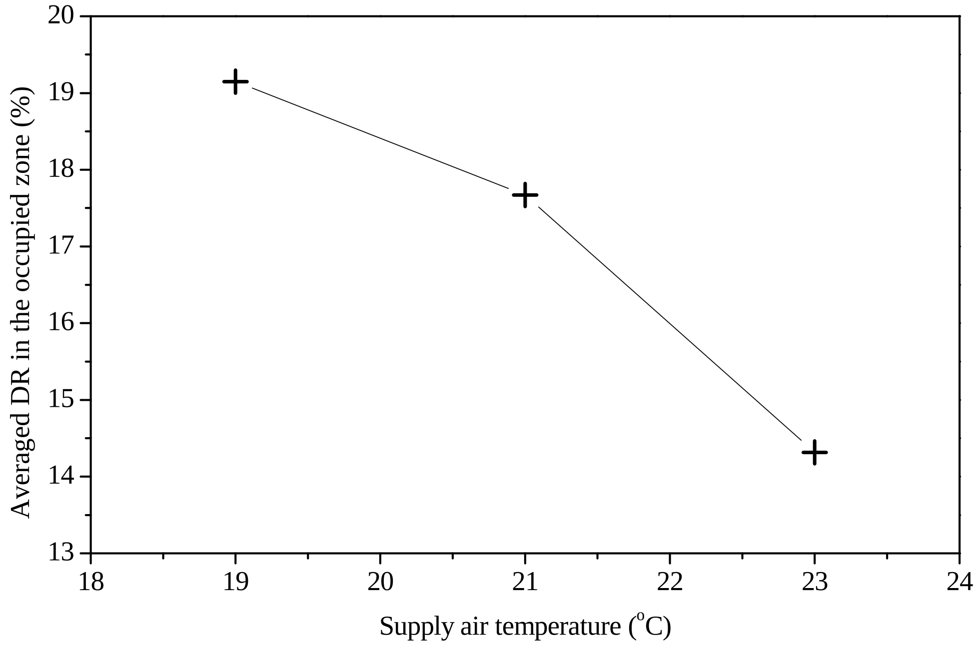

Fig. 5.4 Averaged DR values in the occupied zone at the TAC system arrangement, at different supply air temperatures (Q_s =50 l/s)

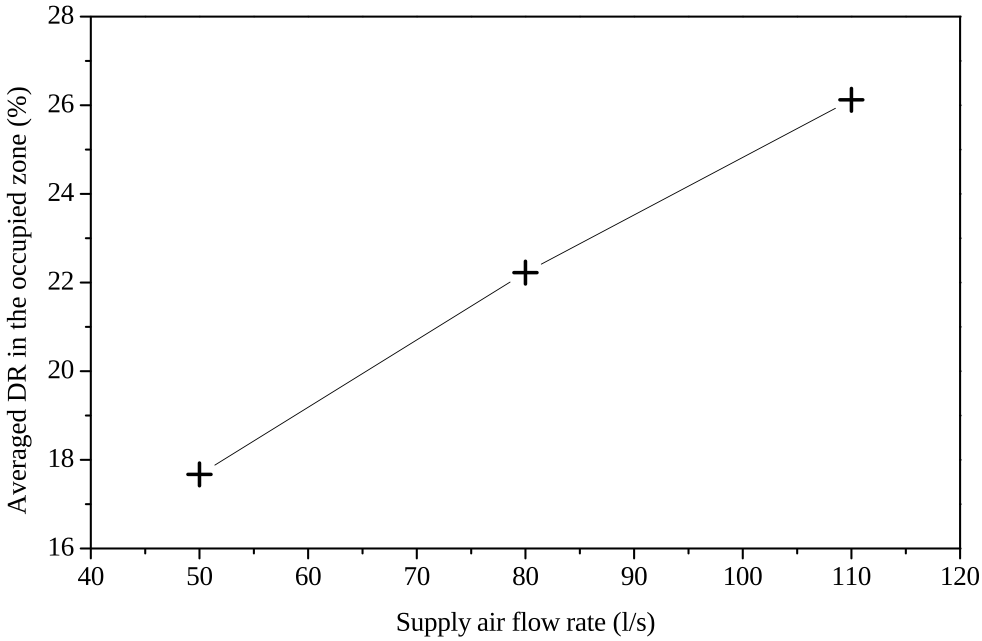

Fig. 5.5 Averaged DR values in the occupied zone at the TAC system arrangement, at different supply air flow rates (t_s =21 °C)

5.3.1.2 Relative humidity (RH)

ASHRAE Standard 55 recommends that the dew-point temperature of occupied spaces should not be less than 2 °C, which corresponds to a calculated lowest humidity ratio of 4.36 g/kg at the standard air pressure, and an upper humidity ratio limit of 12 g/kg, which corresponds to a dew point of 16.8 °C at the standard air pressure [ASHRAE Handbook 2009]. Based on these limits and the measured local dry-bulb temperatures, the lower and upper limits of RH value were calculated and are shown in Fig. 5.6. In this study, values of air relative humidity measured at 0.8 m above the floor level in the occupied zone at the two system arrangements, were averaged to be the mean RHs in the occupied zone, and are also shown in Fig. 9.

As seen, the mean values of RH at the two system arrangements were around 50%, within the recommended limits.

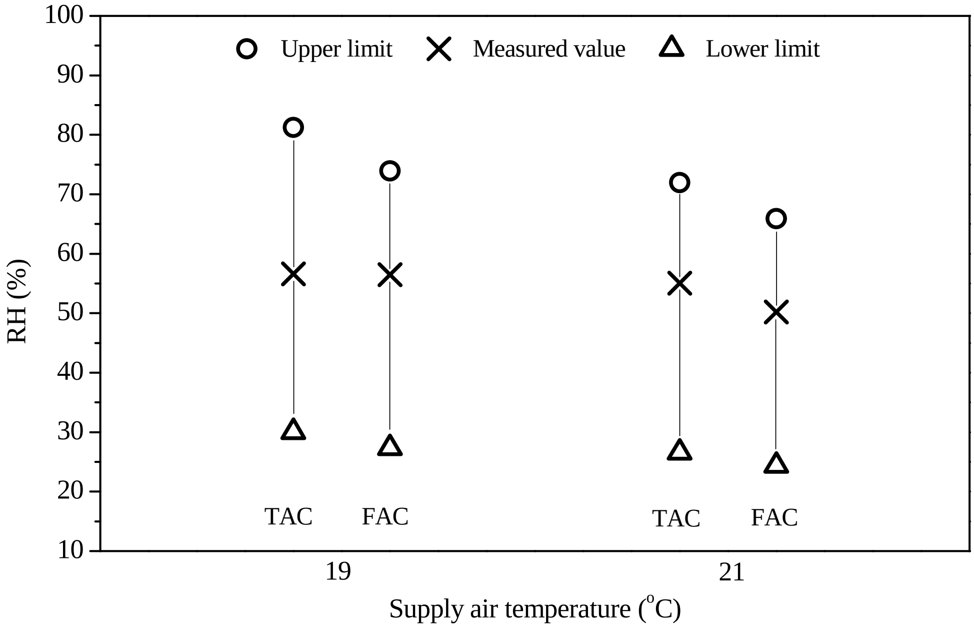

Fig. 5.6 Mean values of RH in the occupied zone at the two system arrangements, at two different supply air temperatures (Q_s=110 l/s)

5.3.2 Ventilation performance

In this study, the ventilation performances in the occupied zone at the two system arrangements were evaluated using ventilation effectiveness index, VE , as the breathing zone of a sleeping person was within the occupied zone:

$$VE=\frac{C_e\text{-}C_s}{C\text{-}C_s} \tag{5.2}$$

Where C_e is the CO_2 concentration in exhaust air, C_s the CO_2 concentration in supply air, and *C* the CO_2 concentration at a measurement position [Gan 1995]. Ventilation effectiveness index reflects the effectiveness of contaminant removal from an occupied zone. The higher the VE is, the better the ventilation performance.

Fig. 5.7 shows the comparisons of measured ventilation effectiveness at two different heights in the occupied zone, at the two system arrangements. It can be seen that the values of VE at the TAC system arrangement were higher than that at the FAC system arrangement. This demonstrated the use of the ductless bed-based TAC system would lead to a better removal of the CO_2 released from the thermal manikin, and result in better indoor air quality in the occupied zone.

Fig. 5.8 shows the measured ventilation effectiveness at two different heights in the occupied zone at TAC system arrangement at two different fresh air flow rates. As seen, all VE values were increased with an increase in fresh air flow rate. This suggested that a higher fresh air flow rate would result in a better ventilation performance when at the ductless bed-based TAC system arrangement.

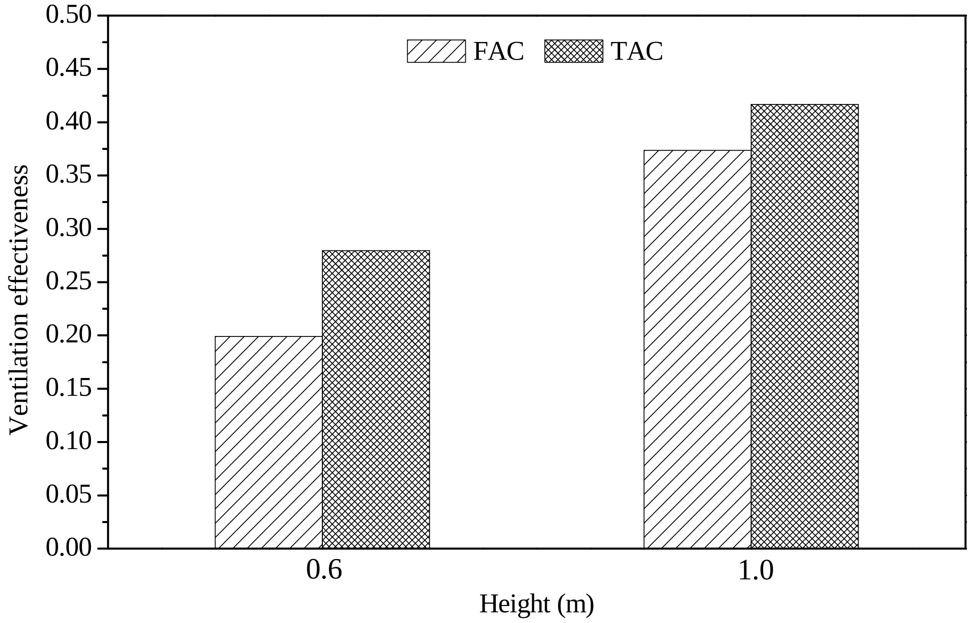

Fig. 5.7 Comparisons of ventilation effectiveness at two different heights in the occupied zone at two system arrangements (t_s =21 °C, Q_s =110 l/s, Q_f =6.5 l/s)

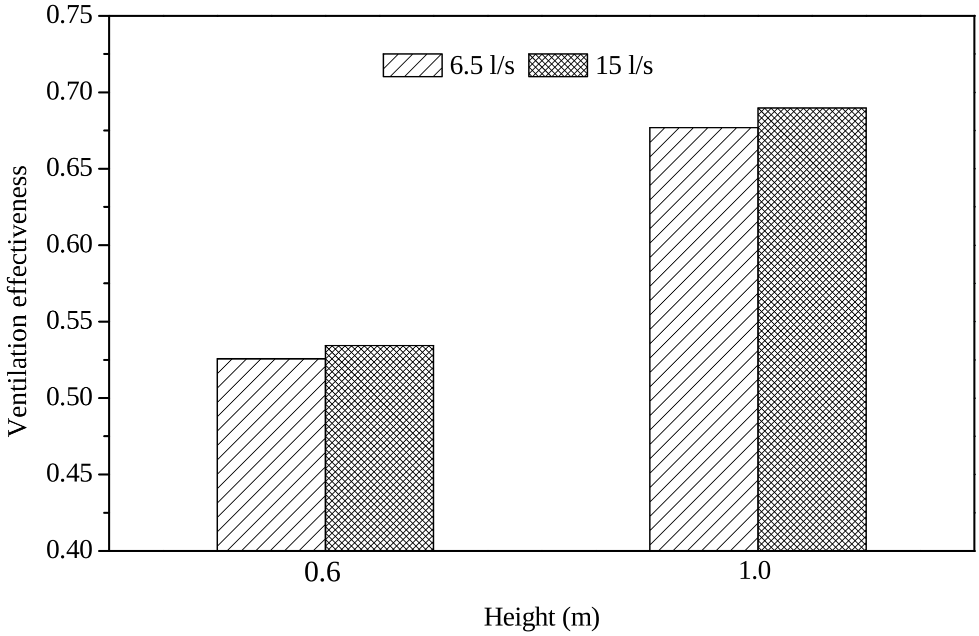

Fig. 5.8 Ventilation effectiveness at two different heights at the ductless bed-based TAC system arrangement at two different fresh air flow rates (t_s =19 °C, Q_s =80 l/s)

The measured thermal and ventilation performance presented above demonstrated that, (1) the use of the ductless bed-based TAC system could result in a higher draft risk than using the FAC system, although both at an acceptable relative humidity level in the occupied zone; (2) the use of the ductless bed-based TAC led to a higher ventilation effectiveness in the occupied zone.

5.3.3 Energy saving performance

In this study, energy saving performances at the two experimental were evaluated in terms of the cooling performance in the occupied zone and the energy utilization coefficient (EUC), and they are presented in this Section.

5.3.3.1 Cooling performance

Fig. 5.9 shows the comparisons of air temperatures in the occupied zone near three different parts of the manikin at the two system arrangements, with two different supply air temperatures. It can be seen that the air temperatures at the above three locations at the TAC system arrangement were 2 °C lower than those at the FAC system arrangement. A higher supply air temperature of 21 °C at the TAC system arrangement and a lower supply air temperature of 19 °C at the FAC system arrangement would result in a similar averaged air temperature in the occupied zone. In other words, similar cooling performances in the occupied zone were achieved at two different supply air temperatures. A higher supply air temperature at the same supply air flow rate meant a lower energy consumption for providing cooling.

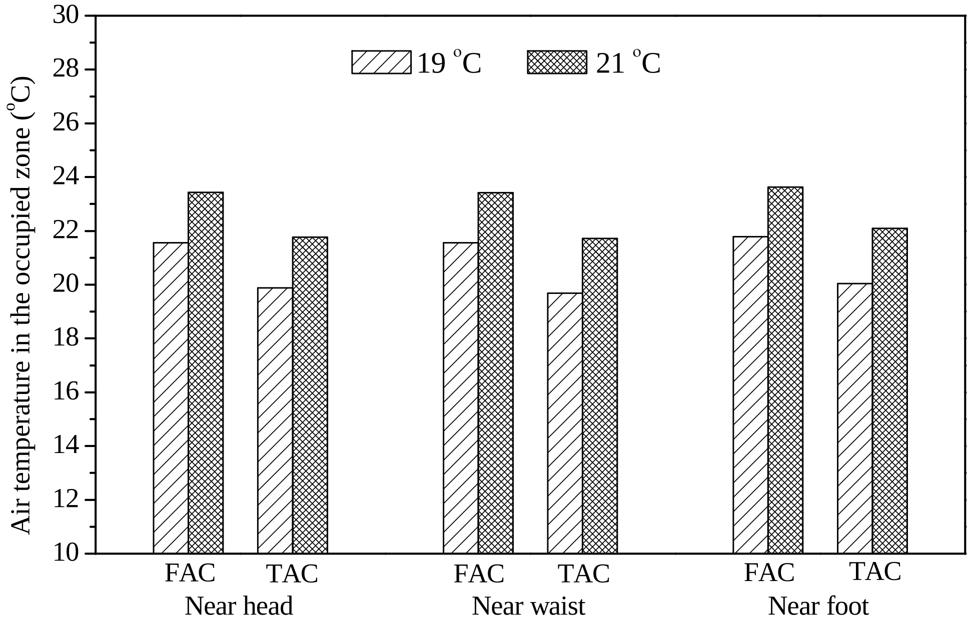

Fig. 5.9 Comparisons of air temperatures in the occupied zone at two experimental system arrangements (Q_s =110 l/s)

5.3.3.2 Energy utilization coefficient

The following modified equation [Liu et al. 2008] for energy utilization coefficient

(EUC) was used:

$$EUC = \frac{(t_{uz} - t_s)}{(t_{oz} - t_s)} \tag{5.3}$$

Where t_{uz} is the average air temperature in the unoccupied zone, t_s the supply air temperature, and t_{oz} the average air temperature in the occupied zone.

Equation (5.3) suggests that energy saving becomes possible if EUC is greater than 1, when the average air temperature in the unoccupied zone is greater than that in the occupied zone, as less cooling energy is used to cool the air in the unoccupied zone. The energy saving potential is expected to increase as the EUC value increases beyond 1. Therefore, at an FAC system arrangement, the resulted EUC should be close to 1. However, at a TAC system arrangement, the resulted EUC is expected to be greater than 1.

Fig. 5.10 shows the values of EUC at two different supply air temperatures of 19 °C and 21 °C but at the same supply air flow rate of 110 l/s at the two experimental system arrangements. The values of EUC at the TAC system arrangement were significantly higher than that at the FAC system arrangement. This was because when using the FAC system, conditioned air was supplied to the entire room, and there was no noticeable air temperature difference between the occupied zone and the unoccupied zone. Therefore, the use of FAC system consumed more energy by unnecessarily removing heat in the unoccupied zone. However, when using the ductless bed-based TAC system, conditioned air was supplied directly into the occupied zone, resulting in a large air temperature difference between the occupied zone and the unoccupied zone.

It was pointed out by a theoretical analysis in a previous related study [Pan et al. 2012] that the presence of the heat gain from an external wall would increase the values of EUC when using the novel bed-based TAC system. In the current study, the values of EUC when using the ductless TAC system, at two different envelope heat gain conditions (Case 6.1 at 504 W and Case 6.2 at 0 W), were evaluated. The results showed that the EUC value, which was evaluated at 1.93 with an envelope heat gain of 504 W, was higher than that without envelope heat gain, at 1.72. This demonstrated that when a bed-based TAC system was used in real buildings, a larger energy saving can be expected.

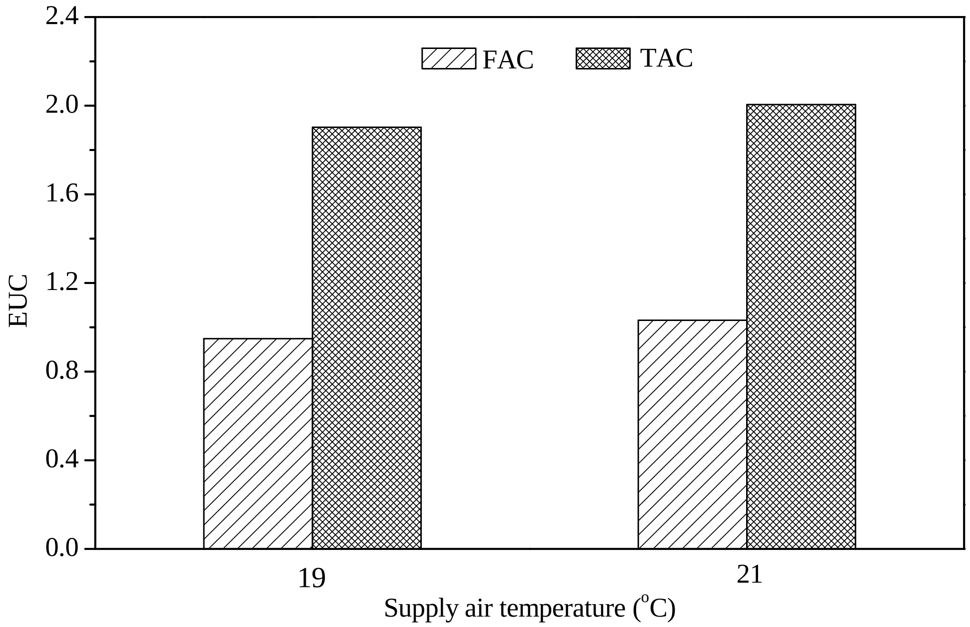

Fig. 5.10 Comparisons of EUC values at two experimental system arrangements

(Q_s=110 l/s)

5.3.4 Measures to improve the thermal performance at the TAC system arrangement

As presented in Sections 5.3.1-5.3.3, using the ductless bed-based TAC system would lead to better ventilation and energy saving performances, but a poor thermal performance in terms of a higher draft risk than using the FAC system.

To improve the thermal performance, it was possible to optimize the supply vane angles at the ductless bed-based TAC system arrangement. Fig. 5.11 shows that when varying the supply vane angles to either +45° or -45°, the averaged DR in the occupied zone could be reduced. A supply vane angle of +45° led to a lower value of averaged DR at 3.4%, which satisfied the recommended maximum level of DR (<20%) [ASHRAE Handbook 2009].

However, while varying the supply vane angle can help reduce draft risk at a supply vane angle of +45°, the value of EUC decreased to 1.09, as shown in Fig. 5.12. Therefore, a proper supply vane angle should be identified, so that while the value of DR can still meet their respective criteria, a higher EUC can also be attained.

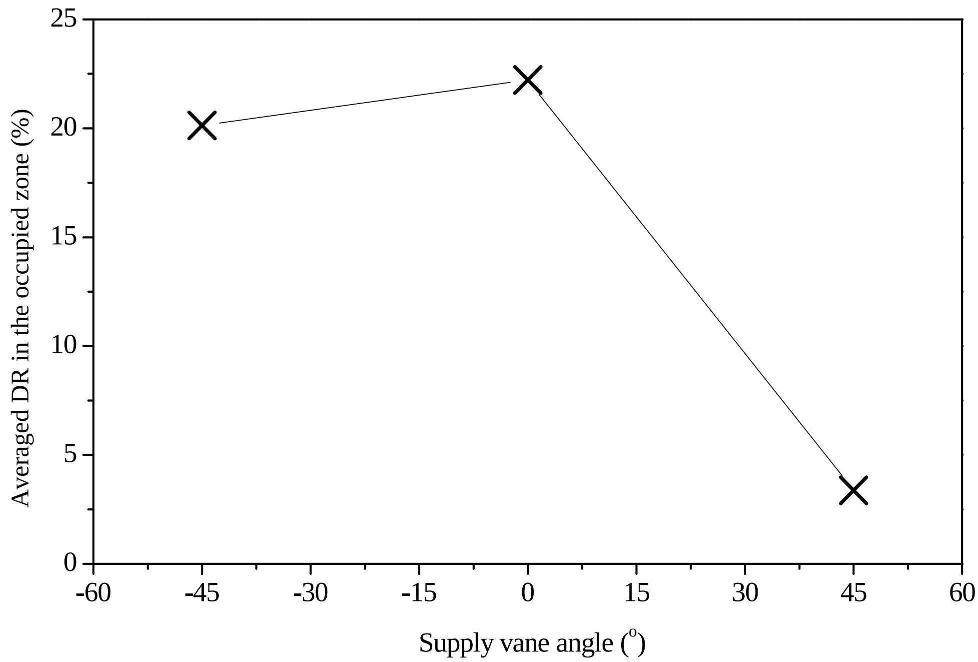

Fig. 5.11 Averaged DR in the occupied zone at the ductless bed-based TAC system arrangement, with different supply vane angles (t_s=21 °C, Q_s=80 l/s)

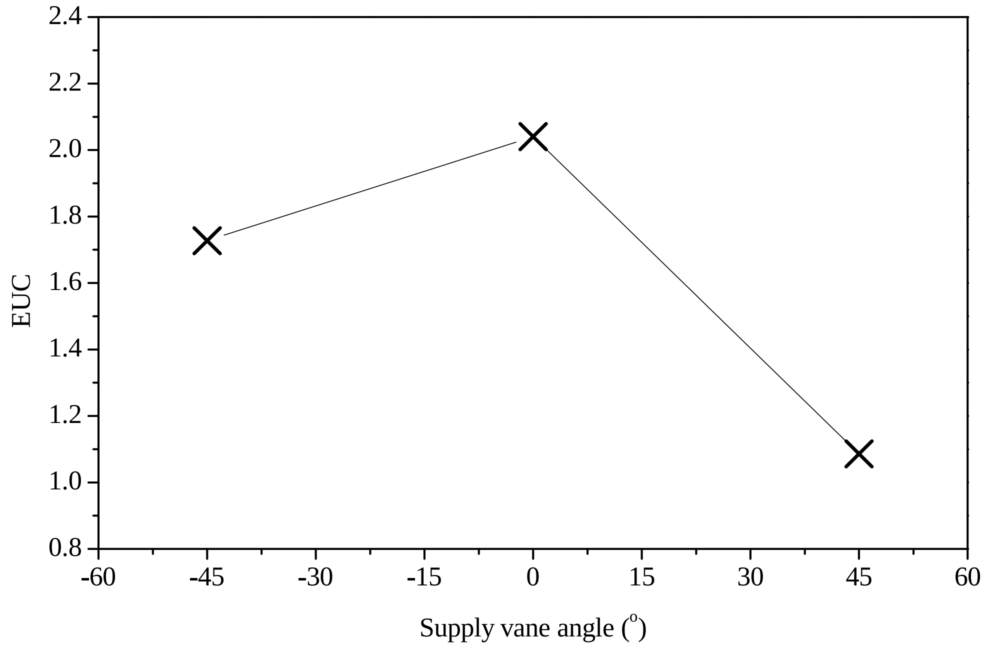

Fig. 5.12 Values of EUC at the ductless bed-based TAC system arrangement, with different supply vane angles (t_s=21 °C, Q_s=80 l/s)

The analysis of experimental error and uncertainty of the used indexes was presented in Appendix B. As seen, the experimental errors and uncertainties satisfied the requirement of analysis, and the analyses of experimental results were reliable.

5.4 Discussions

The first part of the programmed research work reported in this Chapter further developed the previous novel bed-based TAC system [Pan et al. 2012] through addressing its three noticeable inadequacies. Firstly, the ductless bed-based TAC system developed in the current study was more flexible to be integrated into the design of a bed and was more user friendly, because there were neither flexible air ducts nor bulky supply plenums. Secondly, the envelope heat gain was considered to assemble a more realistic real-life application. As compared to the previous study, the presence of envelope heat would actually lead to a larger EUC value. This suggested that a larger energy saving can be achieved when using a bed-based TAC system in real buildings. Thirdly, indoor air quality and humidity distribution profiles were evaluated in the current study, so that a more comprehensive coverage of the issues related to developing bed-based TAC systems was provided. It was demonstrated that, (1) the use of the ductless bed-based TAC system led to a better ventilation effectiveness than the use of a FAC system; (2) the relative humidity values in the occupied zone at the two experimental system arrangements were both at the acceptable level.

Based on the experimental results for the draft risk in the occupied zone when using the TAC system, it can be seen that a lower supply air flow rate or a higher supply air temperature can result in an acceptable draft risk. However, while varying the supply vane angle may also help lower draft risk, it would also lead to a lower EUC value. Therefore, a suitable supply vane angle should be identified, in order to strike a proper balance between achieving energy saving and reducing draft risk.

Consequently, follow-up work should be carried out to further develop the ductless bed-based TAC system, both experimentally and numerically using computational fluid dynamics (CFD) methods, and the study results will be reported in following chapters.

5.5 Conclusions

To address a number of inadequacies in a previous related study for a novel bed-based TAC system, a ductless bed-based TAC system has been developed and its thermal, ventilation and energy saving performances experimentally evaluated, by comparing them with those of a FAC system arrangement. In this Chapter, experimental setup and conditions, and measurement methods are firstly presented, and experimental results of performance evaluation secondly reported and analyzed. The experimental results demonstrated that using the ductless bed-based TAC system could lead to a better ventilation performance and energy saving performance, but a poorer thermal performance in terms of a higher draft risk than using the FAC system. It was shown that the air temperatures in the occupied zone at the TAC system arrangement were 2 °C lower than those at the FAC system arrangement under the same supply air condition. The values of EUC at the TAC system arrangement were nearly two times as much as that at FAC system arrangement. Furthermore, when using the ductless TAC system, with the presence of the envelope heat gain of 504 W, the EUC value was increased by 12%, when compared to the case without envelope heat gain. This suggested that when the ductless bed-based TAC system is applied to real buildings, a greater energy saving can be expected. To reduce the draft risk, when using the TAC system, while still maintaining an acceptable energy saving performance, it was possible to select a proper supply air temperature and air flow rate as well as a proper supply vane angle.

Chapter 6

Experimental and numerical studies on the performance evaluation of the ductless bed-based TAC system with two different return air inlets

6.1 Introduction

As presented in Chapter 5, using the ductless bed-based TAC system would lead to a higher draft risk in the occupied zone. Therefore, to further improve the performance of the TAC system through organizing different return air paths, two settings for the bed-based TAC system were designed and studied, as mentioned in Section 4.4 in Chapter 4. For Setting 1, the same TAC system as that in Chapter 5 was used. For Setting 2, the TAC system was modified by adding a return air plenum with an inlet placed under the bed, as shown in Figs. 4.5 and 4.8 in Chapter 4. Therefore, the performances of the ductless bed-based TAC system at the two different return air inlets settings were experimentally and numerically studied, as the second part of the programmed research work, and are presented in this Chapter. Firstly, the experimental conditions at the two settings are presented, and the experimental results on the operating performances of the bed-based TAC system at the two settings in terms of thermal environment control and energy saving are analyzed and reported. Secondly, to supplement the experimental study for a more detailed analysis on temperature and flow fields, a follow-up numerical study was carried out and is also reported. A CFD method for the experimental setup and experimental bedroom was developed and validated using the experimental data. Using the validated CFD method, the air flow and temperature fields in the experimental bedroom were obtained, which helped explain the differences in operating performances of the bed-based TAC system at the two settings.

6.2 Experimental study

6.2.1 Experimental setup and measurement methods

The experimental setup for the bed-based TAC system at the two settings are described in Section 4.4 and shown in Figs. 4.4, 4.5, 4.7 and 4.8 in Chapter 4. The measurement methods for the two settings are detailed in Section 4.5 in Chapter 4.

6.2.2 Experimental conditions

Table 6.1 summarizes various experimental conditions. There were totally five experimental groups for different purposes. The purposes for Group 1 experiments were to compare the effects of different supply air flow rates on draft risk at the two settings. In Group 2 experiments, the effects of different supply air temperatures on draft risk at the two settings were compared. In addition, the purposes of Groups 3 experiments were to investigate the draft risk in different measurement positions in the occupied zone at the two settings. Moreover, in Group 4 experiments, on one hand, the effects of different supply air flow rates on air diffusion performance were investigated at the two settings; on the other hand, the energy saving performance at the two settings were compared at different supply air flow rates. Finally, in Group 5 experiments, energy saving performances at the two settings were studied at different supply air temperatures.

Table 6.1 Experimental conditions

Group	Case No.	Supply air temperature, t_s (°C)	Supply air flow rate, Q_s (l/s)		Experimental results shown in
			Setting 1	Setting 2	
1	1.1	23	50	50	Fig. 6.1(a)
	1.2	23	80	80	
	1.3	23	110	110	
2	2.1	19	50	50	Fig. 6.1(b)
	2.2	21	50	50	
	2.3	23	50	50	
3	3.1	19	50	50	Fig. 6.2
	3.2	19	110	110	
4	4.1	19	50	50	Fig. 6.3 and Fig. 6.4(a)
	4.2	19	80	80	
	4.3	19	110	110	
5	5.1	19	110	80	Fig. 6.4(b)
	5.2	21	110	80	
	5.3	23	110	80	

6.3 Experimental results and analysis

The operating performances of the bed-based TAC system, in terms of thermal environment control and energy saving performance were experimentally evaluated at the two settings, and are reported in this section.

6.3.1 Thermal environmental control

Thermal environmental control performances for the bed-based TAC system were evaluated at the two settings, in terms of draft risk (DR) and air diffusion performance index (ADPI) in the occupied zone.

6.3.1.1 Draft risk (DR)

The thermal environmental control was evaluated using DR [ASHRAE Standard 55-2013], which is defined in Section 5.3.1.1 in Chapter 5.

The averaged DR values in the occupied zone were obtained by averaging the DR values at the 12 measurement positions at different supply air temperatures and supply air flow rates (Group 1 and Group 2 conditions) at the two settings, as shown in Fig. 6.1(a) and (b), respectively. It can be seen that the averaged DR values at Setting 2 were 4.0 % - 17.8 % lower than those at Setting 1. This indicated that using the bed-based TAC system at Setting 2 helped reduce draft risk. The averaged DR values at the two settings were both decreased with a decrease in supply air flow rate or an increase in supply air temperature, suggesting that draft feeling can be improved by increasing supply air temperature or reducing supply air flow rate.

To have a further detailed examination on draft risk, DR values at 12 positions in the occupied zone at the two settings are depictured in Fig. 6.2, under Group 3 experimental condition. It is seen that DR values at Setting 2 were lower than those at Setting 1 at half of the measurement positions, but very close to those at Setting 1 at the other half positions. When the supply air flow rate was increased to 110 l/s, DR values at most positions became larger, as shown in Fig. 6.2(b). In Fig. 6.2(a), at Setting 1, DR values at measurement positions I1 and I2, J1 and J2, and K1 and K2, which were near the external wall, as shown in Fig. 4.9 in Chapter 4, were higher than those away from the external wall. However, at Setting 2, DR values were close to one another. The difference in DR value at Setting 1 may well be due to the flow induced by the stronger convection from the external wall. This will be further explained in the numerical study.

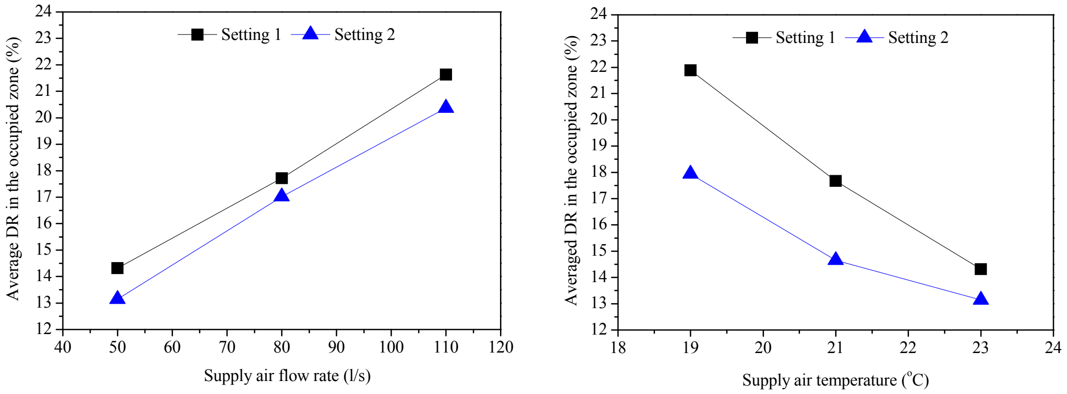

(a) At different supply air flow rates (t_s=23 °C)

(b) At different supply air temperatures (Q_s =50 l/s)

Fig. 6.1 Averaged DR values in the occupied zone at the two settings

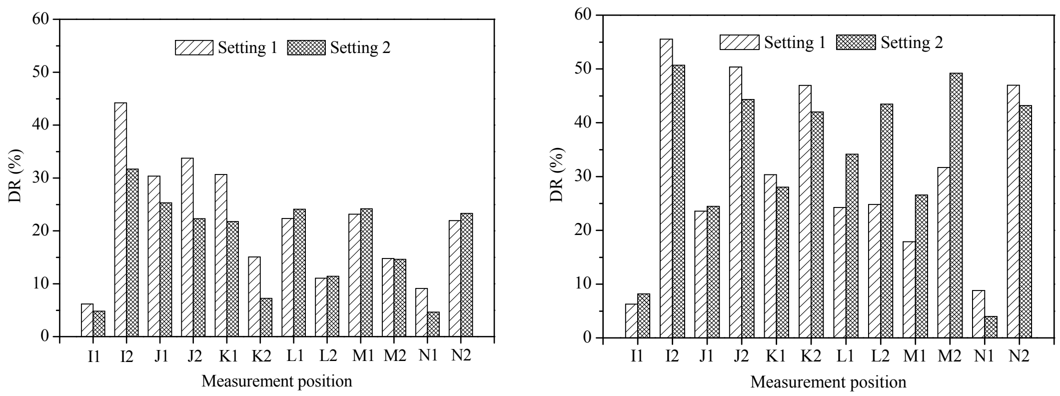

(a) t_s=19 °C, Q_s=50 l/s

(b) t_s=19 °C, Q_s=110 l/s

Fig. 6.2 Values of DR at each measurement position in the occupied zone at the two settings

(I1 represents 0.8 m above the floor level, and I2 1.0 m, at measurement location I)

6.3.1.2 Air diffusion performance index (ADPI)

ADPI [ASHRAE Standard 113-2013] has been used to evaluate the performances of air distribution and thermal environmental control in a specified zone at a given supply air flow rate, temperature and space cooling load. However, ADPI was initially proposed for evaluating the air diffusion performance in an entire air conditioned space. In this study, modifications were therefore introduced to make the index more suitable to assess the air diffusion in the occupied zone, as follows:

$$ADPI = \frac{\begin{array}{c}\textit{Number of measuring positions where the measured} \\ \textit{parameters meet the } \text{respective } \textit{criteria in the occupied zone}\end{array}}{\textit{Total number of measurement positions in the occupied zone}} \qquad (6.1)$$

In Equation (6.1), EDT (effective draft temperature, °C) and air velocity in the occupied zone were the designed parameters and their respective acceptable values of -1.7 °C <EDT< +1.1 °C and air velocity ≤ 0.35 m/s were taken as the criterion values, according to ASHRAE Standard 55-2013.

EDT was calculated according to the following equation:

$$EDT=(t-t_{oz})-8.0(v-0.15) \qquad (6.2)$$

Where t is the measured air temperature at a measurement position, t_{oz} the average air temperature in the occupied zone, and v air velocity at a measurement position.

Using Equation (6.2), EDT values in the occupied zone were evaluated. According to Equation (6.1), ADPI values at the two settings under different supply air flow rates were calculated and are shown in Fig. 6.3. It can be seen that an increase in supply air flow rate resulted in a significant decrease in ADPI values, or a poor air diffusion performance, except under the flow rate of 110 l/s at Setting 1. At Setting 2, ADPI values were obviously higher than those at Setting 1 under a lower supply air flow rate, i.e., 50 l/s and 80 l/s. However, when the supply air flow rate was increased to 110 l/s, the ADPI value at Setting 2 was lower than that at Setting 1. This was because the return air inlet at Setting 1 was placed below the supply air outlet, leading to a shortcut between supply air and return air at a lower supply air flow rate. However, when a larger supply air flow rate was used, the supply air could be delivered to the entire occupied zone. On the contrary, at Setting 2, when the supply air flow rate was increased to a high level, the supply air in the occupied zone was influenced by both the supply air outlet and the return air inlet, which led to a non-uniform thermal environment in the occupied zone and thus a poorer air diffusion performance.

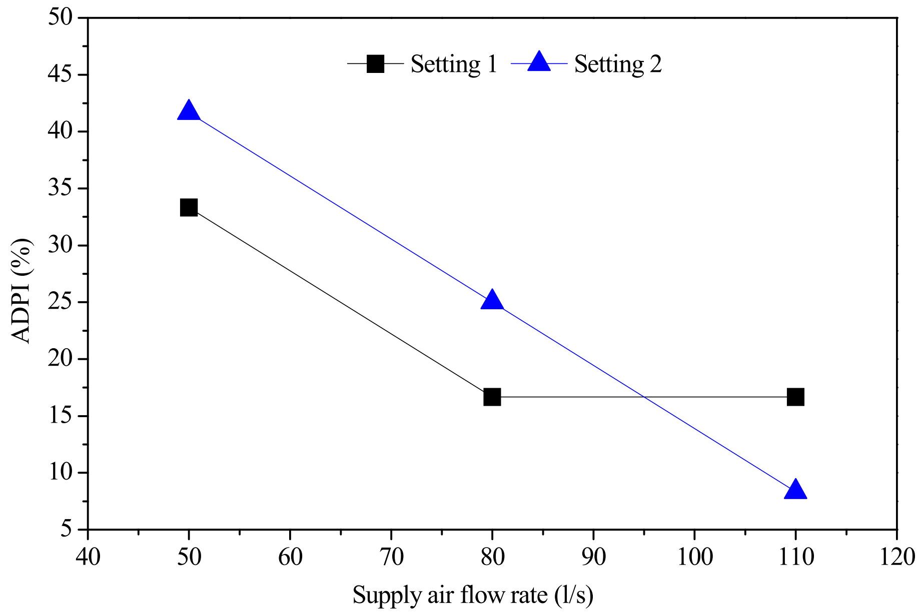

Fig. 6.3 Values of ADPI in the occupied zone at the two settings, under different supply air flow rates (t_s =19 °C)

6.3.2 Energy saving

Energy saving performance of the bed-based TAC system was evaluated at the two settings, in terms of the EUC, which is defined in Section 5.3.3.2 in Chapter 5.

Fig. 6.4 shows EUC values at three different supply air flow rates and three different supply air temperatures, respectively, at the two settings. EUC values at Setting 2 were 3.8 % - 7.8 % lower than those at Setting 1. As seen in Figs. 4.7 and 4.8 in Chapter 4, the conditioned air at Setting 2 was delivered to the occupied zone and forward flowed into return inlet, so that the flow distance and duration of the supply air staying in the occupied zone at Setting 2 were longer than those at Setting 1, resulting in more heat exchange between the conditioned air and the air in the unoccupied zone, and consequently a lower value of t_{uz}. Therefore, a poorer energy saving potential was resulted in at Setting 2 than at Setting 1.

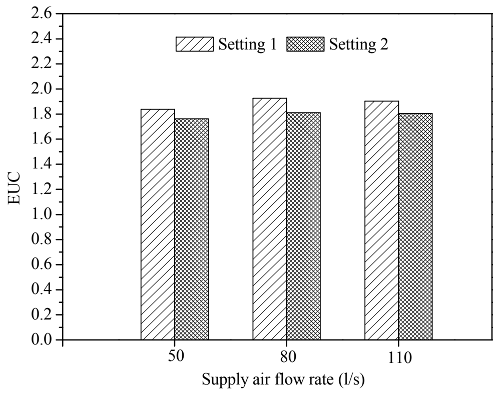

(a) at different supply air flow rates (t_s =19 °C)

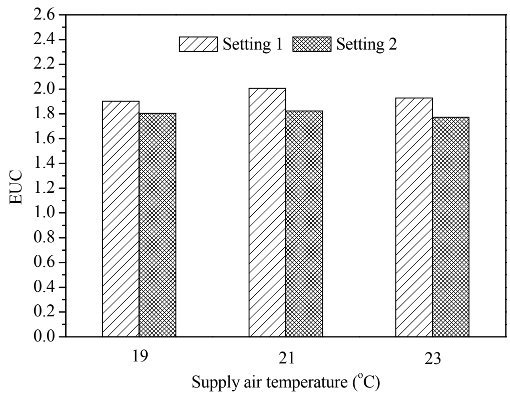

(b) at different supply air temperatures (Q_s=110 l/s)

Fig. 6.4 EUC values at the two settings

The analysis of experimental error and uncertainty of the used indexes was presented in Appendix B. As seen, the experimental errors and uncertainties satisfied the requirement of analysis, and the analyses of experimental results were reliable.

6.4 Numerical study

Although the operating performances of the bed-based TAC system in terms of thermal environment control and energy saving were experimentally evaluated and compared at the two settings, there were limitations as the operating parameters were only measured at limited numbers of measurement positions. Therefore, to supplement the experimental study for a more detailed analysis on the air temperature and flow fields inside the experimental bedroom, a follow-up numerical study was carried out. A CFD method for the experimental setup was developed and experimentally validated. Using the validated CFD method, the temperature and flow fields inside the experimental bedroom were predicted, which helped explain the differences in operating performance of the bed-based TAC system at the two different settings.

6.4.1 The CFD method

A commercial CFD code (Fluent) was used to solve the following steady state, viscous and 3D governing equations for the flow field inside the experimental bedroom. The governing equations are as follows:

Continuity equation:

$$\frac{\partial u_i}{\partial x_i} = 0 \tag{6.3}$$

Momentum equation:

$$u_j \frac{\partial u_i}{\partial x_j} = -\frac{1}{\rho}\frac{\partial P}{\partial x_i} + \nu \frac{\partial^2 u_i}{\partial x_j x_j} + \frac{1}{\rho}\frac{\partial}{\partial x_j}\left(-\rho \overline{u' u_j'}\right) - g_i \beta \Delta T \tag{6.4}$$

Where p is the static pressure, and $\overset{=}{\tau}$ the stress tensor.

Energy equation:

$$c_p u_j \frac{\partial T}{\partial x_j} = \frac{\lambda}{\rho}\frac{\partial^2 T}{\partial x_j x_j} + \frac{1}{\rho}\frac{\partial}{\partial x_j}\left(-\rho c_p \overline{u_j' \theta'}\right) + \frac{Q}{\rho} \tag{6.5}$$

When using CFD method, the mesh structure is very important for computational stability and results accuracy. For simulating airflow around complicated geometries, unstructured grids are more flexible in grid distribution and therefore often used. However, for simple geometries, structured grids can be easily generated with high mesh quality and a lower number of mesh elements. Therefore, grids were separately generated for the occupied zone and the unoccupied zone. The sectional views of the mesh for the computational domain including both the occupied and the unoccupied zones at the two settings are shown in Fig. 6.5. In the occupied zone, due to the complex geometry of thermal manikin surface, unstructured grids (tetrahedral meshes) were generated and prism mesh was used for the entire wall representing the manikin surface. The height of the first layer for prism mesh from the surface of thermal manikin was set at 0.4 mm, and 10 layers of prism mesh were generated in wall-normal direction to guarantee $y+<1$ and to provide a better computational result [ANSYS 2010], as shown in Fig. 6.6(b). In the unoccupied zone, structured grids were generated, as shown in Fig. 6.5.

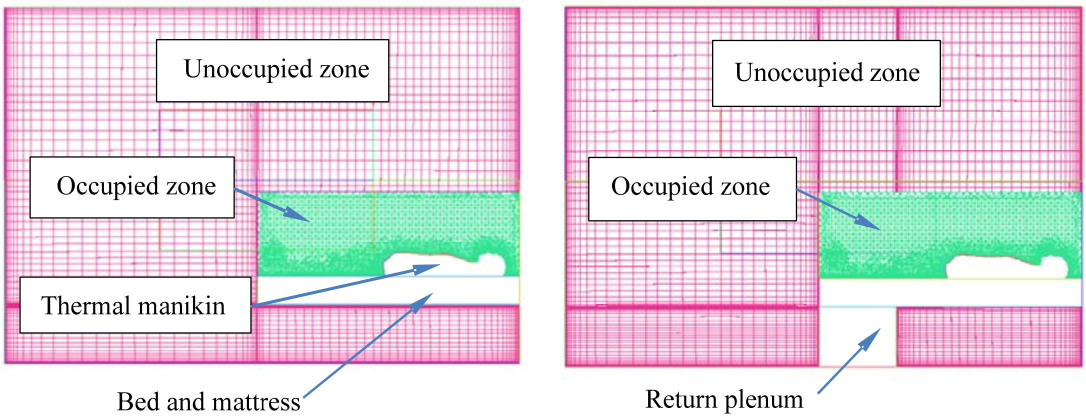

(a) Setting 1 (b) Setting 2

Fig. 6.5 Sections of computational domain mesh at the two settings

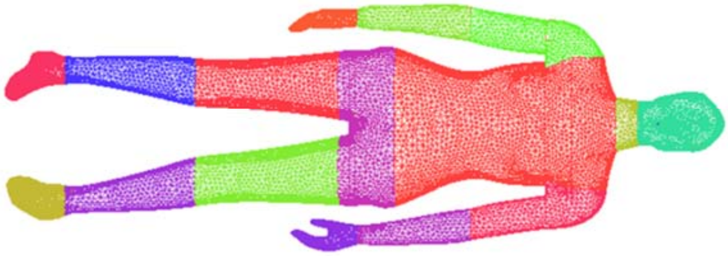

(a) Surface mesh of the thermal manikin

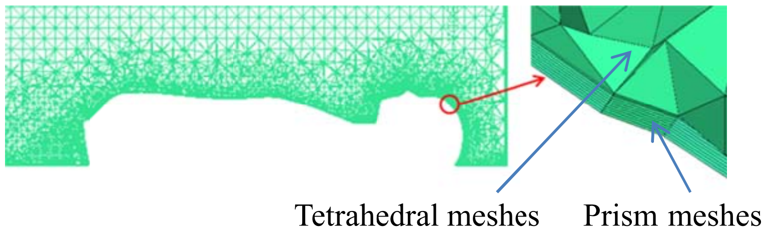

(b) Detailed mesh structure for the region near the thermal manikin

Fig. 6.6 Mesh details for the thermal manikin

The radiation heat exchange between any two surfaces depends partly on their sizes, separation distance and orientation. These parameters were calculated using a geometric function called "view factor" available in the CFD code. A surface-to-surface (S2S) radiation model was used to compute the radiation heat exchange between the surfaces in the experimental bedroom. In this radiation model, the surfaces were assumed to be gray, and the emissivities of each surface are shown in Table 6.2. Details of the surface-to-surface radiation model can be found in a previous related study [Raithby and Chui 1990].

The boundary conditions for the CFD method are summarized in Table 6.2, and the different study cases in Table 6.3. The purpose of carrying out Group 1 numerical study was for validating the CFD method and that for Group 2 to show the detailed air velocity and temperature fields inside the experimental bedroom, which helped explain the differences in the operating performances of the bed-based TAC system at the two different settings, identified in the experimental study reported in Sections 6.2 and 6.3.

Table 6.2 Boundary conditions

Boundary	Boundary conditions
Supply outlet	Air flow rate from 50 to 110 l/s, air temperature from 19 ºC to 23 ºC.
Return inlet	Pressure outlet.
Thermal manikin	16 body parts with fixed skin heat flux, emissivity: 0.07.
External wall	Fixed heat flux: 18W/m^2, emissivity: 0.1.
Window	Fixed heat flux: 20W/m^2, emissivity 0.94.
Bed	Adiabatic wall, emissivity of 0.77.
Floor	Adiabatic wall, emissivity of 0.2.
Other walls	Adiabatic wall, emissivity of 0.07.

Table 6.3 Numerical study conditions

Group	Case No.	Supply air temperature, t_s (°C)	Supply air flow rate, Q_s (l/s)		Numerical results shown in
			Setting 1	Setting 2	
1	1.1	23	80	-	Figs. 6.7 and 6.8
2	2.1	19	50	50	Figs. 10, 11 and 12
	2.2	19	110	110	

6.4.2 Validation of the CFD method

Because only the arrangements for the return air path at the two settings were not the same, the flow mechanisms of forced, natural and mixed convections inside the bedroom were similar, which created the same flow characteristics with impingement, separation, circulation, reattachment, vortices and buoyancy at the two settings [Zhai et al. 2007]. Furthermore, the heat transfer characteristics due to convection and radiation were also the same at the two settings [Zhai et al. 2007]. Therefore, following the validation procedures and criteria recommended in a previous study [Chen et al. 2002], the experimental validation of the CFD method was only performed for case 1.1 at Setting 1, by comparing air temperatures and velocities at four measurement locations: D, G, L and M, as shown in Fig. 6.7 and Fig. 6.8, respectively.

(1) Mesh sensitivity

Case 1.1 was simulated with different mesh sizes to guarantee the grid independence of the results. Fig. 6.7 shows the predicted temperature and velocity at four selected measurement locations for grid sizes with 1.6 million, 2 million and 2.4 million mesh elements. As seen, the obtained results were close to one another, with the maximum difference of 0.5 °C (about 3 %) and 0.04 m/s (about 10 %). Therefore, these results can be considered to be grid independent.

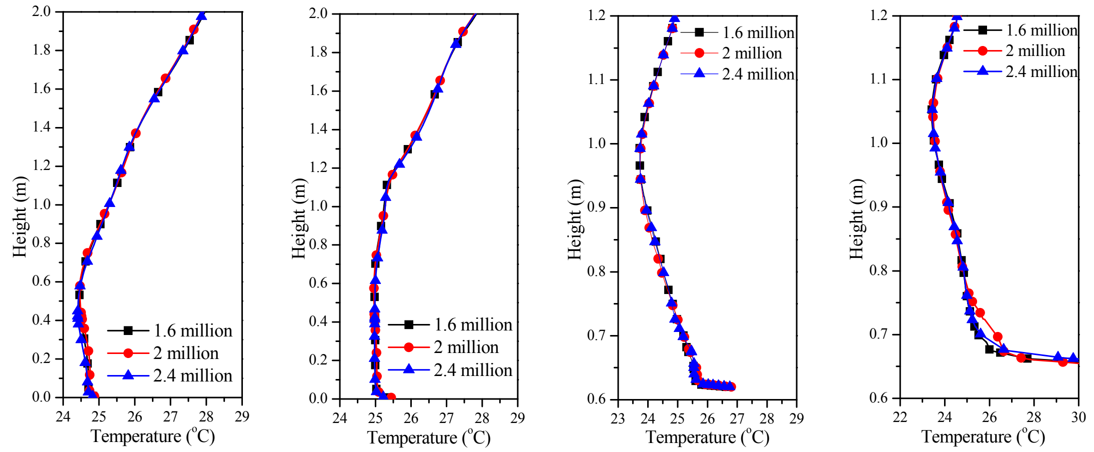

Location D Location G Location L Location M

(a) Temperature

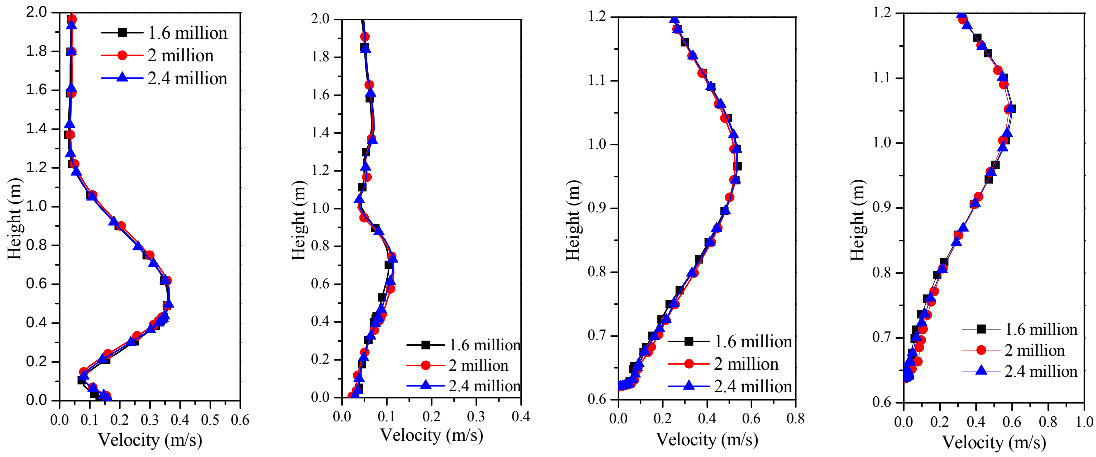

Location D Location G Location L Location M

(b) Velocity

Fig. 6.7 The air temperatures and velocities predicted using different number of mesh, at Setting 1

(2) Selection of turbulence model

The use of three different turbulence models: SST, Standard k-epsilon and RNG k-epsilon, was studied and the calculated air temperatures and velocities at four measurement locations were compared with the measured data. As shown in Fig. 6.8(a), the predicted air temperatures using SST model was the closest to experimental values. Fig. 6.8(b) shows, except for Location G, SST performed better for predicting air velocity profile. Therefore, SST performed the best in predicting air temperature and velocity profiles. The averaged absolute differences between the measured and the predicted temperatures using SST model were 0.01 °C in the unoccupied zone and 0.02 °C in the occupied zone, and those between the measured and the predicted velocities using SST model -0.03 m/s in the unoccupied zone and 0.09 m/s in the occupied zone, respectively. Furthermore, both the predicted and measured temperature and velocity demonstrated similar variation patterns, also shown in Fig. 6.8(a) and Fig. 6.8(b), respectively. Following the suggestions in a previous CFD study [Chen and Srebric 2002], it was considered that the CFD method developed was validated.

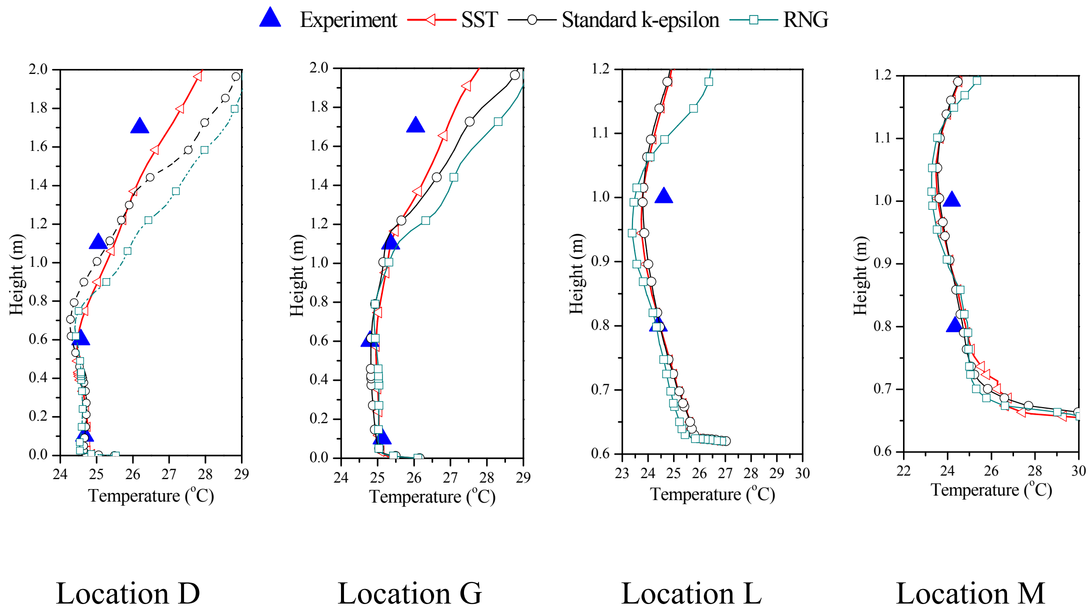

(a) Temperature

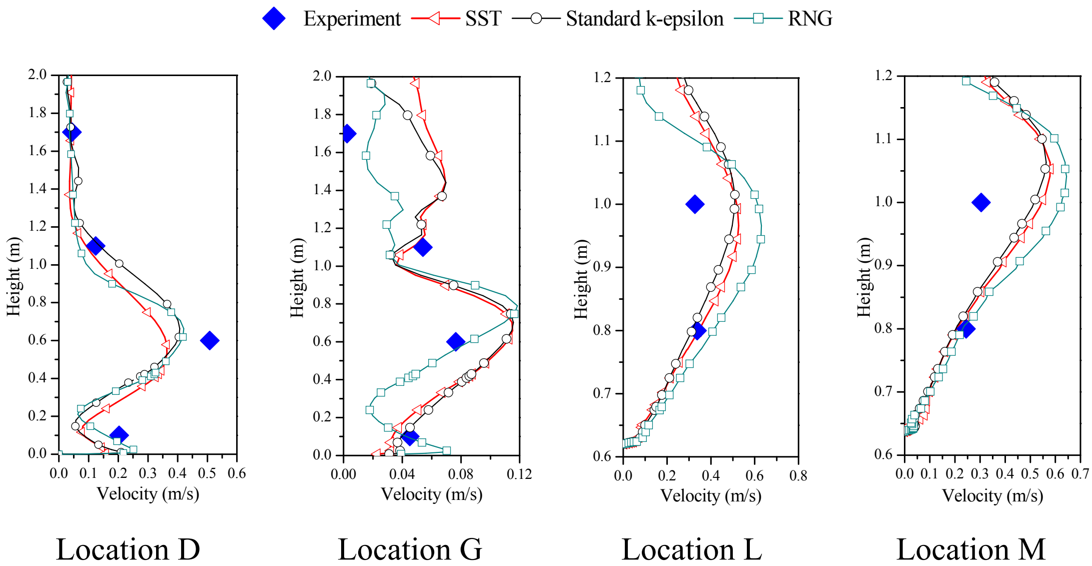

(b) Velocity

Fig. 6.8 The comparisons between predicted and measured data using different turbulence models, at Setting 1

6.5 Numerical results and analysis

Using the validated CFD method, detailed information on air velocity and temperature fields inside the experimental bedroom was made available, which helped explain the differences in the operating performances for the bed-based TAC system at the two settings. Two sectional planes inside the experimental bedroom, where the numerical results of air temperature and flow fields are illustrated in Fig. 6.9. Plane A is perpendicular to X-axis, placed at the middle of the width of the experimental bedroom, and Plane B perpendicular to Y-axis, placed at the middle of the bed.

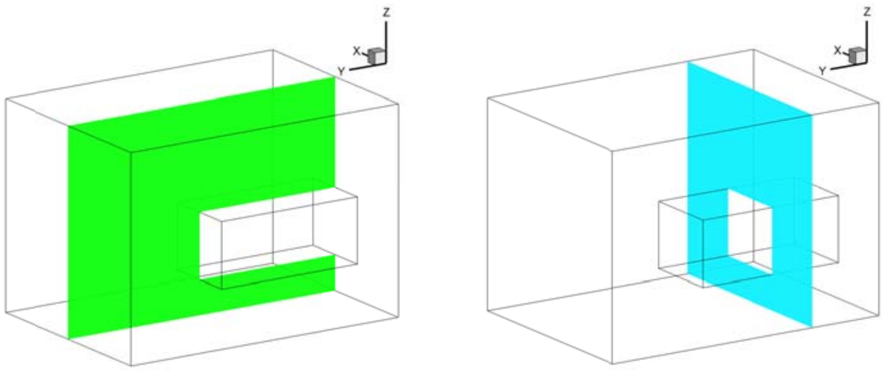

(a) Plane A (b) Plane B

Fig. 6.9 Two sectional planes for the experimental bedroom

Fig. 6.10 shows the air velocity field at Plane A at different supply air flow rates, at the two settings. As seen, an obvious stronger jet flow region above the thermal manikin at Setting 2 than that at Setting 1 was observed. This was because the return inlet at Setting 2 was placed away from the supply outlet which weakened the direct back flow to the return inlet. The stronger jet flow at Setting 2 resulted in more supply air delivered to the unoccupied zone, leading to lower EUC values. For Setting 1, the strength of jet flow was lowered and cooled air delivered closer to the thermal manikin, especially at a lower supply air flow rate, leading to a higher draft risk.

Fig. 6.11 shows the temperature fields at Plane B at different supply air flow rates, at the two settings. Fig. 6.11(a) illustrates a lower temperature region near the thermal manikin at Setting 1, caused by the cooled air directly delivered to this region. Unlike at Setting 1, air temperature near the thermal manikin at Setting 2 was much higher, as seen in Fig. 6.11(b). At a higher supply air flow rate, the jet flow resulted in a lower temperature region above the thermal manikin and an increase in air temperature near the thermal manikin. This indicated that much more cooled air was delivered to outside of the occupied zone at Setting 2, leading to a lower EUC value, and less cooled air near the thermal manikin leading to a higher temperature in this region.

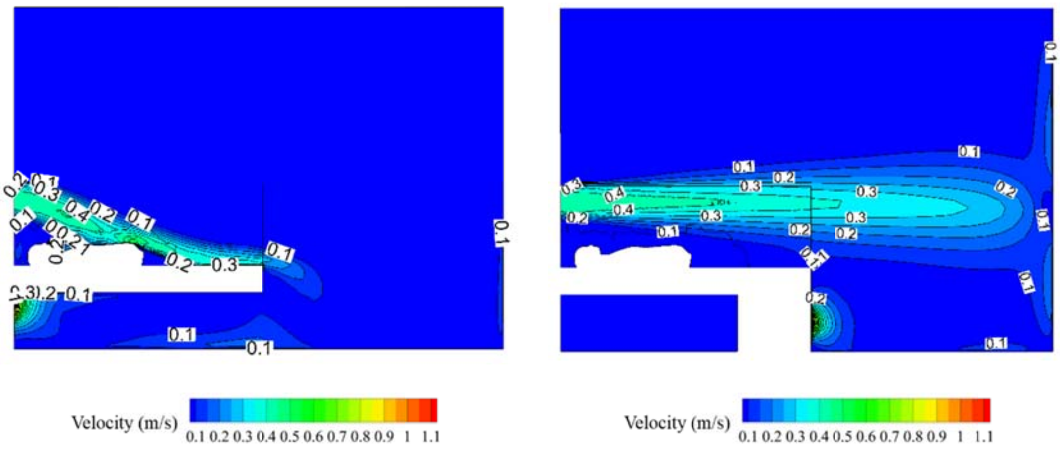

(a) Setting 1 (t_s=19 ºC, Q_s=50 l/s)

(b) Setting 2 (t_s=19 ºC, Q_s=50 l/s)

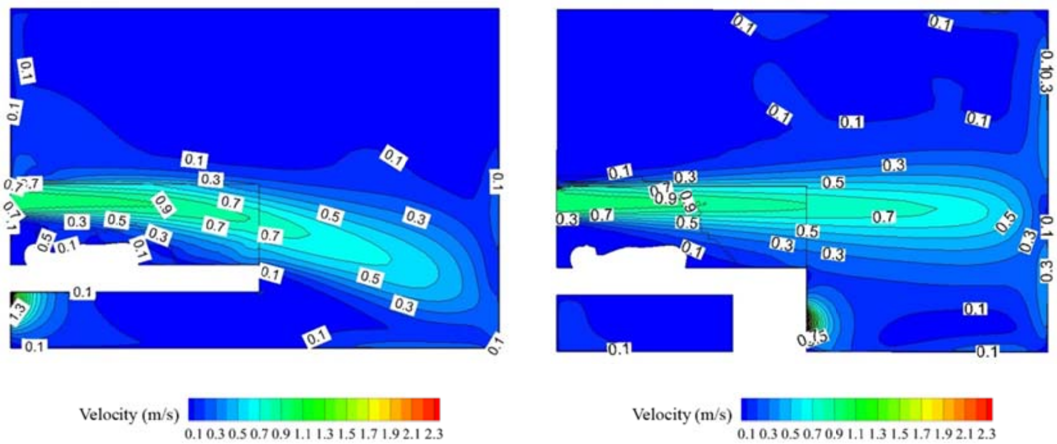

(c) Setting 1 (t_s=19 ºC, Q_s=110 l/s)

(d) Setting 2 (t_s=19 ºC, Q_s=110 l/s)

Fig. 6.10 Velocity fields at Plane A at different flow rates, at the two settings

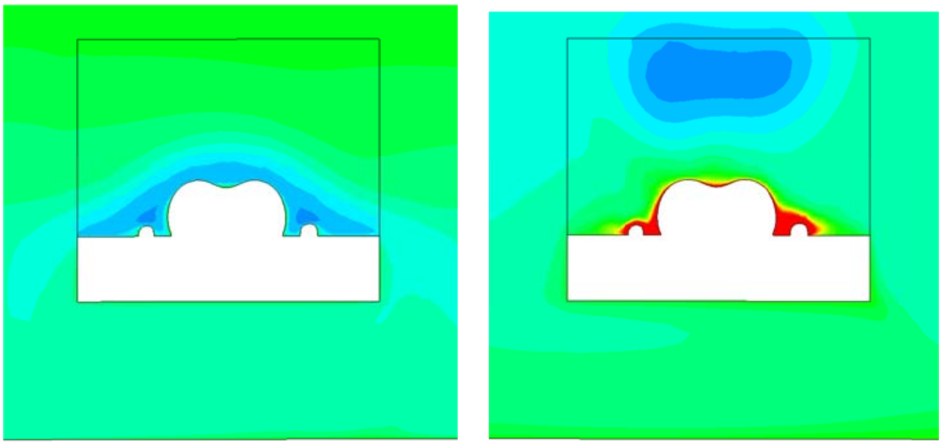

(a) Setting 1 (t_s=19 ºC, Q_s=50 l/s)   (b) Setting 2 (t_s=19 ºC, Q_s=50 l/s)

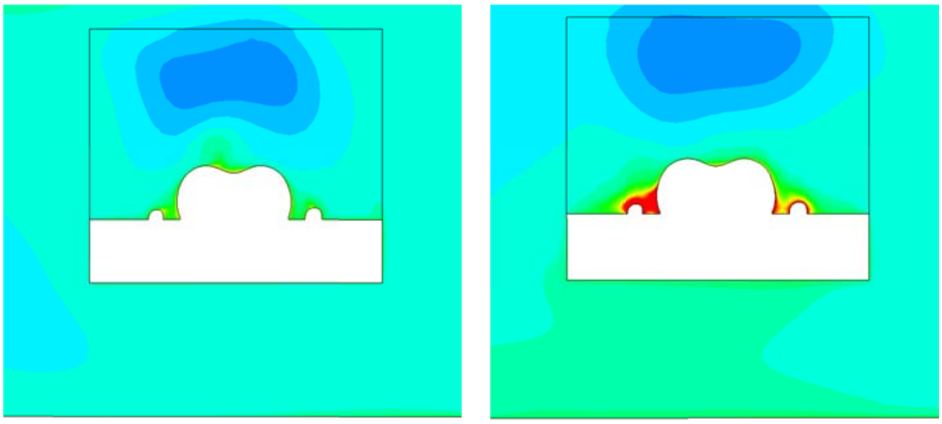

(c) Setting 1 (t_s=19 ºC, Q_s=110 l/s)   (d) Setting 2 (t_s=19 ºC, Q_s=110 l/s)

Fig. 6.11 Temperature fields at Plane B at different flow rates, at the two settings

Fig. 6.12 shows the velocity field and streamlines at Plane B at different air flow rates, at the two settings. When the supply air flow rate was low, the air in the lower temperature region flowed out of the occupied zone at Setting 1, which was caused by the extraction of return inlet. At Setting 2, however, air flowed from the unoccupied higher temperature zone into the occupied zone, as a result of the entrainment of jet flow. When the supply air flow rate was higher, entrainment occurred at both settings, causing high temperature air flowing into the occupied zone.

In addition, high temperature of the external wall resulted in a stronger convection and buoyancy flow region at Setting 1, which influenced the air flow on the right-hand side of the occupied zone, as shown in Fig. 6.12(a), noting that the right-hand side of the occupied zone was near the external wall, as shown in Fig. 4.9 in Chapter 4. This resulted in increased DR values on the right-hand side of the experimental bedroom. At Setting 2, the stronger jet flow extracted air from the unoccupied zone into the occupied zone, and weakened the effect on air flow of high temperature external wall. Therefore, the DR values shown in Fig. 6.12 at Setting 2 were more symmetric between the right-hand side and left-hand side in the experimental bedroom.

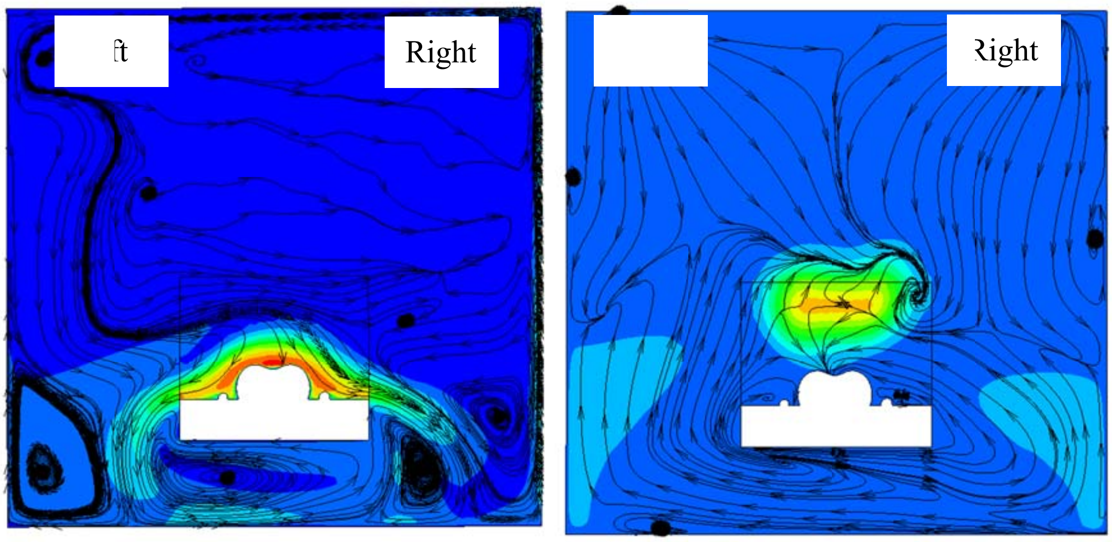

(a) Setting 1 (t_s=19 ºC, Q_s=50 l/s) (b) Setting 2 (t_s=19 ºC, Q_s=50 l/s)

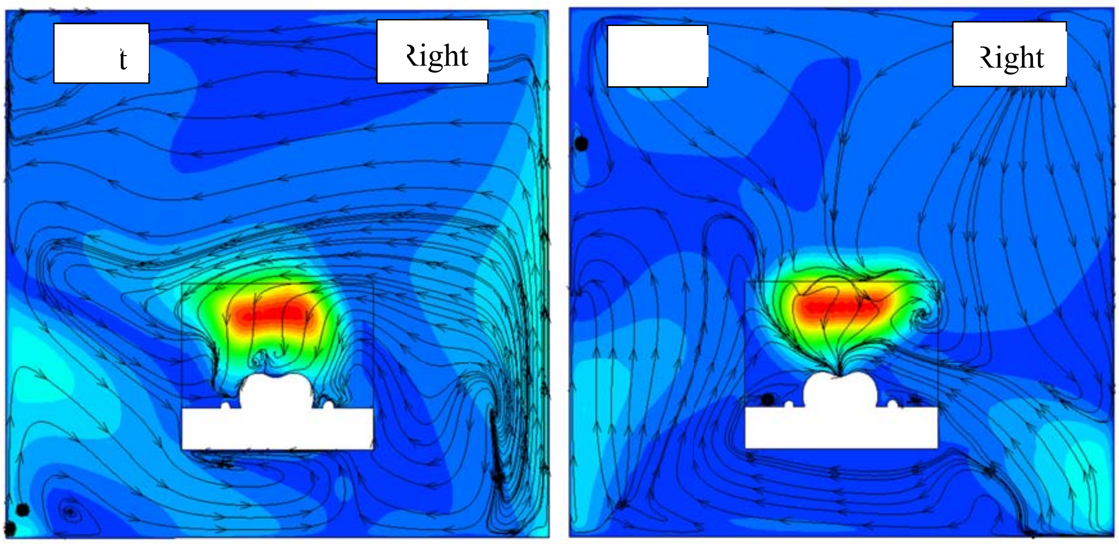

(c) Setting 1 (t_s=19 ºC, Q_s=110 l/s) (d) Setting 2 (t_s=19 ºC, Q_s=110 l/s)

Fig. 6.12 Velocity fields and streamlines at Plane B at different flow rates, at the two settings

From Figs. 6.10 to 6.12, the following observations that helped better explain the experimental results are as follows:

(1) Compared to at Setting 2, cooled air was delivered closer to thermal manikin at Setting 1, creating a lower temperature and higher velocity region near the thermal manikin, resulting in a higher DR value, as illustrated in Section 6.3.1.1. Furthermore, the stronger jet flow at Setting 2 weakened the effect of high temperature external wall on air flow, resulting in a more symmetric DR distribution in the experimental bedroom, as reported in Section 6.3.1.1.

(2) At a lower supply flow rate, an air flow shortcut reduced the diffusion effectiveness of cooled air in the occupied zone at Setting 1. When the supply air flow rate was increased to a high level, the effect of shortcut was decreased at Setting 1, and jet flow at Setting 2 became stronger, resulting in a better air diffusion performance at Setting 1 than at Setting 2, as stated in Section 6.3.1.2.

(3) The stronger jet flow at Setting 2 entrained the air from the unoccupied zone at a higher temperature, and at the same time, delivered more cooled air into the unoccupied zone. This reduced the temperature difference between the occupied

zone and unoccupied zone, resulting in lower EUC values, as presented in Section 6.3.2.

6.6 Conclusions

In this Chapter, the performances of the ductless bed-based TAC system at two different settings were experimentally and numerically evaluated in terms of thermal environmental control and energy saving.

The study results demonstrated that at Setting 2, 4.0 % to 17.8 % improvement in thermal environmental control performance due to a lower draft risk, but at 3.8 % to 7.8 % more energy consumption, were resulted in. Moreover, at Setting 2, the ductless bed-based TAC system performed better at lower supply air flow rates (50 and 80 l/s) with a better air diffusion performance. The detailed air flow field and temperature field inside the experimental bedroom predicted by the CFD method clearly illustrated the causes of the differences in operating performance of the ductless bed-based TAC system at the two settings in terms of DR, ADPI and EUC. Therefore, it was helpful to increase the thermal comfort level when using the ductless bed-based TAC system at the expense of saving less energy by placing a return air plenum with return air inlet under the bed, and such a design of TAC system is more applicable to the real life in a bedroom.

Chapter 7

Performance evaluation of an air conditioning system with different heights of supply outlet applied to a sleeping environment

7.1 Introduction

To address a number of inadequacies for a previous bed-based TAC system, the ductless bed-based TAC system was developed to make it applicable to a real bedroom, and its operating performances in terms of ventilation effectiveness, thermal environmental control and energy saving were investigated and are reported in Chapter 5. It was revealed that the TAC and FAC system arrangements have their own pros and cons with respect to ventilation, thermal control and energy saving performances, and for an A/C applied to a sleeping environment, the height of its supply outlet would significantly affect its operating performances. Hence, a follow-up study on the A/C system to obtain the best performances considering the above three aspects became necessary.

Therefore, a numerical study using CFD methods on evaluating the operating performances of an A/C system installed in the experimental bedroom with its supply outlet placed at five different heights has been carried out, as the third part of the programmed research work, and the study results are presented in this Chapter. The study was carried out in two steps: a numerical simulation using CFD method, and performance evaluations based on the CFD simulation results. Firstly, the detailed distributions of air flow, temperature and CO_2 concentration inside the bedroom were simulated using CFD, when the A/C system was operated at different supply air temperatures, flow rates and fresh air flow rates, with its supply outlet placed at five different heights. Secondly, based on the simulation results, three performance evaluation indexes, i.e., ventilation effectiveness (VE), thermal environmental control in terms of draft risk (DR) and energy saving in terms of Energy Utilization Coeffiecient (EUC), for the A/C system operated at different operating conditions, were obtained and analyzed. Finally, in view of the inadequacy of using separately each of the three performance evaluation indexes, an evaluation tool called TOPSIS (Technique for Order Preference by Similarity to an Ideal Solution) [Yoon and Hwang 1995] was employed to evaluate the overall performance of the A/C system at various operating conditions, through integrating the indexes for ventilation effectiveness, thermal environmental control and energy saving.

7.2 Methodology

The methodology used in this numerical study is shown in Fig. 7.1. As seen, there were two steps. In the first step, a CFD method for the A/C system and the experimental bedroom was firstly established and validated with experimental results. Then, the validated CFD method was used to numerically study air temperature, velocity and CO_2 concentration distributions inside the experimental bedroom when the A/C system was operated at different supply air conditions and with its supply outlet placed at five different heights. In the second step, based on the simulation results obtained in Step 1, the performance evaluations were carried out in two parts: performance evaluation for the A/C system using three separate indexes: ventilation effectiveness, thermal environmental control and energy saving, and an overall performance evaluation using the TOPSIS method.

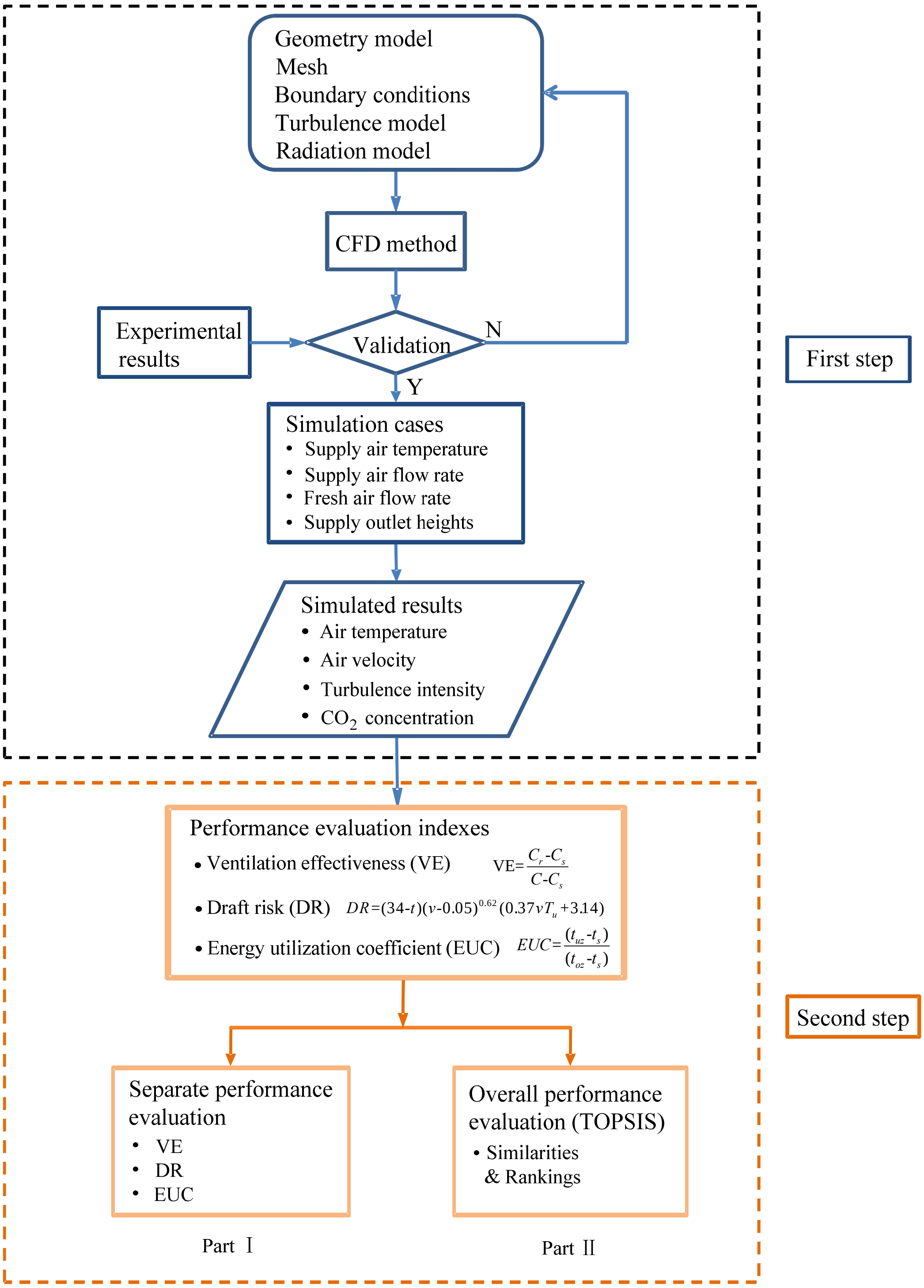

Fig. 7.1 Flow chart for the methodology used in the numerical study

7.2.1 Numerical study using CFD method

7.2.1.1 Geometry model

A geometry model was built for the experimental bedroom, shown in Fig. 4.3 in Chapter 4, with its dimensions shown in Fig. 7.2. As mentioned, the operating performances of an A/C system applied to a sleeping environment were significantly affected by the height of its supply outlet. Therefore, in this study, the height of supply outlet was set at five different levels: 800, 1100, 1400, 1700 and 2000 mm above the floor level, as also shown in Fig. 7.2, respectively. These five heights were designated as the following five system settings: H800, H1100, H1400, H1700 and H2000. The detailed information of the experimental bedroom, thermal manikin and instrumentation is presented in Chapter 4.

7.2.1.2 CFD method

A commercial CFD code [ANSYS 2010] was used to compute the air flow and heat transfer inside the experimental bedroom. The flow field was calculated by the three-dimensional and steady-state Reynolds averaged Navier-Stokes (RANS) equations, combined with continuity and energy equations. The boundary conditions for the CFD study are summarized in Table 6.2 in Chapter 6. The SIMPLE algorithm was used with a second order scheme for the convective terms. The SST turbulence model [Menter 1994], which took advantages of both k-ε model and k-ω model, was validated to have the best performance in predicting air temperature and velocity profiles inside the experimental bedroom, as reported in Section 6.4.2.2 in Chapter 6.

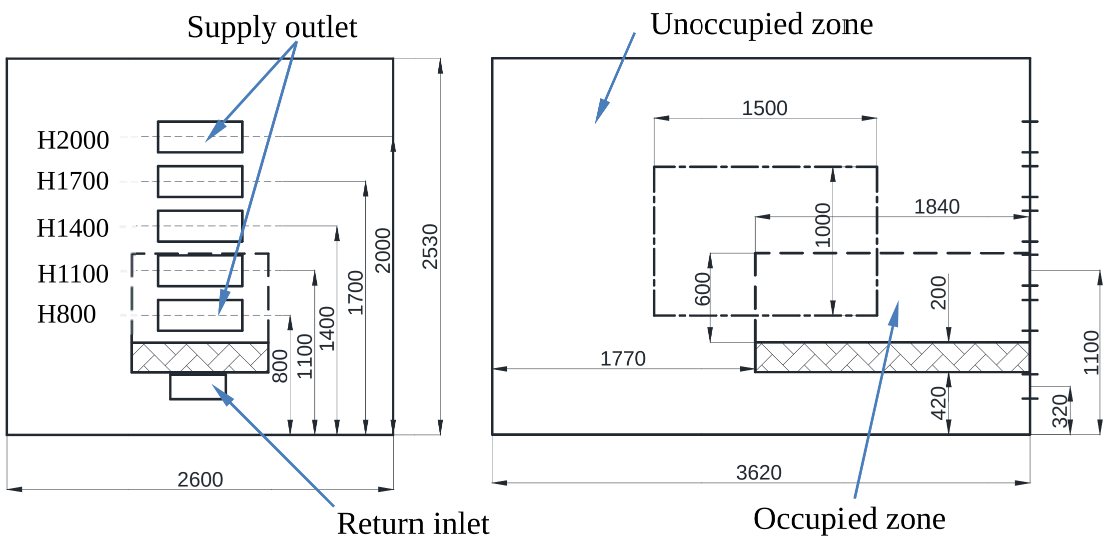

Fig. 7.2 Schematics of five system settings used in the numerical study

The surface-to-surface (S2S) radiation model was used to compute the radiation heat exchange between the surfaces in the experimental bedroom, as presented in Section 6.4.1 in Chapter 6.

To predict the CO_2 concentration distributions in the bedroom, the conservation equations of species transport were solved:

$$\nabla(\rho\vec{u}Y_i) - \nabla\vec{J}_i = S_i \tag{7.1}$$

$$\vec{J}_i = -(\rho D_{i,m} + \frac{\mu_t}{Sc_t})\nabla Y_i - D_{T,i}\frac{\nabla T}{T} \tag{7.2}$$

7.2.1.3 Studied cases

In this study, a supply air temperature between 21 °C and 27 °C and a supply air flow rate between 20 l/s and 110 l/s were used. To study the effects of fresh air on ventilation performance, fresh air flow rate was set at 0, 6.5 and 13 l/s, respectively. The details of all simulated cases are listed in Table 7.1. There were totally 9 study conditions at each setting, and therefore totally 45 cases. The purposes for study conditions 2-5 were to compare VE, DR and EUC values at different supply air flow rates, and that of study conditions 1, 3, 8 and 9 to compare DR and EUC values at different supply air temperatures, at the five height settings. Moreover, in study conditions 3, 6 and 7, the effects of fresh air on VE values were comparatively evaluated at the five height settings. With the 9 study conditions at the five settings, the total 45 study cases were resulted in.

Table 7.1 All study cases

Conditions	t_s (°C)	Q_s (l/s)	Q_f (l/s)	Case No.				
				H800	H1100	H1400	H1700	H2000
1	21	50	6.5	1.1	2.1	3.1	4.1	5.1
2	23	20	6.5	1.2	2.2	3.2	4.2	5.2
3	23	50	6.5	1.3	2.3	3.3	4.3	5.3
4	23	80	6.5	1.4	2.4	3.4	4.4	5.4
5	23	110	6.5	1.5	2.5	3.5	4.5	5.5
6	23	50	0	1.6	2.6	3.6	4.6	5.6
7	23	50	13	1.7	2.7	3.7	4.7	5.7
8	25	50	6.5	1.8	2.8	3.8	4.8	5.8
9	27	50	6.5	1.9	2.9	3.9	4.9	5.9

7.2.2 Experimental validation of the CFD method

To validate the CFD method, an A/C system at H1100 setting, which was actually the same as the ductless bed-based TAC system described in Chapter 6, was established in the experimental bedroom, as shown in Fig. 4.3. The dimensions of the experimental bedroom and measurement locations for air temperatures, air velocity and CO_2 concentration are shown in Fig. 4.9.

Because only the heights of the supply outlet at the five height settings were different, the flow mechanisms of forced, natural and mixed convections inside the bedroom were similar, which created the same flow characteristics with impingement, separation, circulation, reattachment, vortices and buoyancy at the five settings [Zhai et al. 2007]. Furthermore, the heat transfer characteristics due to convection and radiation were also the same at the five settings [Zhai et al. 2007]. Therefore, following the validation procedures and criterion recommended in a previously reported study [Chen and Srebric 2002], the experimental validation of the CFD method was only performed at H1100 setting, at the validating cases listed in Table 7.2. On the other hand, since the A/C system at H1100 setting was the same as the ductless bed-based TAC system, the CFD method used to predict the temperature and flow fields inside the experimental bedroom was already validated using the related experimental results, as presented in Section 6.4.2 in Chapter 6. Hence, additional validation of the CFD method on predicting the CO_2 concentration distributions was validated and is reported in this Section. The measured and simulated averaged CO_2 concentrations near the mouth of the thermal manikin and in the unoccupied zone were used to validate the CFD method in predicting CO_2 concentration distributions.

Table 7.2 Validation cases for predicting CO_2 concentration distributions

Cases for validation	t_s (°C)	Q_s (l/s)	Q_f (l/s)
1	19	80	0
2	19	80	6.5
3	19	80	15

Fig. 7.3 shows that the comparisons between the measured and simulated CO_2 concentrations near the mouth of the manikin and at B1.7 and F1.7 measurement positions under different fresh air flow rates. As seen, the simulated data agreed well with the measured ones in these measurement positions and under different fresh air flow rates. Based on the suggestions from a previously reported CFD study [Sørensen 2002], it was considered that this CFD method was validated with an accepted accuracy and can well be used to simulate air flow, air temperature and CO_2 transportation inside the bedroom.

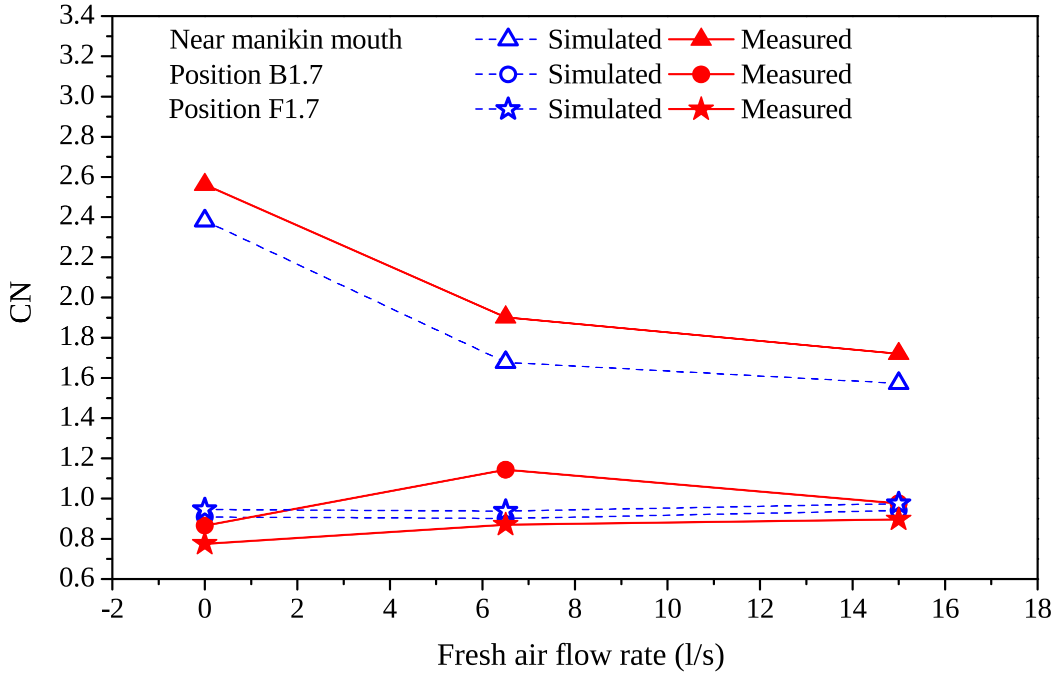

Fig. 7.3 The comparisons between the simulated and measured CO_2 concentrations near manikin mouth and unoccupied zone, at B1.7 and F1.7 positions ($CN=(C-C_s)/(C_r-C_s)$ [Kobayashi and Chen 2003], B1.7 represents 1.7m above the floor level at location B)

7.2.3 Evaluation index

In this Chapter, the operating performances of the A/C system applied to a sleeping environment were evaluated using the following three indexes: ventilation effectiveness (VE), draft risk (DR) for thermal environmental control and energy utilization coefficient (EUC) for energy saving, at different operating conditions.

7.3 Results and analysis

Numerical studies using the validated CFD method have been carried out for all the studied cases shown in Table 7.1, and their corresponding VE, DR and EUC values were obtained using the simulation results. The performance evaluations were carried out in two parts: performance evaluation of the A/C system using three separate indexes VE, DR and EUC, and overall performance evaluation using the TOPSIS method.

7.3.1 Performance evaluations using separate indexes

Fig. 7.4 shows the comparisons of simulated VE values in the occupied zone at the five height settings. It can be seen that when the fresh air flow rate was increased, a better ventilation performance was resulted in. On the other hand, different ventilation performances were demonstrated at the different heights of supply outlets. With the same rate of increase in fresh air supply, VE values were increased more at H1100 and H800 settings than at the other three settings, as shown in Fig. 7.4(a). As seen from Fig. 7.4(b), at these three settings, an increase in total supply air flow rate did not significantly influence ventilation effectiveness as compared to at H800 and

H1100 settings. Therefore, the ventilation performances of the A/C system at H800 and H1100 settings were better than that at other three settings, with an increased fresh air supply or the total supply air leading to a higher VE value. As shown in Fig. 7.2, the supply outlets at H800 and H1100 settings were actually placed in the occupied zone and could therefore deliver directly the fresh air into the occupied zone, resulting in a lower CO_2 concentration level and better ventilation performance.

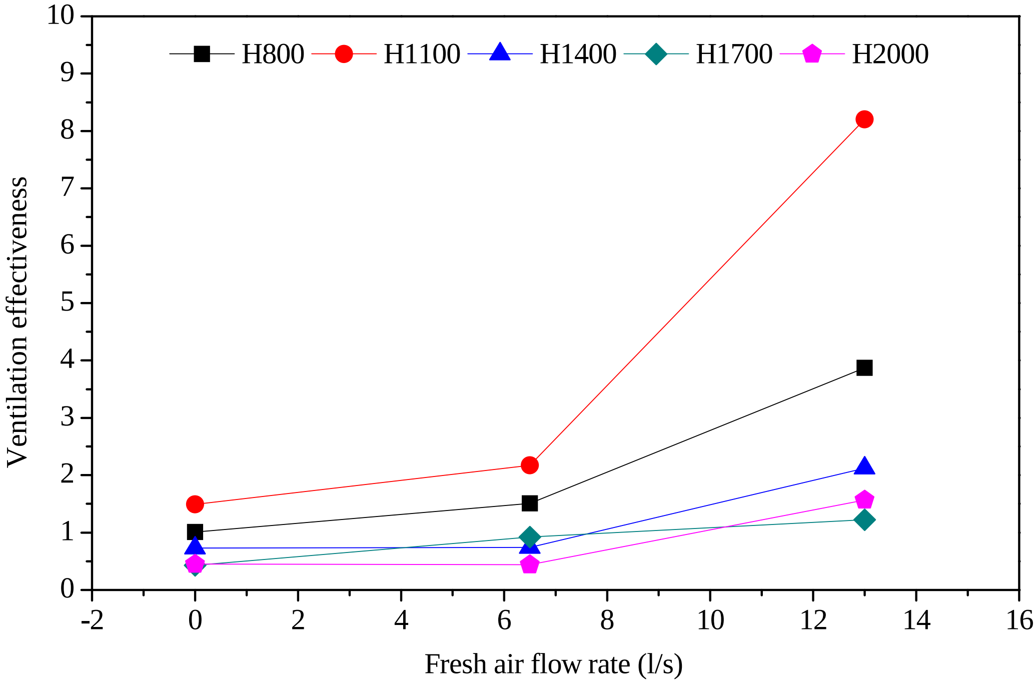

(a) At different fresh air flow rates

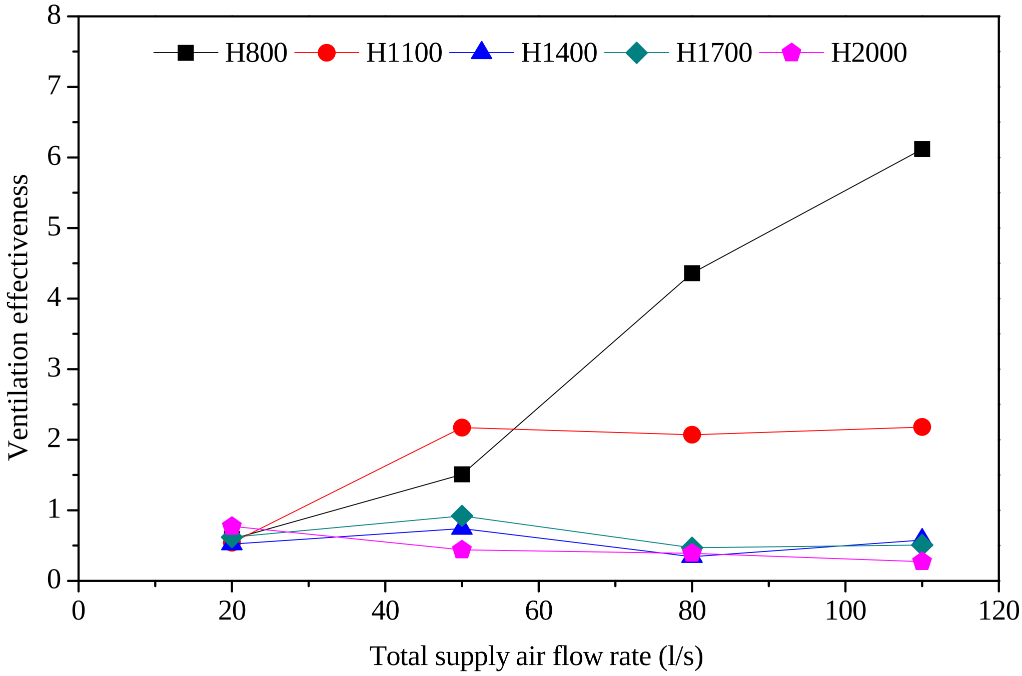

(b) At different total supply air flow rates

Fig. 7.4 Comparisons of VE values in the occupied zone, at the five settings

From Fig. 7.5 showing the averaged DR values in the occupied zone at different supply air conditions, averaged DR values at H800 and H1100 settings were higher than that of other three settings. Fig. 7.5(a) shows that the values of DR were increased sharply with an increase in supply air flow rate at H800 and H1100 settings, and that at the other three settings remained at relatively lower values. This was because the supply outlets at H800 and H1100 settings were placed at relatively lower levels in the occupied zone so that the air was colder and at a higher velocity. Fig. 7.5(b) shows that the variations in supply air temperature led to moderate changes in averaged DR values at the five settings, and that an increase in supply air temperature would help reduce the draft risk at the five settings.

As shown in Fig. 7.6, energy saving performance of the A/C system under study at H800 and H1100 settings was better than that at the other three settings, in particular at a higher supply air flow rate. This was because when the supply outlet was placed at a lower level, a higher supply air flow rate meant more conditioned air was used to decrease the air temperature in the occupied zone. On the contrary, more conditioned air was used to cool down air in the unoccupied zone when the supply outlet was placed at a higher level, at for example H2000 setting.

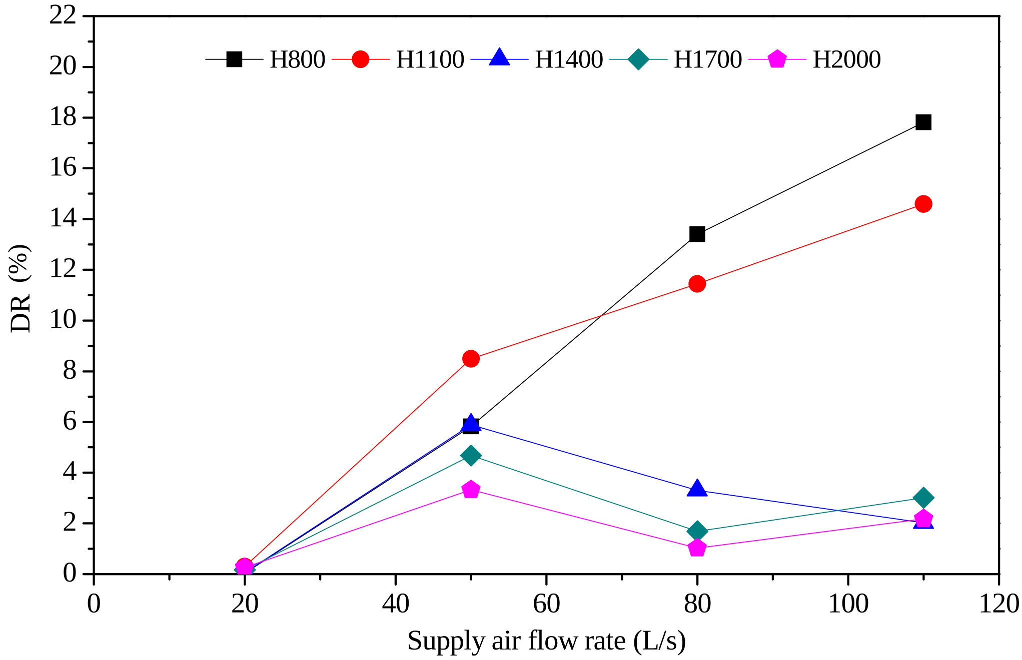

(a) At different supply air flow rates

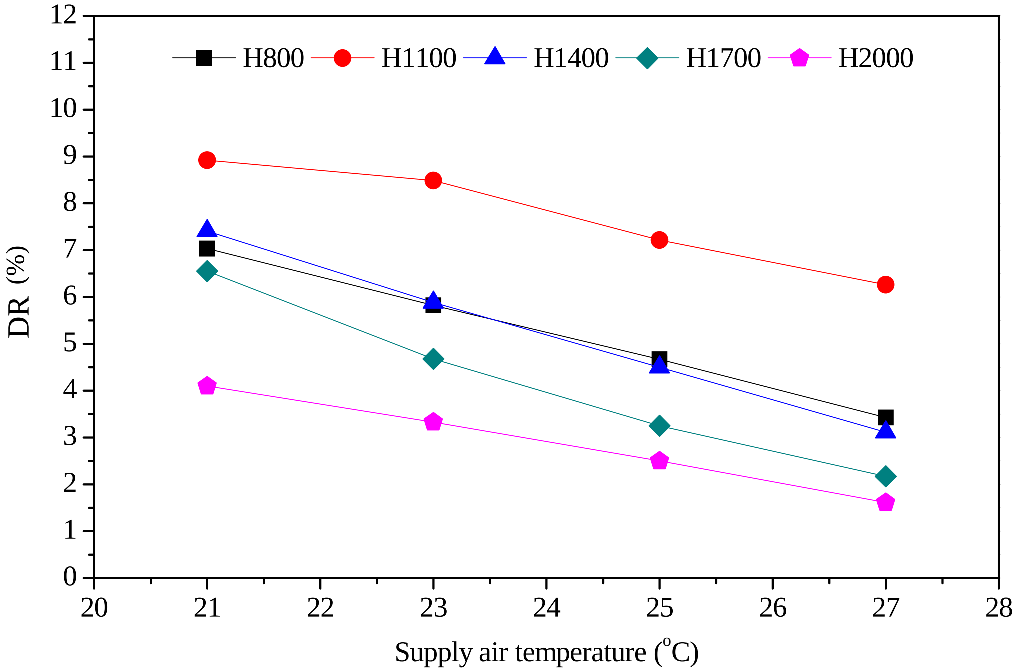

(b) At different supply air temperatures

Fig. 7.5 Comparisons of averaged DR in the occupied zone at the five settings

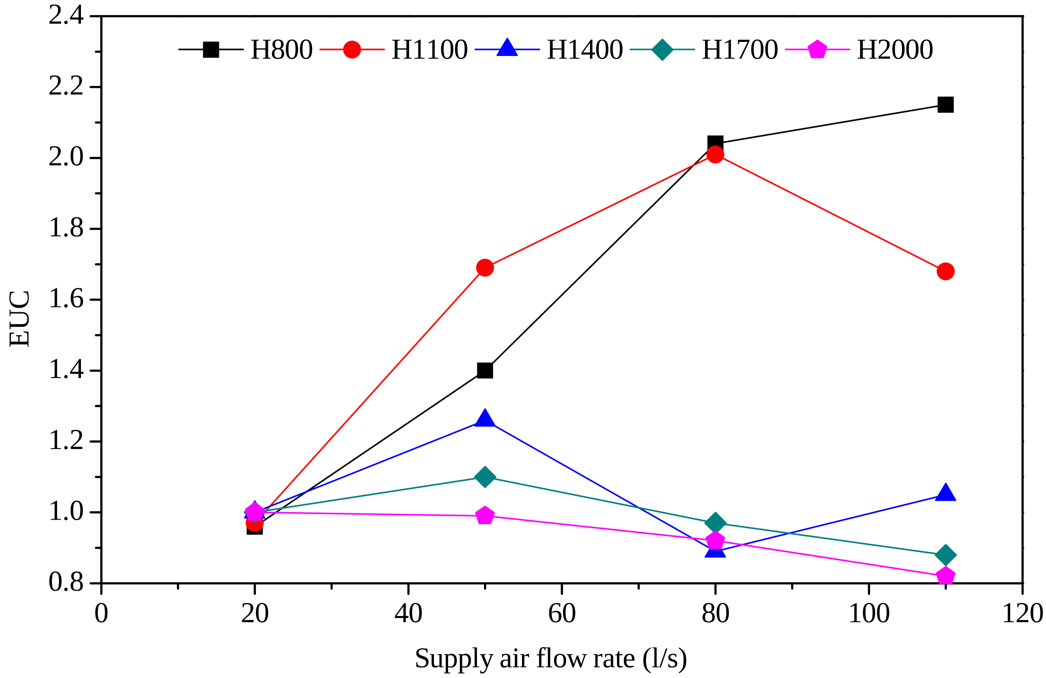

(a) At different supply air flow rates

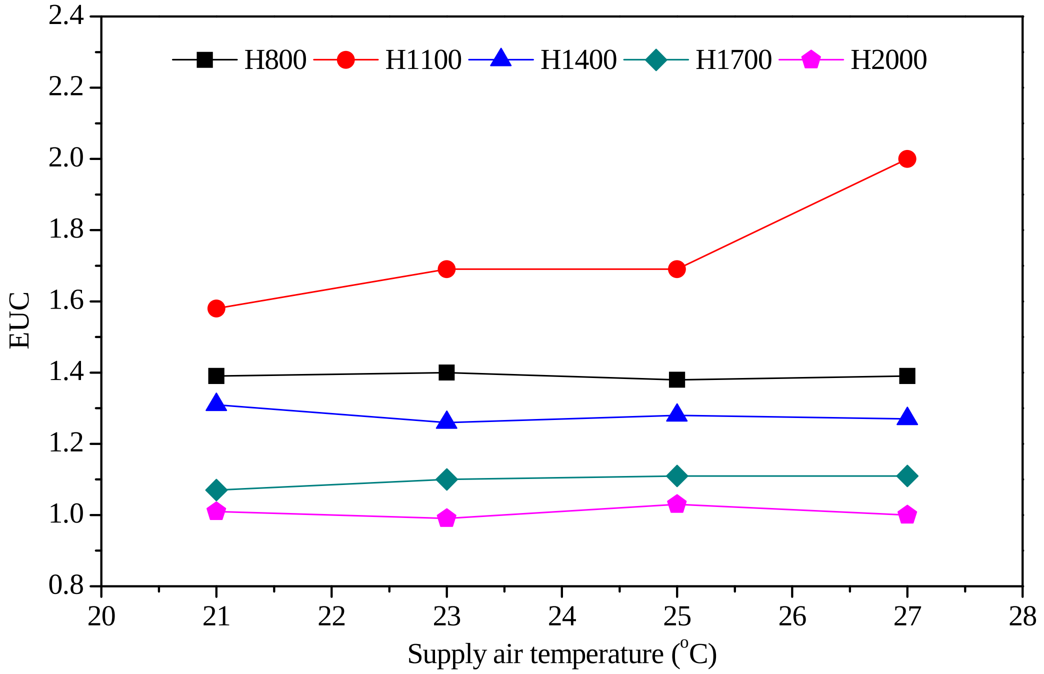

(b) At different supply air temperatures

Fig. 7.6 Comparisons of EUC values, at the five settings

From the above analysis, it can be seen that VE values were influenced by both the total supply air flow rate and the fresh air supply, and DR and EUC values by supply air temperatures and flow rates. At different settings, the degrees of influence of these operating parameters on ventilation, thermal environmental control and energy saving performances were different. For example, when the supply air flow rate was increased from 20 l/s to 110 l/s, the EUC value was increased by 1.19 at H800 setting, but was decreased by 0.18 at H2000 setting. At a specific setting, a change in one of these parameters may lead to conflicts amongst the three aspects of performance evaluation. For instance, at H800 setting, an increase in the toal supply air flow rate raised DR value in the occupied zone, suggesting a negative effect on the thermal environmental control there. However, the same increase would result in a higher EUC value suggesting a better energy saving performance. Therefore, it was indeed inadequate to evaluate the overall performance of the A/C system under study using each of these indexes separately. Hence, an evaluating tool for overall performance evaluation based on multiple separate evaluation index, TOPSIS method, was adopted to evaluate the overall performance of the A/C system applied to a sleeping environment, by integrating altogether the three performance indexes.

7.3.2 Overall performance evaluation using the TOPSIS method

An evaluating tool, called TOPSIS method, was used to assist the overall performance evaluation. TOPSIS method is a simple ranking method by making full use of index information, and thus provides rankings of different alternatives [Chen and Huang 1992, Yoon and Hwang 1995].

The overall performance of the A/C system under study, considering altogether the three indexes: VE, DR and EUC, was evaluated using the TOPSIS method. The procedure of using the TOPSIS method is shown in Fig. 7.7. Firstly, the original values of the three indexes at various study cases were normalized; secondly, the normalized values were multiplied by the weights for each index to obtain the weighted normalized values; thirdly, based on the normalized values, a positive ideal solution can be obtained and the similarities of each study case to this ideal solution calculated and then a ranking given. The final outputs from the TOPSIS method were the similarities of each study case to a positive ideal solution [Gao et al. 2009], and the rankings based on these similarities. The detailed calculation procudures is presented in Appendix C. According to the TOPSIS theory, the higher the value of similarity, the higher the ranking of a study case and the better the overall performance of the study case.

As shown in Fig. 7.7, when using the TOPSIS method, the determination of weights for each of the evaluating indexes was critical. For the A/C system under study, the weights of each of the three indexes acturally reflected their relative importance in the overall performance evaluation and can be decided based on (a) objective approach: the actural values of an index at various study cases, or (b) subjective approach: an assessor's subjective preference on an index. Therefore, the weights for each of the indexes were calculated by using the objective and subjective approaches respectively, and are shown in Table 7.3. The objective approach used in this study was the Entropy Approach based on Shannon's entropy theory [Shannon and Weaver 1947], and it assigned weight to an index according to the dispersion of its values of each index. According to the entropy theory, the less dispersion the lower weight of the index [Diakoulaki et al. 1995]. The weights calculated for each index using Entropy Approach are shown in Table 7.3. As seen, the weights for VE and DR were much higher than that for EUC, suggesting that as compared to VE and DR, the EUC values would have less variations and was therefore less important.

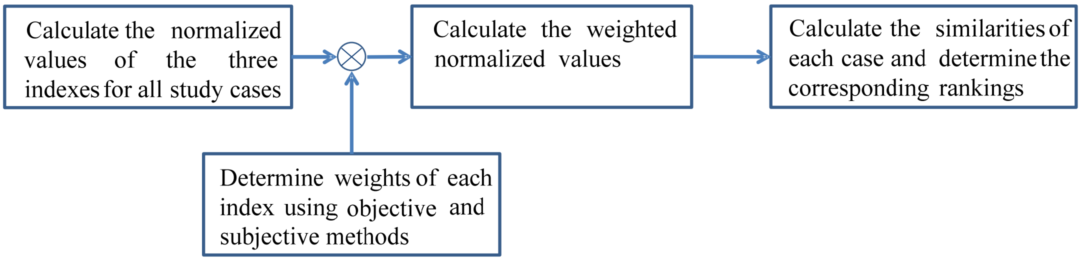

Fig. 7.7 Calculation flowchart for the TOPSIS method

Table 7.3 Weights for each index calculated using objective and subjective approaches

Weight calculation approach		Preference orders		Weights		
				VE	DR	EUC
Objective	Entropy	-	-	0.55	0.40	0.05
Subjective	AHP	AV1	VE ≻ DR ≻ EUC	0.54	0.30	0.16
		AV2	VE ≻ EUC ≻ DR	0.54	0.16	0.30
		AD1	DR ≻ VE ≻ EUC	0.30	0.54	0.16
		AD2	DR ≻ EUC ≻ VE	0.16	0.54	0.30
		AE1	EUC ≻ VE ≻ DR	0.30	0.16	0.54
		AE2	EUC ≻ DR ≻ VE	0.16	0.30	0.54

The subjective approach used in this study was Analytic Hierarchy Process (AHP) [40]. It converts the natural thoughts of a human being into an explicit process [Sharma et al. 2008], using a relational scale [Yoon and Hwang 1995]. The scales from 1 to 3 can be selected, where scale 1 means equal importance, scale 3 moderate importance, and scale 2 lies between scales 1 and 3. In this study reported in this Chapter, in view of that different assessors might have different preferences on each index, six types of preference orders for the three indexes were proposed and the weights for each index under different orders calculated [Khorshidi 2013], as also shown in Table 7.3. For example, the preference order of AV1 represents the preference order of $\mathrm{VE} \succ \mathrm{DR} \succ \mathrm{EUC}$. This preference order suggested that an assessor would assign the highest weight to VE, a lower weight to DR and the lowest to EUC. To calculate the weights for each index, a 3×3 pair-wise matrix consisting of the relative importances of the three indexes for this preference order was constructed, as shown in Table 7.4, and a principal eigen vector (0.847, 0.466, 0.257) corresponding to the maximum eigenvalue (3.01) of the above matrix was obtained. Finally, the weights were calculated at 0.54 for VE, 0.30 for DR and 0.16 for EUC, respectively, using the principal eigen vector, and are shown in Table 7.3.

On the basis the final outputs of calculated similarities by TOPSIS method, two types of evaluation were carried out: overall performance of each study case for all the cases, and overall performance of each setting among the five height settings .

Table 7.4 Relative importance of the three indexes for the preference order of AV1

Index	VE	DR	EUC
VE	1 (VE/VE)	2 (VE/DR)	3 (VE/EUC)
DR	1/2 (DR/VE)	1 (DR/DR)	2 (DR/EUC)
EUC	1/3 (EUC/VE)	1/2 (EUC/DR)	1 (EUC/EUC)

7.3.2.1 Overall performance evaluation for different study cases

The overall rankings of all study cases were obtained based on the values of similarity, as shown in Table 7.5. It indicates that Case 2.7 was the best case under most situations, due to its best ventilation performance and higher energy saving performance. However, for the preference order of AD2, its thermal environmental control performance was relatively bad, but acceptable.

Table 7.5 Overall rankings of study cases based on similarities calculated by TOPSIS method

Settings	Study case no.	Entropy	AHP					
			AV1	AV2	AD1	AD2	AE1	AE2
H800	1.1	36	36	21	36	37	23	38
	1.2	7	9	19	4	3	20	8
	1.3	27	23	14	30	30	14	22
	1.4	4	4	3	42	43	3	24
	1.5	2	2	2	43	44	2	31
	1.6	35	37	32	32	32	25	28
	1.7	3	3	4	3	22	4	3
	1.8	18	16	13	20	21	13	11
	1.9	13	11	12	12	11	12	4
H1100	2.1	43	41	17	41	41	15	42
	2.2	12	15	22	7	5	22	9
	2.3	25	14	6	38	39	8	25
	2.4	42	29	9	44	42	6	37
	2.5	45	38	10	45	45	9	45
	2.6	41	39	15	40	40	11	34
	2.7	1	1	1	1	31	1	1
	2.8	21	12	8	33	35	7	13
	2.9	5	5	5	24	27	5	2

Table 7.5 Overall rankings of study cases based on similarities calculated by TOPSIS method (continued)

Settings	Study case no.	Entropy	AHP					
			AV1	AV2	AD1	AD2	AE1	AE2
H1400	3.1	44	45	44	39	38	42	43
	3.2	10	13	20	6	4	21	7
	3.3	39	42	41	35	34	37	39
	3.4	33	35	40	25	20	43	35
	3.5	19	22	29	14	10	28	16
	3.6	38	43	42	34	33	38	40
	3.7	11	6	7	23	28	10	20
	3.8	32	31	31	27	24	27	23
	3.9	20	20	23	15	13	18	10
H1700	4.1	40	44	43	37	36	45	44
	4.2	8	10	18	5	2	19	6
	4.3	34	34	33	29	25	34	32
	4.4	17	21	30	13	9	31	17
	4.5	26	28	37	19	17	39	30
	4.6	37	40	45	31	29	44	41
	4.7	28	25	24	28	26	32	36
	4.8	22	24	28	18	16	30	19
	4.9	16	19	25	11	8	24	12
H2000	5.1	31	33	36	26	23	40	33
	5.2	6	8	16	2	1	16	5
	5.3	30	32	39	22	19	41	29
	5.4	15	18	27	8	6	29	15
	5.5	23	26	35	16	15	36	27
	5.6	29	30	38	21	18	35	26
	5.7	9	7	11	10	12	17	18
	5.8	24	27	34	17	14	33	21
	5.9	14	17	26	9	7	26	14

When following the Entropy Approach to determine the weights, the weight for EUC were very low, which weakened the advantages of H800 and H1100 settings in terms of energy saving. There were cases at these two settings which were ranked relatively lower due to relatively higher draft risk.

When following the AHP method, the overall performances for different study cases were differed at different preference orders. For the preference order of AV2, the study cases at H800 and H1100 settings gained higher rankings for their better performances on ventilation effectiveness and energy saving. Among them, for cases with higher fresh air flow rates and supply air flow rates, such as Cases 1.4, 1.5, 1.7, 2.7 and 2.9, shown in Figs. 7.4(a) and (b), better ventilation performances were achieved, leading to higher overall rankings. Furthermore, the cases with higher overall rankings were less influenced by the relative importance of DR and EUC, such as Cases 1.5 and 2.7. The overall rankings for cases for the preference orders of AV1 and AV2 were mostly similar to each other. For preference orders of AD1 and AD2, cases with lower supply flow rates or higher levels of supply outlets with lower DR values were ranked higher overall, such as Cases 1.2, 2.2, 3.2 4.2 and 5.2, as shown in Fig. 7.5(a). In addition, the change of relative importance in EUC may result in obvious variations in overall rankings, like case 2.7, which gained overall ranking of 1 for preference order of AD1 but 31 for AD2. This was because when VE was given the lowest preference, its obvious advantage in ventilation effectiveness cannot offset its disadvantage in thermal environmental control. For the preference orders of AE1 and AE2, the overall rankings for different study cases depended mainly on the weights of the second place index. When VE was more important than

DR, the study cases at H800 and H1100 settings and those with higher fresh air flow rates gained higher overall rankings. When DR was more important than VE, the study cases with lower supply air flow rates and those with higher supply outlets were ranked higher overall, such as Cases 1.2, 2.2, 3.2, 4.2 and 5.2, as shown in Table 7.5.

7.3.2.2 Overall performance evaluations for the five settings

To compare the overall performance of the A/C system under study at the five height settings, the similarities of all study cases at each setting were averaged, and are presented in Fig. 7.8.

Fig. 7.8 indicates that when following objective approachs, the mean similarities at the five settings were close to one another, with the mean similarity at H800 setting being the highest. When following subjective approach, the mean similaries were different at different preference orders. When VE was at the first place, i.e., AV1 and AV2, the mean similarities at both H800 and H1100 settings were higher than those at other three settings, due to their better ventilation performances. In particular for the preference order of AV2, where DR was at the last place, the differences between mean similarities at H800 and H1100 settings and those at other three settings were increased, due to the decreased negative effects for DR at H800 and H1100 settings. When the DR was at the first place, i.e., AD1 and AD2, the mean similarities at H1400, H1700 and H2000 settings were higher, since the DR values at those settings were lower. For preference order of AE1, the mean similarities were higher at H800 and H1100 settings for their better ventilation and energy saving performances, and the lower weight assigned to thermal environmental control. For preference order of AE2, it was difficult to determine the best setting, since the mean similarities at the five settings were close to one another. No one performed better in every index. For example, at H800 and H1100 settings, while better ventilation and energy saving performances were achieved, a higher draft risk was also resulted in. At the other three settings, while draft risks were lower, ventilation effectiveness and energy saving performances were worse. Hence, when ventilation effectiveness was at the second place, the overall performances at the five settings were almost the same.

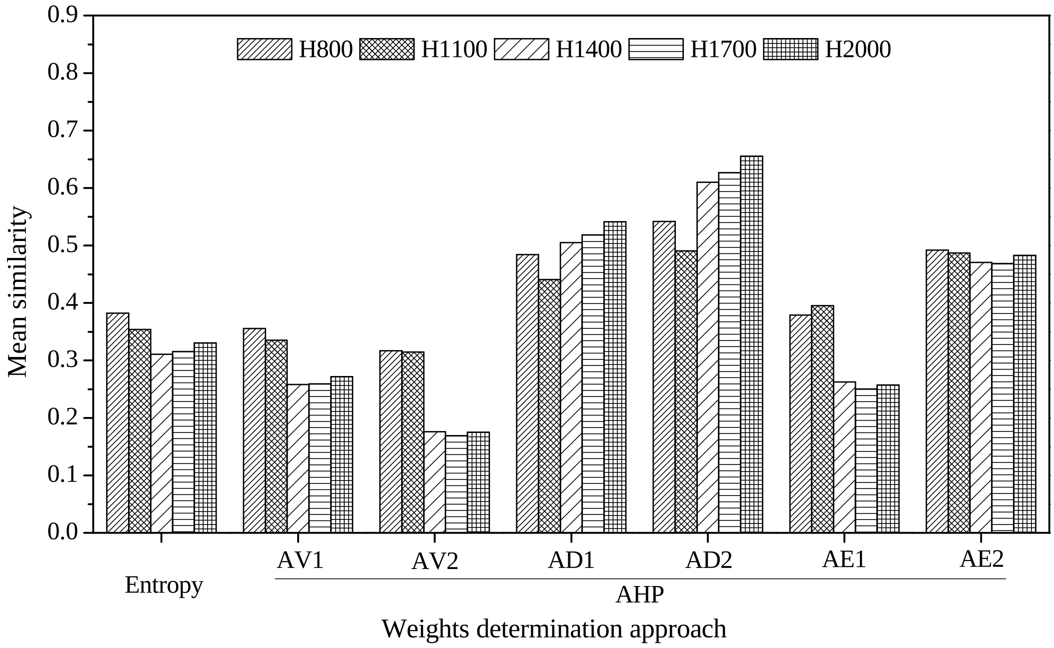

Fig. 7.8 Mean similarities at the five settings, using different weights determination approaches

Based on the above analysis, the followings can be observed:

(1) The best performance case was achieved at a supply air temperature of 23 °C, an air flow rate of 50 l/s and a fresh air flow rate of 13 l/s at H1100 setting. Generally, at H800 setting, better overall performances were achieved than at the other four settings when using objective approaches with ventilation effectiveness being given the highest weight.

(2) When the objective weight determination approach was applied, at the settings

with a lower level of supply outlet, a slightly better overall performance was resulted in. When subjective weight determination approach was used, different results were resulted in with different preference orders. If thermal environmental control was favored more by an assessor, a better overall performance was resulted in at the setting with a higher level of supply outlet. If ventilation effectiveness or energy saving performances was favored most, the best overall performance was resulted in at the settings with lower levels of supply outlet.

(3) In this Chapter, TOPSIS method was used to evaluate the overall performance of the A/C system under different operating conditions at the five settings. As demonstrated, overall performance rankings depended on the weights assigned to each index. In particular, for the subjective weights determination approach, the weights of each index were subject to an assessor’s preferences. Because of different preferences on ventilation effectiveness, thermal environmental control and energy saving, different weights would be assigned for the three indexes, and thus different evaluation results of overall performances would be resulted in.

7.4 Conclusions

This Chapter reports on the third part of the programmed research work, which is the study on the performance evaluations of an A/C system installed in the experimental bedroom with its supply of outlets positioned at five different heights. Two steps were included in the study, a numerical simulation using CFD method and performance evaluations based on the CFD simulation results. The detailed distributions of air flow, temperature and CO_2 concentration inside the experimental bedroom where the A/C system was operated at different conditions with its supply outlet placed at 5 different heights were simulated using CFD method. Based on the CFD simulation results, the operating performance of the A/C system in terms of ventilation effectiveness, thermal environmental control and energy saving were evaluated using three indexes VE, DR and EUC separately and using the TOPSIS method for overall performance evaluation. The study results indicated that the best overall performance was achieved at a supply air temperature of 23 °C, an air flow rate of 50 l/s and a fresh air flow rate of 13 l/s at H1100 setting. Among the five height settings, the A/C system performed the best at H800 setting. However, the overall performance rankings depended on the weights assigned to each index. Therefore, an assessor’s preferences and the weight determination approach had also a role to play in influencing the overall performance evaluation of the studied A/C system.

Chapter 8

Operating parameter optimization of the ductless bed-based TAC system for a thermally neutral environment with minimum energy use

8.1 Introduction

In Chapters 5 and 6, the first two parts of the programmed research work on studying the operating performances of the ductless bed-based TAC systems applied to sleeping environments are reported. The study results indicated that a TAC system can be integrated with a bed for use in sleeping environments. Furthermore, it was noted that previous investigations on studying the thermal comfort in sleeping environments were carried out [Pan et al. 2012, Lin and Deng 2006]. A comfort equation applicable to sleeping environments [Lin and Deng 2008a], which was developed by modifying Fanger's comfort equation for daytime [Fanger 1970], indicated that the total insulation value of beddings and bed would significantly affect thermal neutral temperatures in sleeping environments. Based on this comfort equation, a further study revealed the relationships between the total insulation value of beddings and bed and thermal neutral temperatures [Pan et al. 2011]. However, how to set the operating parameters of a bed-based TAC system to maintain a thermally neutral sleeping environment at a minimized energy use remained to be studied.

Therefore, in this Chapter, an optimization study on the operating parameters of the ductless bed-based TAC system installed in the experimental bedroom at two different total insulation values of beddings and bed to obtain a thermally neutral sleeping environment at minimum energy use is reported, as the fourth part of the programmed research work. Firstly, a CFD method was applied to calculating the values of PMV and EUC under 16 simulation cases. Secondly, based on the simulation results, the DOE (design of experiment) method was applied to identifying operating parameters, individually or combined, which would significantly affect thermal neutrality and energy use, and linear regression models for PMV and EUC using the identified parameters were respectively established. Finally, the linear regression models were used to obtain the optimum operating parameters of the bed-based TAC system, so that a thermally neutral sleeping environment can be maintained at a minimum energy use.

8.2 Methodology

The methodology used in the optimization study reported in this Chapter is schematically shown in Fig. 8.1. Firstly, according to the ranges of supply air temperature, supply air flow rate and supply air relative humidity [Lin and Deng 2006], simulation cases were determined through a full-factorial design approach. The air flow, temperature and relative humidity distributions inside the experimental bedroom were predicted using a CFD method. Secondly, the PMV and EUC values at 16 simulation cases were evaluated using the simulation results, respectively. Thirdly, linear regression models for PMV and EUC were respectively obtained using the DOE method, which helped identify those operating parameters, individually or combined, that significantly affect thermal neutrality and energy use. Finally, the optimum operating parameters for the bed-based TAC system were obtained by numerically solving the linear regression models for PMV and EUC.

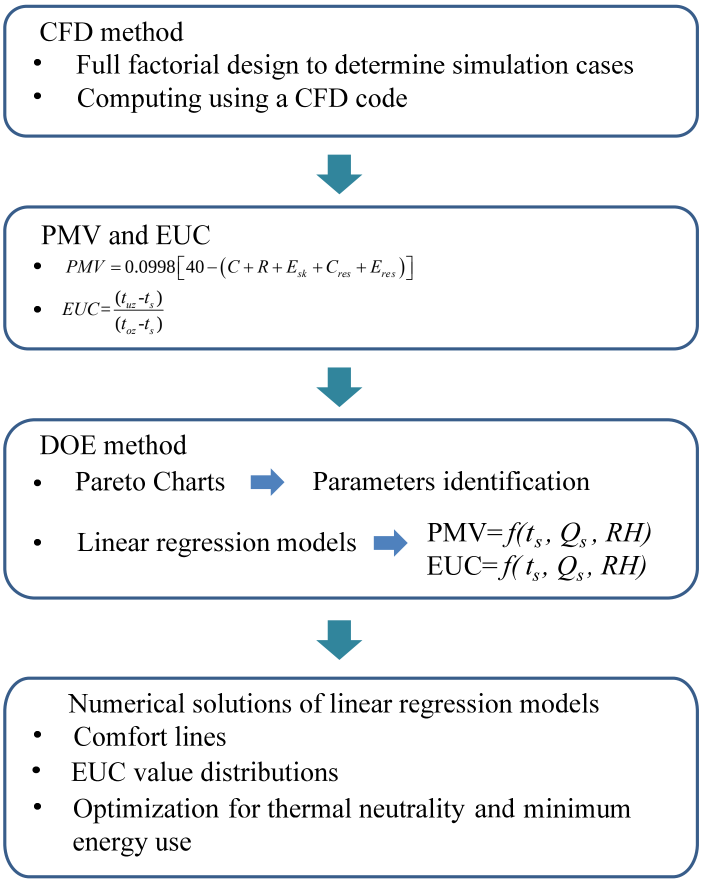

Fig. 8.1 Flow chart for the methodology used

8.2.1 CFD method

8.2.1.1 Geometry model and mesh generation

The simulated experimental bedroom is described in Chapter 4 and shown in Figs. 4.4 and 4.7. Grids used in the CFD method were separately generated for the occupied zone and the unoccupied zone, as detailed in Section 6.4.1 in Chapter 6.

8.2.1.2 Governing equations

A commercial CFD code [ANSYS 2010] was used to compute the air flow field and heat transfer inside the experimental bedroom. The air flow field was calculated by the three-dimensional and steady-state Reynolds averaged Navier-Stokes (RANS) equations, combined with continuity and energy equations, as presented in Section 6.4.1 in Chapter 6. The SST turbulence model [Menter 1994], which takes advantages of both the *k-ε* model and the *k-ω* model, was used for modelling the turbulent flow. The surface-to-surface (S2S) radiation model was used to compute the radiation heat exchange among the surfaces in the bedroom.

To predict the moisture transfer between the surface of the thermal manikin and its surrounding environments, a species transport model was used. The conservation equation for species transport was:

$$\nabla \cdot (\rho \vec{v} Y_i) = \nabla[(\rho D_{i,m} + \frac{\mu_t}{Sc_t})\nabla Y_i] + S_i \tag{8.1}$$

Where Y_i is the local mass fraction of the i^{th} species, $D_{i,m}$ the mass diffusion coefficient for species i in the mixture, Sc_t the turbulent Schmidt Number, and S_i

source term.

8.2.1.3 Boundary conditions

(1) Skin surface temperature

Mean skin surface temperature, t_{sk}, was an important factor influencing human's thermal sensation. The following linear regression equation, which was proposed by Fanger [1970], was used to evaluate the value of t_{sk}:

$$t_{sk} = 35.7 - 0.0275(M - W) \tag{8.2}$$

The metabolic rate (M) of a sleeping person is 40 W/m^2, and the workload (W) is zero, therefore, the mean skin temperature would be 34.6 ºC.

(2) The total insulation value of beddings and bed

The total insulation value of beddings and bed plays an important role in determining the thermal neutrality of a sleeping environment [Lin and Deng 2008b, McCullough et al. 1987] and a previous related study [Lin and Deng 2008b] was carried out to determine the total insulation values of various combinations of beddings and bed. Table 8.1 shows the total insulation values of beddings and bed at two levels, which were part of the outcomes of the previous study [Lin and Deng 2008b], a low level when the thermal manikin was naked, and a high level when it was covered with a blanket with a total body coverage of 94.1% by blanket and bed. Since these two sets of the total insulation values were typical, they were used in the current optimization study by designating two study Groups, Group N where the total insulation value for naked thermal manikin of 0.98 clo was used, and Group B where that for blanket covered thermal manikin of 2.11 clo was used. Although only two sets of the total insulation value of beddings and bed were considered in the current study, the results obtained from the study would provide a base for further studying the impacts of other sets of the total insulation value on thermal neutrality and energy use

Table 8.1 The total insulation values of beddings and bed at two levels used in the study [Lin and Deng 2008b]

	Naked	Covered by Blanket
Coverage of beddings and bed	23.3%	94.1%
Detailed description	-	100% cotton
Weight per unit area (kg/m^2)	-	0.3308
Thickness (mm)	-	3.03
Thermal resistance (m^2K/W)	-	0.121
Thermal conductivity (w/mK）	-	0.02504
Calculated density (kg/m^3)	-	109
Total insulation value of beddings and bed (clo)	0.98	2.11

(3) Moisture diffusion

To predict the moisture transfer between the surface of the thermal manikin and the surrounding environment, air moisture content was taken as 10 g/kg air at the surfaces of the thermal manikin according a previous study [Sevilgen and Kilic 2011]. The gradient of air moisture content at the all other solid surfaces was taken as zero [Sevilgen and Kilic 2011].

8.2.2 Simulation cases

A two-level three-parameter full-factorial approach for simulation was used to determine simulation cases, as shown in Table 8.2. The operating parameters, supply air temperature, supply air flow rate and supply air relative humidity, were designated as the three parameters where using the full-factorial approach. Each of these parameters was studied at two levels: a low and a high level. The minimum number of simulation cases for the two-level three-parameter approach was therefore 2^3 or 8, as shown in Table 8.3. Moreover, as mentioned in Section 8.2.1, with respect to the influence of the total insulation value of beddings and bed on thermal neutrality of a sleeping environment, two study Groups were designated, Group N and Group B. Correspondingly, in each group, there were 8 simulation cases and therefore totally, there were 16 simulation cases, as shown in Table 8.3.

Table 8.2 Design parameters and their low-high levels used in the study

Parameters	Low level	High level
t_s (ºC)	21	25
Q_s (l/s)	20	50
RH_s (%)	40	70

Table 8.3 Simulation cases

Study Group	Case no.	t_s (ºC)	Q_s (l/s)	RH_s (%)
N	1.1	21	20	40
	1.2	21	20	70
	1.3	21	50	40
	1.4	21	50	70
	1.5	25	20	40
	1.6	25	20	70
	1.7	25	50	40
	1.8	25	50	70
B	2.1	21	20	40
	2.2	21	20	70
	2.3	21	50	40
	2.4	21	50	70
	2.5	25	20	40
	2.6	25	20	70
	2.7	25	50	40
	2.8	25	50	70

8.2.3 PMV evaluation for sleeping environments

Based on the well-known Fanger's thermal comfort model [Fanger 1970] and considering the heat generation and balance for a sleeping person, Lin and Deng [2008a] developed an equation to evaluate the PMV index in sleeping environments:

$$PMV = 0.0998\left[40 - \left(C + R + E_{sk} + C_{res} + E_{res}\right)\right] \tag{8.3}$$

In Equation (8.3), C+R is the total heat flux generated from a human body. In this study, the CFD method provided the numerical value of C+R, as part of the simulation outputs.

Evaporative heat loss from skin, E_{sk}, depended on the amount of moisture on skin and the difference between the water vapor pressure at the surface of a human body and that in the ambient environment, and was evaluated by:

$$E_{sk} = \frac{i_m L_R w(p_{sk,s} - p_a)}{R_t} = 0.06 h i_m L_R (P_{sk,s} - P_a) \tag{8.4}$$

Respiratory heat loss, q_{res}, is often expressed in terms of sensible heat loss, C_{res}, and latent heat loss, E_{res}. Sensible loss (C_{res}) and latent loss (E_{res}) due to respiration can be estimated, respectively, by the following equations [Lin and Deng 2008a]:

$$C_{res} = 0.0014 M (34 - t_a) \tag{8.5}$$

$$E_{res} = 0.0173 M (5.87 - p_a) \tag{8.6}$$

8.2.4 Energy use

The energy use by the ductless bed-based TAC system under study was indirectly evaluated using energy utilization coefficient (EUC) which relates to the temperature difference between the occupied zone and the unoccupied zone, and is defined in Section 5.3.3.2 in Chapter 5.

8.3 Results and analysis

Using the simulated air temperature, humidity and flow distributions inside the experimental bedroom from the CFD method, the PMV and EUC values were evaluated for the 16 simulation cases as detailed in Table 8.3. To analyze the simulation results and carry out optimization, two analytical tools of the DOE method were applied: Pareto Chart plotting and linear regression modelling [Antony 2003]. By plotting Pareto Chart, the operating parameters, individually or combined, that can significantly affect thermal neutrality and energy use, were identified. Then, linear regression models for PMV and EUC using the identified parameters were developed. Comfort lines and EUC values at different operating parameters were then studied using the obtained linear regression models. Finally, the linear regression models were used to optimize the operating parameters of the bed-based TAC system.

8.3.1 Analysis of operating parameters' effect through plotting Pareto Chart

A Pareto Chart is a simple bar chart that ranks the effects of related parameters in a descending order. It allows one to detect the effect of each of the parameters, individually or combined, which are the most important to a process or design. It displays the absolute values of the effects, and a reference line can be drawn to estimate the significance of these effects on a Pareto Chart. The effect value for the reference line can be estimated using Length's pseudo-standard error (PSE) method [Lenth 1989] when the effect of a parameter extends past this reference line to the right hand side of the line on a Pareto Chart, then parameter is potentially important and significant with a 95% confidence level [Antony 2003]. Following the standard method for plotting a Pareto Chart [Antony 2003, Lenth 1989], the Pareto Charts for the effects of individual parameters and their combinations on PMV and EUC were produced as shown in Figs. 8.2 and 8.3. It can be seen from Fig. 8.2(a) and Fig. 8.3(a) that, at Group N, Q_s, t_s, RH_s and $Q_s \times t_s$ had significant effects, and at Group B, Q_s, t_s, and $Q_s \times t_s$ had the significant effects, on PMV. Although the effect value of RH_s on the PMV was lower than that of the reference line, it was still more significant than other remaining combined operating parameters and was hence still taken as a significant parameter. On the other hand, Fig. 8.2(b) and Fig. 8.3(b) show that, at both Group N and Group B, Q_s, t_s and $Q_s \times t_s$ had significant effects on the EUC. Using the Pareto Chart, the parameters, individually or combined, having significant effects on PMV and EUC were identified, and used in the linear regression models to be established.

8.3.2 Prediction of linear regression models

Linear regression models were established for PMV and EUC based on the identified individual or combined operating parameters using the least square technique. P-values of the identified individually or combined operating parameters which were statistically significant were evaluated. The significances of each of the identified individual or combined parameters were judged by their P-values being closer to zero. For a 95% confidence level, the P-value should not be greater than 0.05. The P-values for those identified parameters, individually or combined, were all less than 0.05, as shown in Table 8.4. Correspondingly, the regression coefficients for these identified parameters were evaluated and are also shown in Table 4.

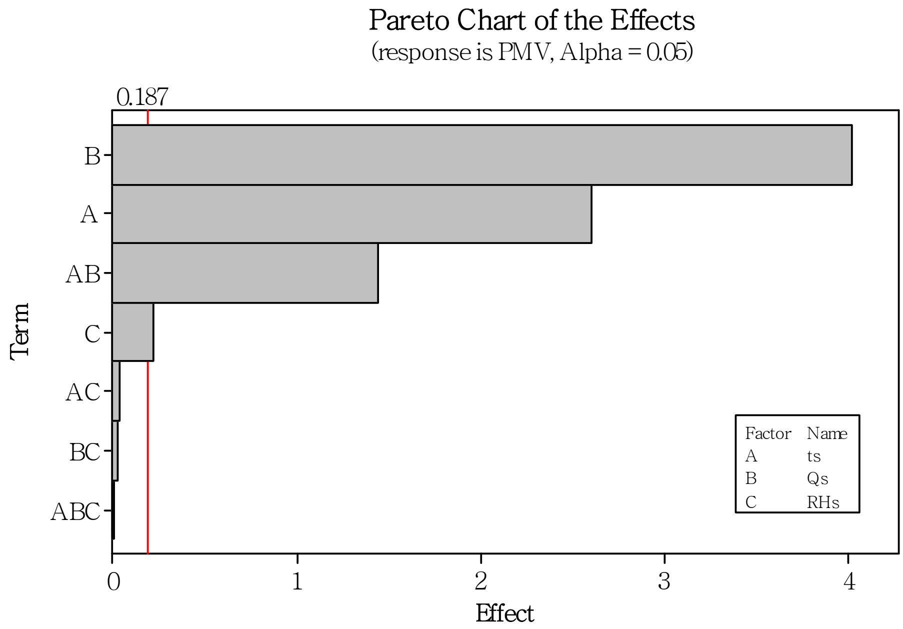

(a) for PMV

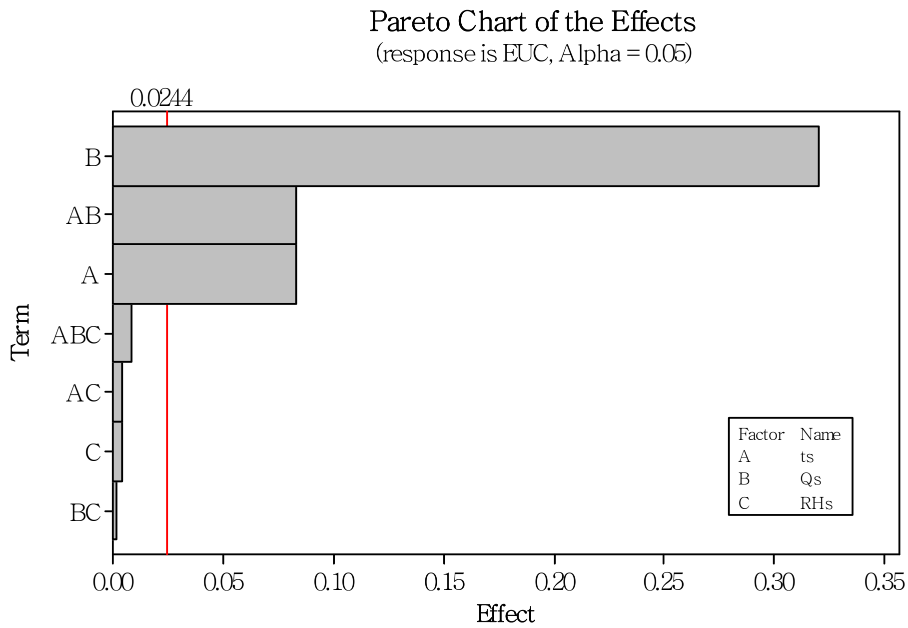

(b) for EUC

Fig. 8.2 Pareto chart of the individual and combined operating parameters on PMV and EUC (Group N)

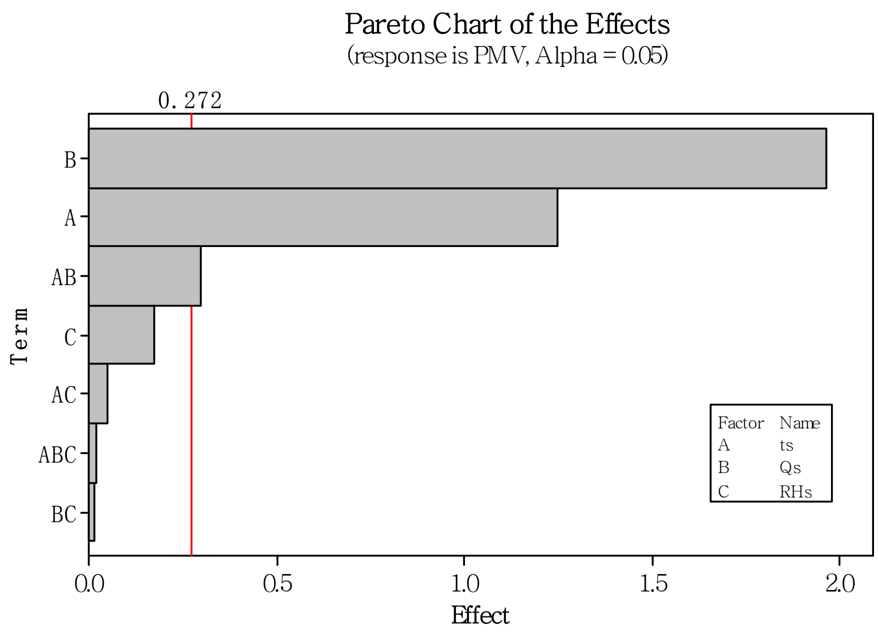

(a) for PMV

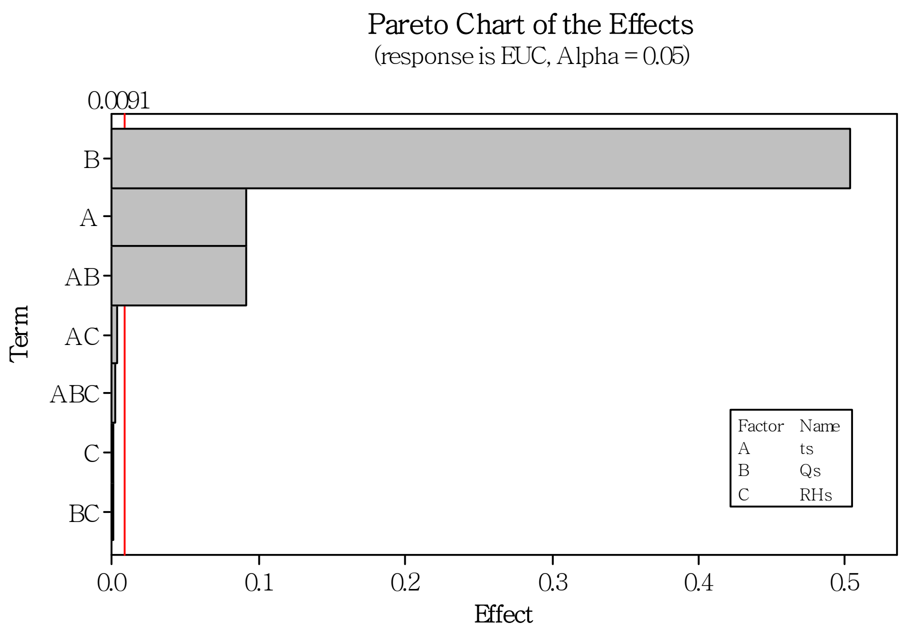

(b) for EUC

Fig. 8.3 Pareto chart of the individual and combined operating parameters on PMV and EUC (Group B)

Table 8.4 Regression coefficients and P-values of the identified individual or combined operating parameters for PMV and EUC

Group	Responses	Parameter / combinations	Regression coefficient	P-value
N	PMV	t_s	-0.192	0.002
		Q_s	-0.689	0.000
		RH_s	0.00753	0.004
		$t_s \times Q_s$	0.0241	0.000
	EUC	t_s	0.0279	0.001
		Q_s	0.0427	0.000
		$t_s \times Q_s$	-0.00139	0.000
B	PMV	t_s	0.137	0.006
		Q_s	-0.181	0.000
		RH_s	0.00589	0.011
		$t_s \times Q_s$	0.00502	0.002
	EUC	t_s	0.0306	0.000
		Q_s	0.0521	0.000
		$t_s \times Q_s$	-0.00153	0.000

Based on effect analysis presented in Section 8.3.1 and combined with the evaluated P-values in Table 8.4, linear regression models for PMV and EUC for the two Groups were obtained:

For Group N:

$$PMV = 7.74 - 0.192t_s - 0.689Q_s + 0.0241t_sQ_s + 0.00753RH_S \tag{8.7}$$

(Coefficient of determination: 99.99%)

$$EUC = 0.108 + 0.0279 t_s + 0.0427 Q_s - 0.00139 t_s Q_S \quad (8.8)$$

(Coefficient of determination: 99.90%)

For Group B:

$$PMV = -0.054 + 0.137 t_s - 0.181 Q_s + 0.00589 RH_s + 0.00502 t_s Q_s \quad (8.9)$$

(Coefficient of determination: 99.95%)

$$EUC = -0.0670 + 0.0306 t_s + 0.0521 Q_s - 0.00153 t_s Q_s \quad (8.10)$$

(Coefficient of determination: 99.98%)

The applicable ranges of all the parameters in the linear regression models were between the high- and low- level for t_s, Q_s and RH_s, as shown in Table 8.2. To analyze the performance of the TAC system under different operating parameters within the applicable ranges, linear regression models of PMV and EUC, i.e., equations (8.7-8.10) were numerically solved. Considering that the effects of t_s, Q_s and RH_s on PMV and EUC were significantly different as mentioned in Section 8.3.1, various calculation steps were chosen, at 0.1 ºC for t_s, 1 l/s for Q_s and 5% for RH_s. This gave rise to a total of 7200 numbers of different operating points.

8.3.3 Comfort line

The operating parameters, under which an indoor environment is thermally neutral, would form a line, called a comfort line. Using the numerical solutions for the linear regression models, the operating points where the PMV was equal to zero with an error of ±0.05 were obtained to form the comfort line. Using the comfort line, how to realize a thermally neutral environment can be illustrated.

Fig. 8.4 shows that the influence of RH_s on the thermal neutrality of the sleeping environment was relatively small. A change in RH_s from 40% to 70% can be compensated by only a 0.4 - 0.7 ºC (at Group N) or 0.4 ºC (at Group B) decrease in supply air temperature. The higher the Q_s, the less the decrease in t_s with an increase in RH_s at Group N. This suggested that at a higher Q_s and t_s, a larger increase in Q_s or a smaller decrease in t_s can compensate an increase in RH_s for Group N.

On the other hand, the total insulation value of beddings and bed would significantly influence the operating parameters under the thermal neutral condition, as shown in Fig. 8.4. When the total insulation value of beddings and bed was at a high level, Q_s

was at a higher level and t_s was at a lower level, compared to that when the total insulation value of beddings and bed was at a lower level.

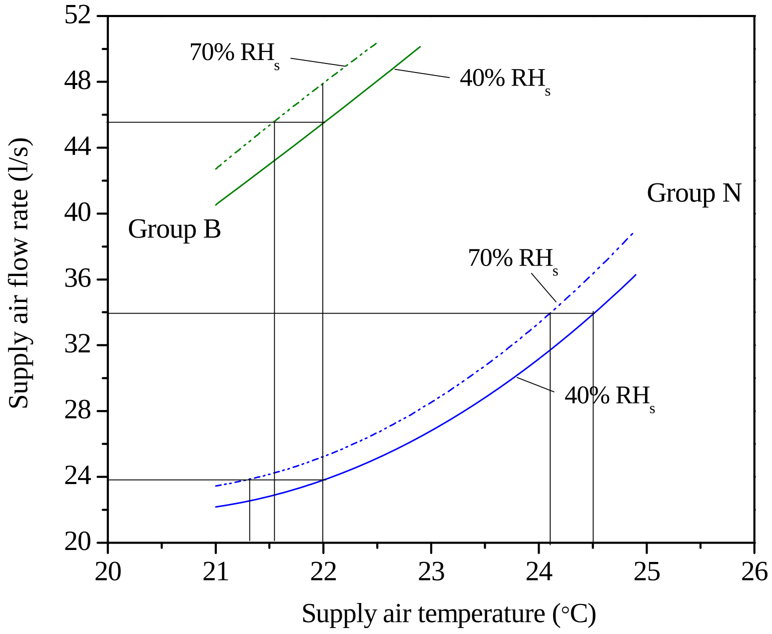

Fig. 8.4 Comfort lines for the two Groups

8.3.4 EUC values at different operating parameters

Using the numerical solutions of the linear regression models obtained in Section 8.3.2, EUC values under different identified operating parameters were obtained for the two Groups, as shown in Figs. 8.5 and 8.6. It can be seen that for both Groups, at a constant t_s, an increase in Q_s led to an increase in EUC, and at a constant Q_s, an increase in t_s resulted in a decrease in EUC. It can also be seen that EUC values were affected more by Q_s than t_s, as shown in Figs. 8.5 and 8.6.

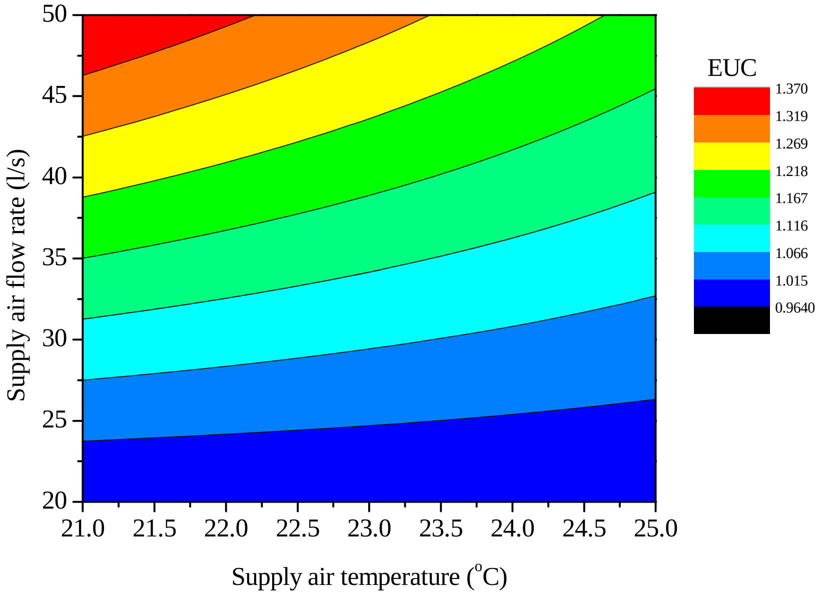

Fig. 8.5 EUC values at Group N

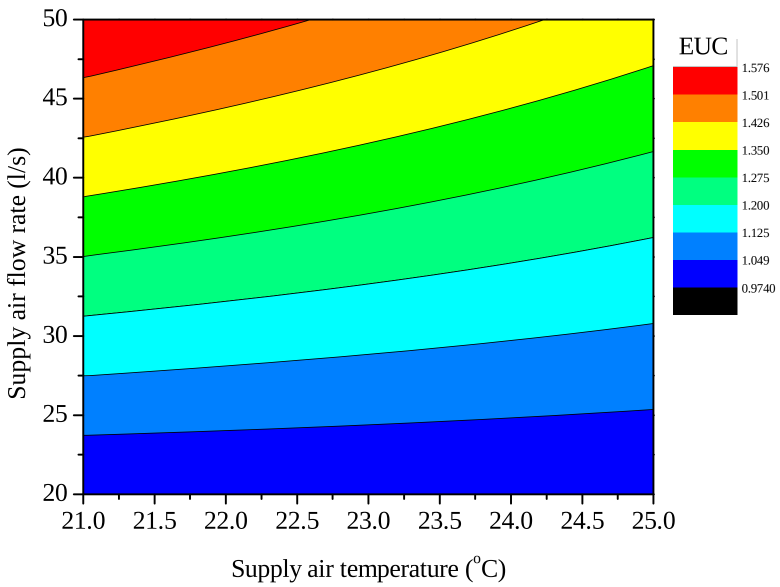

Fig. 8.6 EUC values at Group B

Combining Figs. 8.4, 8.5, and 8.6, it can be seen that, at a specific total insulation value of beddings and bed, an increase in both Q_s and t_s contributed to a better thermally neutral environment. However, an increase in Q_s led to a lower EUC value compared to an increase in t_s. Therefore, there existed a balance point between maximizing EUC and maintaining PMV close to zero and an optimization was carried out and is reported in next Section.

8.3.5 Operating parameters optimization

8.3.5.1 Optimization analysis and results

PMV and EUC values at different operating points at the two groups were plotted to form PMV-EUC Charts, shown in Figs. 8.7 and 8.8, respectively. In general, the operating zones which were formed by high-low limits of the operating parameters at Group N were located in the region with lower PMV and EUC values, but those at Group B in the region with higher PMV and EUC values. Therefore, different optimum operating parameters would be expected.

On the PMV-EUC Charts, vertical lines for PMV=0 can be drawn, as shown in Figs.

8.7 and 8.8. On these lines, a higher EUC corresponded to higher t_s, Q_s and RH_s. Furthermore, all the operating points on lines of PMV=0 would lead to thermal neutrality since PMV=0. Therefore, one particular operating point with the Maximum EUC value on this line can be viewed as the optimum operating point at which the TAC system could maintain a thermally neutral environment at a minimum energy use. This point can be identified through numerically solving the linear regression models presented in Section 8.3.2.

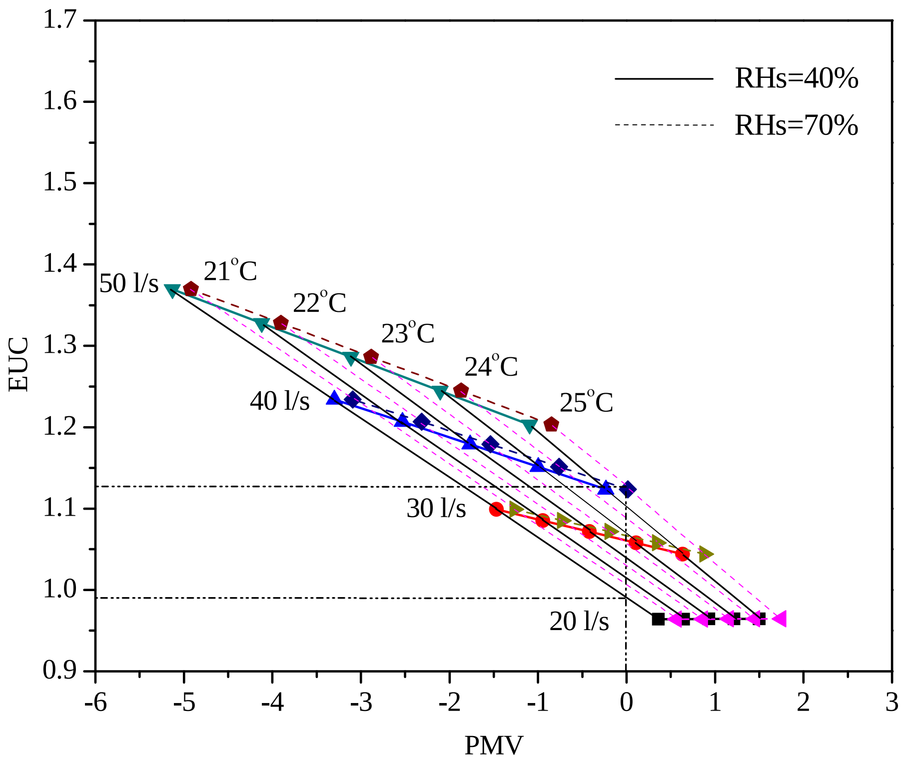

Fig. 8.7 PMV-EUC Chart for Group N

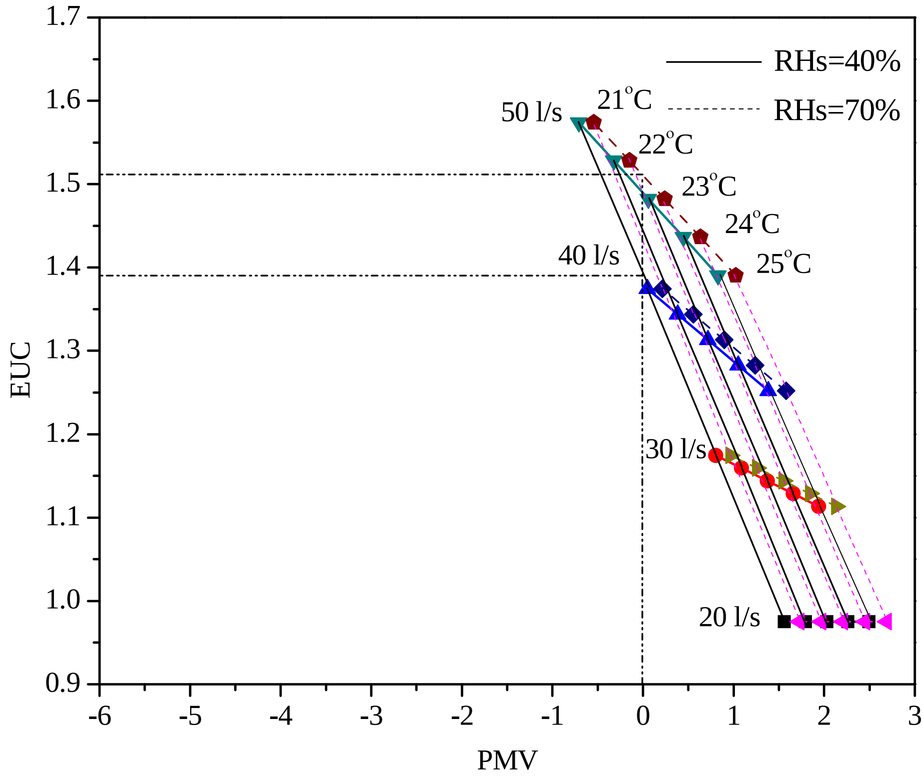

Fig. 8.8 PMV-EUC Chart for Group B

The optimum operating parameters at the two Groups were thus obtained and are shown in Table 8.5. It can be seen that when the human body was either naked or covered with a blanket, the optimum operating point for the ductless bed-based TAC system can be determined to maintain a thermally neutral environment at a minimum energy use.

Table 8.5 The optimum operating parameters of the TAC system for the two Groups

Group	t_s (ºC)	Q_s (l/s)	RH_s (%)
N	24.8	39	70
B	22.3	50	70

8.3.5.2 Validation of the optimization results

To validate the above optimization results obtained through using the linear regression models, CFD simulations were carried out using the operating parameter values at the optimum operating point, shown in Table 8.5, as inputs. The PMV and EUC values output from the CFD method are presented in Table 8.6, which also lists those predicted by using the linear regression models. It can be seen that the PMV and EUC values obtained using CFD method agreed reasonably well with that predicted using the linear regression models. Therefore, the use of linear regression models can suitably help determine the optimum operating parameters of a TAC system, at which while thermally neutral environment was maintained, energy use for the TAC system was minimized.

Table 8.6 The PMV and EUC values at optimum operating points obtained using linear regression models and CFD method

Group	Objectives		Linear regression models		CFD	
	PMV	EUC	PMV	EUC	PMV	EUC
N	0	Max	-0.05	1.12	-0.21	1.15
B	0	Max	-0.04	1.51	0.14	1.40

In the current study, only eight simulation cases for each Group were studied using CFD method to obtain linear regression models, which were consequently used for optimization. However, if the same optimization results should have been obtained using CFD method, 7200 simulation cases should have been done. This meant the optimization jointly using both the DOE method and CFD method could save much calculating time.

8.4 Conclusions

This Chapter reports on an optimization study on the operating parameters of the ductless bed-based TAC system at two different total insulation values of beddings and bed to achieve a thermally neutral environment and a minimum energy use. A CFD method was firstly applied to calculating the PMV and EUC values for 16 simulation cases. Based on the results from the simulation cases, using the DOE method, linear regression models for PMV and EUC were respectively established, and then numerically solved to obtain the optimum operating parameters. The study results suggested that for a bed-based TAC system, at a specified total insulation value of beddings and bed, increases in supply air flow rate, supply air RH and supply air temperature would lead to a lower energy use when still maintaining a thermal comfortable level. Under a given total insulation value of beddings and bed, jointly using the DOE method and CFD method can help find the optimum operating parameters of the bed-based TAC system, at which a thermally neutral sleeping environment was maintained at minimum energy use.

Chapter 9

Conclusions and Future Work

9.1 Conclusions

A programmed research work on studying thermal environmental control, indoor air quality and energy efficiency using task\ambient air conditioning (TAC) systems in sleeping environments in the subtropics has been successfully carried out and is reported in this thesis. There are four parts in the programmed research work, and they are presented in Chapters 5 to 8, respectively, of the thesis. The conclusions of the Thesis are as follows:

1) To address the inadequacies of a previous bed-based TAC system, a ductless bed-based TAC system has been developed and its thermal, ventilation and energy saving performances experimentally studied, by comparing them with those of a full volume air conditioning (FAC) system and the study results are reported in Chapter 5. Firstly, the measured thermal performances in the experimental bedroom at the two different system arrangements in terms of Draft Risk (DR) and Relative Humidity (RH) in the occupied zone, are presented. Secondly, the measured ventilation performances, in terms of ventilation effectiveness at the two system arrangements were compared. Furthermore, the measured energy saving performances in terms of cooling performance and Energy Utilization Coefficient (EUC) at the two system arrangements were compared. Finally, an improvement method by varying the supply vane angle was proposed to reduce the draft risk in the occupied zone when using the ductless TAC. The experimental results demonstrated that using the

ductless bed-based TAC could lead to a better ventilation performance and energy saving performance, but a poor thermal performance in terms of a higher draft risk than using the FAC system. To reduce the draft risk, while still maintaining an acceptable energy saving performance, it was possible to select a proper supply air temperature and air flow rate as well as a proper supply vane angle. Moreover, the study results also suggested that a larger energy saving can be achieved when a bed-based TAC system is applied to real buildings with envelope heat gains.

2) Using the developed ductless bed-based TAC system, reported in Chapter 5, may lead to a higher draft risk in an occupied zone. Therefore, to further improve the operating performance of the ductless bed-based TAC system through organizing return air paths, two system settings for the TAC system were designed and their performances in terms of thermal environmental control and energy saving are experimentally and numerically studied. The study results, reported in Chapter 6, demonstrated that at Setting 2, 4.0 % to 17.8 % improvement in thermal environmental control performance due to a lower draft risk, but with 3.8 % to 7.8 % more energy consumption, were resulted in. Moreover, at Setting 2, the ductless bed-based TAC system performed better at lower supply air flow rates (50 and 80 l/s) with a better air diffusion performance. A CFD method developed to predict the temperature and flow fields inside the experimental bedroom was experimentally validated. The detailed air flow field and temperature field inside the experimental bedroom predicted by the validated CFD method clearly illustrated the causes of the differences in operating performance of the bed-based TAC system at the two settings in terms of DR, ADPI and EUC. Therefore, it was helpful to increase the thermal comfort level when using the ductless bed-based TAC system at the expense

of saving less energy by placing a return air plenum with return air inlet under the bed, and such a design of TAC system is more applicable to the real life in a bedroom.

3) For an A/C system applied to a sleeping environment, the height of its supply outlet could significantly affect its operating performance. Therefore, a study on the performance evaluations of an A/C system installed in the experimental bedroom with its supply of outlets positioned at five different heights was carried out and the study results are reported in Chapter 7. Two steps were included in the study, a numerical simulation using CFD method and performance evaluations based on the CFD simulation results. The CFD method was experimentally validated with respect to its thermal control and energy saving, as reported in Chapter 5, and with respect to its predictions on CO_2 concentration distribution through carrying out additional experiments reported in Chapter 6. The detailed distributions of air flow, temperature and CO_2 concentration inside the bedroom where the A/C system was operated at different conditions with its supply outlet placed at 5 different heights were simulated using the validated CFD method. Based on the CFD simulation results, the operating performances of the A/C system at five different height settings in terms of ventilation effectiveness, thermal environmental control and energy saving were respectively evaluated using three separate indexes of VE, DR and EUC and using the TOPSIS method for the overall performance evaluation. The study results indicated that the best overall performance was achieved at a supply air temperature of 23 °C, an air flow rate of 50 l/s and a fresh air flow rate of 13 l/s at H1100 setting. Among the five height settings, the A/C system performed the best at H800 setting. However, the overall performance rankings depended on the weights assigned to

each index. Therefore, an assessor's preferences and the weight determination approach had also a role to play in influencing the overall performance evaluation of the studied A/C system.

4) In the last part of the programmed research work, an optimization study on the operating parameters (supply air temperature, supply air flow rate and supply air humidity) of the ductless bed-based TAC system at two different total insulation values of beddings and bed to achieve a thermally neutral sleeping environment with the minimum energy use was carried out and the study results are presented in Chapter 8. A CFD method was firstly applied to calculating the PMV and EUC values for 16 simulation cases. Based on the simulation results, the DOE method was applied to identifying operating parameters, individually or combined, which would significantly affect thermal neutrality and energy use, and linear regression models for PMV and EUC using the identified parameters were established, respectively. Thereafter, the linear regression models were used to obtain the optimum operating parameters of the bed-based TAC system, so that a thermally neutral sleeping environment can be maintained at a minimum energy use. The study results suggested that for a bed-based TAC system, at a specific total insulation value of beddings and bed, increases in supply air flow rate, supply air RH and supply air temperature would lead to a lower energy use when indoor thermal comfort was maintained. Under a given total insulation value of beddings and bed, jointly using the DOE method and CFD method can help find the optimum operating parameters of the bed-based TAC system, at which a thermally neutral sleeping environment was maintained at minimum energy use.

The outcomes of the completed programmed research work reported in this thesis have made significant contributions to studying the thermal environmental control, indoor air quality and energy efficiency using task\ambient air conditioning (TAC) systems in sleeping environments in the subtropics. This would in turn help maintain an appropriate indoor thermal environment and suitable air quality at a low energy use in sleeping environments in the sub-tropics. The long-term significance of the work is its contribution to developing advanced air conditioning technology for sleeping environments to achieve a high level of indoor thermal comfort and air quality for sleepers at a low energy use.

9.2 Proposed future work

A number of future studies following on the successful completion of the programmed research work reported in this thesis are proposed:

1) In the experimental study reported in Chapter 5, envelope heat gain to the experimental bedroom was considered but at a constant value of 504 w. However, Lin and Deng [2004] pointed out that the total cooling loads in bedrooms in Hong Kong, of which the envelope heat gain accounted for more than 70%, varied significantly overnight. Since envelope heat gain would impact the energy saving performance when using a bed-based TAC system in a bedroom, follow-up studies on using the bed-based TAC system with continuously varying envelope heat gain overnight should be therefore carried out.

2) The TOPSIS method has been employed to evaluate the overall performance of an A/C system at various operating conditions, through integrating individual performance indexes for ventilation effectiveness, thermal environmental control and energy saving, as reported in Chapter 7. However, the complexity and cost of the A/C system were not considered in the overall performance evaluation in the current study. In order to make an A/C system applicable to real life situation, these two factors should also be considered in the overall performance evaluation in a future study.

3) In the optimization study of the operating parameters reported in Chapter 8, only three operating parameters of the TAC system (supply air temperature, supply air flow rate and supply air relative humidity) were considered. Other factors, such as the total heat gain and its sensible heat ratio, different TAC system configurations, etc., should be considered in a future follow-up study.

Appendix A

Photos of the experimental setup

Photo 1 Overview of the environmental chamber

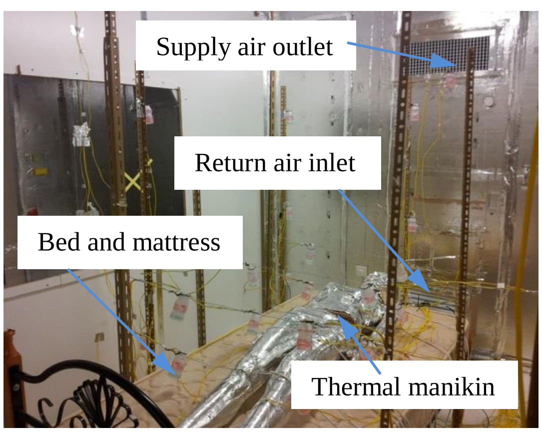

Photo 2 The experimental bedroom

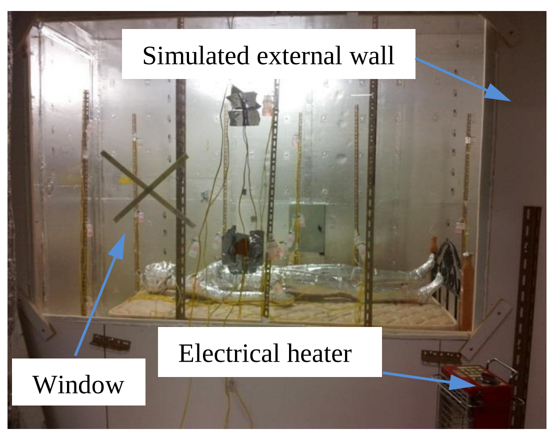

Photo 3 The outdoor environment

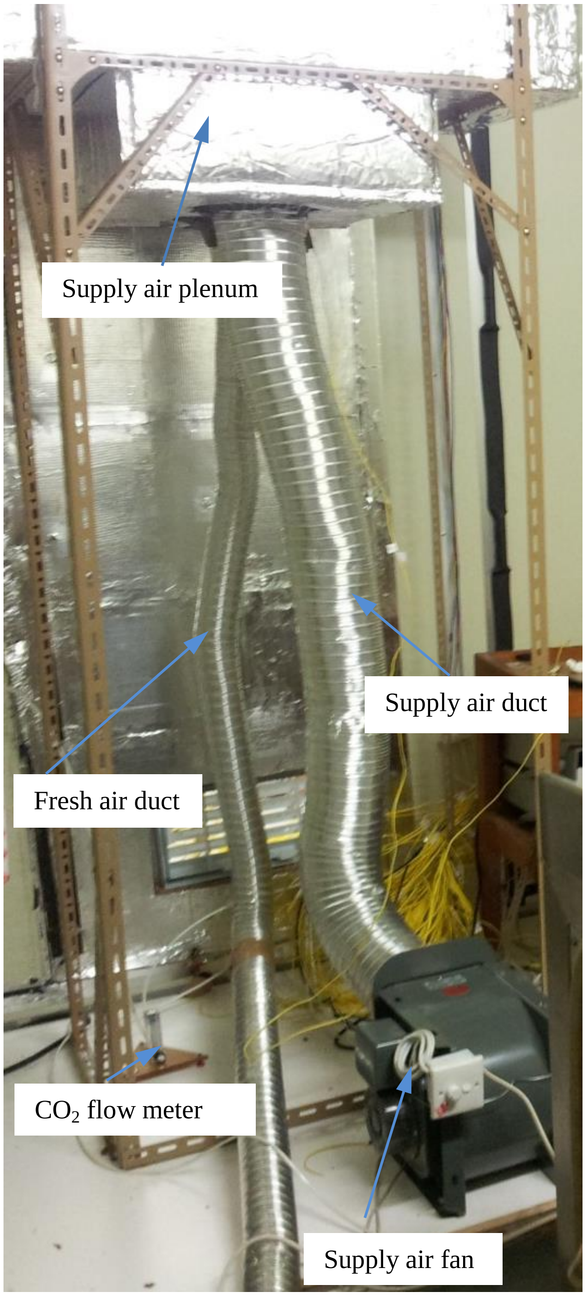

Photo 4 Supply air plenum and flexible ducts

Photo 5 Fresh air duct

Photo 6 The CO_2 tank

Photo 7 Load Generation Units

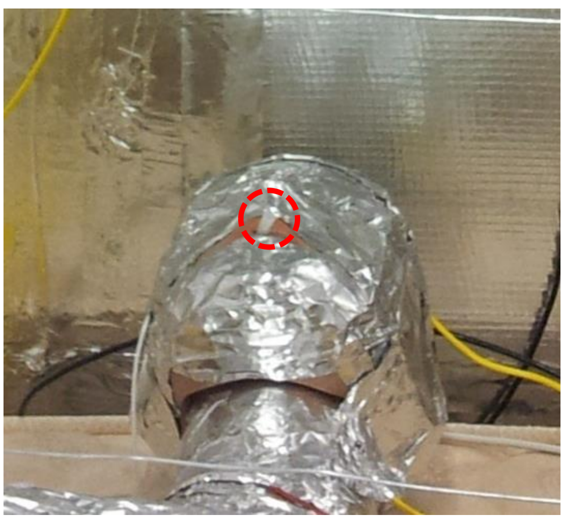

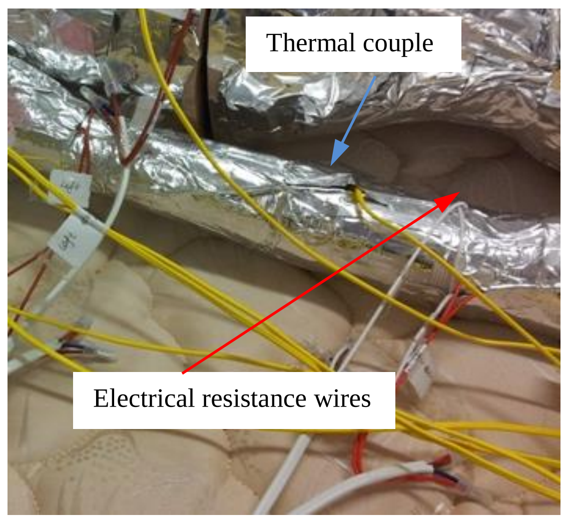

Photo 8 The CO_2 releasing outlet from the thermal manikin

Photo 9 Electric resistance wires and thermal couples used in the thermal manikin

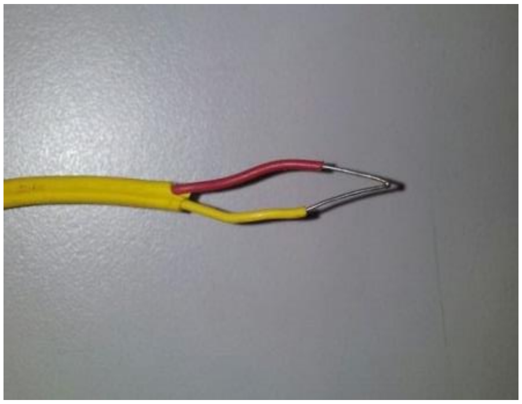

Photo 10 K-type Thermal Couple

Photo 11 TSI Air Velocity Transducer 8475

Photo 12 Air Flow Meter

Photo 13 Airdata Multimeter ADM-870

Photo 14 Telaire 7001 CO_2 Monitor

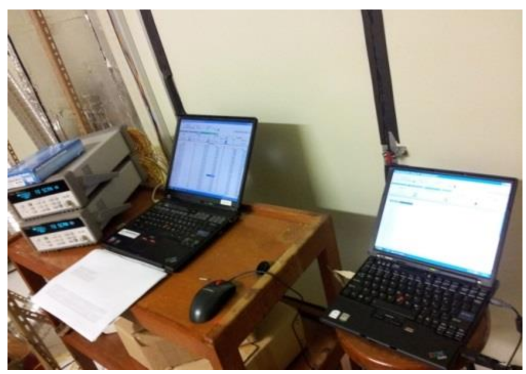

Photo 15 Agilent 34970A Data

Acquisition/Switch units

Appendix B

Experimentation and uncertainty analysis

According to the principles and theories [Coleman and Steele 1989, Cumming et al. 2007] on experimental error and uncertainty of measurement, calculation was carried out and results are listed as following.

Table B.1 Experimental errors for cases in Chapter 5

Cases	Location	Δt	Δv	ΔC	Δ Averaged DR		Δ EUC		Δ VE		Δ RH	
		(^{o}C)	(%)	(ppm)	FAC	TAC	FAC	TAC	FAC	TAC	FAC	TAC
1.1	-	1	4%	50	-	-	$\pm$0.16	$\pm$0.16	-	-	0.0022	0.0023
1.2	-	1	4%	50	-	-	0.07	0.24	-	-	0.002	0.0021
2.1	-	1	4%	50	-	0.64	-	-	-	-	-	-
2.2	-	1	4%	50	-	0.56	-	-	-	-	-	-
2.3	-	1	4%	50	-	0.54	-	-	-	-	-	-
3.1	-	1	4%	50	-	0.56	-	-	-	-	-	-
3.2	-	1	4%	50	-	0.72	-	-	-	-	-	-
3.3	-	1	4%	50	-	0.89	-	-	-	-	-	-
4.1	0.6	1	4%	50	-	-	-	-	-	0.026	-	-
	1.0	1	4%	50	-	-	-	-	-	0.043	-	-
4.2	0.6	1	4%	50	-	-	-	-	-	0.019	-	-
	1.0	1	4%	50	-	-	-	-	-	0.032	-	-
5.1	-	1	4%	50	-	0.72	-	0.18	-	-	-	-
5.2	-	1	4%	50	-	0.66	-	0.06	-	-	-	-
5.3	-	1	4%	50	-	0.14	-	0.11	-	-	-	-
6.1	-	1	4%	50	-	-	-	0.13	-	-	-	-
6.2	-	1	4%	50	-	-	-	0.25	-	-	-	-
1.2	0.6	1	4%	50	-	-	-	-	0.015	0.021	-	-
1.2	1.0	1	4%	50	-	-	-	-	0	0.046	-	-

Table B.2 Experimental uncertainties for cases in Chapter 5

Cases	Location	u(t)	u(v)	u(CO_2)	u(Averaged DR)		u(EUC)		VE		RH	
					FAC	TAC	FAC	TAC	FAC	TAC	FAC	TAC
1.1	-	0.58	0.023	28.87	-	-	$\pm$0.16	$\pm$0.16	-	-	0.0013	0.0013
1.2	-	0.58	0.023	28.87	-	-	0.07	0.24	-	-	0.0012	0.0012
2.1	-	0.58	0.023	28.87	-	0.37	-	-	-	-	-	-
2.2	-	0.58	0.023	28.87	-	0.32	-	-	-	-	-	-
2.3	-	0.58	0.023	28.87	-	0.31	-	-	-	-	-	-
3.1	-	0.58	0.023	28.87	-	0.32	-	-	-	-	-	-
3.2	-	0.58	0.023	28.87	-	0.41	-	-	-	-	-	-
3.3	-	0.58	0.023	28.87	-	0.51	-	-	-	-	-	-
4.1	0.6	0.58	0.023	28.87	-	-	-	-	-	0.075	-	-
	1.0	0.58	0.023	28.87	-	-	-	-	-	0.12	-	-
4.2	0.6	0.58	0.023	28.87	-	-	-	-	-	0.055	-	-
	1.0	0.58	0.023	28.87	-	-	-	-	-	0.092	-	-
5.1	-	0.58	0.023	28.87	-	0.41	-	0.10	-	-	-	-
5.2	-	0.58	0.023	28.87	-	0.38	-	0.037	-	-	-	-
5.3	-	0.58	0.023	28.87	-	0.080	-	0.064	-	-	-	-
6.1	-	0.58	0.023	28.87	-	-	-	0.07	-	-	-	-
6.2	-	0.58	0.023	28.87	-	-	-	0.15	-	-	-	-
1.2	0.6	0.58	0.023	28.87	-	-	-	-	0.044	0.060	-	-
1.2	1.0	0.58	0.023	28.87	-	-	-	-	0	0.13	-	-

Table B.3 Experimental errors for cases in Chapter 6

Group	Case No.	EUC		DR	
		Setting 1	Setting 2	Setting 1	Setting 2
1	1.1	-	-	0.54	0.50
	1.2	-	-	0.67	0.65
	1.3	-	-	0.83	0.76
2	2.1	-	-	0.64	0.53
	2.2	-	-	0.56	0.49
	2.3	-	-	0.54	0.54
3	3.1	-	-	-	-
	3.2	-	-	-	-
4	4.1	0.082	0.081	-	-
	4.2	0.13	0.14	-	-
	4.3	0.16	0.17	-	-
5	5.1	0.03	0.028	-	-
	5.2	0.056	0.064	-	-
	5.3	0.067	0.064	-	-

Table B.4 Experimental uncertainties for cases in Chapter 6

Group	Case No.	EUC		DR	
		Setting 1	Setting 2	Setting 1	Setting 2
1	1.1	-	-	0.31	0.29
	1.2	-	-	0.39	0.37
	1.3	-	-	0.48	0.44
2	2.1	-	-	0.37	0.30
	2.2	-	-	0.32	0.28
	2.3	-	-	0.31	0.29
3	3.1	-	-	-	-
	3.2	-	-	-	-
4	4.1	0.047	0.047	-	-
	4.2	0.074	0.082	-	-
	4.3	0.094	0.097	-	-
5	5.1	0.094	0.097	-	-
	5.2	0.14	0.15	-	-
	5.3	0.15	0.15	-	-

Table B.5 Experimental errors and uncertainties of DR values for cases 3.1 in Chapter 6

Positions	Setting 1		Setting 2	
	Error	Uncertainty	Error	uncertainty
I 0.8	0.62	0.36	0.51	0.29
I 1.0	4.21	2.43	2.88	1.66
J 0.8	2.66	1.54	2.33	1.34
J 1.0	3.10	1.79	2.07	1.19
K 0.8	2.79	1.61	2.02	1.17
K 1.0	1.40	0.81	0.71	0.41
L 0.8	2.02	1.17	2.23	1.29
L 1.0	1.06	0.61	1.12	0.65
M 0.8	2.02	1.17	2.15	1.24
M 1.0	1.35	0.78	1.34	0.77
N 0.8	0.82	0.47	0.49	0.28
N 1.0	1.83	1.06	2.03	1.17

Table B.6 Experimental errors and uncertainties of DR values for cases 3.2 in Chapter 6

Positions	Setting 1		Setting 2	
	Error	Uncertainty	Error	uncertainty
I 0.8	0.59	0.59	0.72	0.72
I 1.0	5.76	5.76	5.09	5.09
J 0.8	1.94	1.94	2.11	2.11
J 1.0	4.98	4.98	4.22	4.22
K 0.8	2.67	2.67	2.44	2.44
K 1.0	4.63	4.63	3.98	3.98
L 0.8	2.06	2.06	3.05	3.05
L 1.0	2.12	2.12	4.17	4.17
M 0.8	1.48	1.48	2.23	2.23
M 1.0	2.74	2.74	4.79	4.79
N 0.8	0.75	0.75	0.45	0.45
N 1.0	4.43	4.43	3.97	3.97

Appendix C

Calculation procedures of TOPSIS method

The TOPSIS method can be summarized in a series of steps, shown in Fig. C.1. The calculation of TOPSIS method was detailed presented as following:

Step 1: Calculate the original values of the three indexes (VE, DR and EUC) at various study cases.

Table C.1 Original values of the three indexes

Settings	Case no.	Criteria		
		VE	DR	EUC
H800	1.1	0.59	0.04	0.96
	1.2	1.51	5.82	1.4
	1.3	4.36	13.4	2.04
	1.4	6.12	17.82	2.15
	1.5	1.01	5.93	1.4
	1.6	3.87	6.1	1.41
	1.7	1.51	4.67	1.38
	1.8	1.44	3.43	1.39
	1.9	1.54	2.17	0.99
H1100	2.1	0.54	0.3	0.97
	2.2	2.17	8.49	1.69
	2.3	2.07	11.45	2.01
	2.4	2.18	14.59	1.68
	2.5	1.49	8.51	1.69
	2.6	8.20	8.68	1.7
	2.7	2.05	7.22	1.69
	2.8	2.43	6.26	2
	2.9	2.09	4.58	1.94

Table C.1 Original values of the three indexes (continued)

Settings	Case no.	Criteria		
		VE	DR	EUC
H1400	3.1	0.52	0.06	1.00
	3.2	0.74	5.88	1.26
	3.3	0.34	3.31	0.89
	3.4	0.58	2.03	1.05
	3.5	0.73	5.85	1.25
	3.6	2.12	5.71	1.26
	3.7	0.90	4.5	1.28
	3.8	0.95	3.11	1.27
	3.9	1.02	1.62	1.09
H1700	4.1	0.62	0.17	1.00
	4.2	0.92	4.68	1.1
	4.3	0.47	1.69	0.97
	4.4	0.51	3.01	0.88
	4.5	0.43	4.93	1.08
	4.6	1.22	5.01	1.08
	4.7	0.82	3.25	1.11
	4.8	0.79	2.17	1.11
	4.9	0.66	1.14	1.07
H2000	5.1	0.77	0.26	1.00
	5.2	0.44	3.33	0.99
	5.3	0.39	1.02	0.92
	5.4	0.27	2.18	0.82
	5.5	0.45	3.13	1.00
	5.6	1.57	3.22	0.98
	5.7	0.36	2.5	1.03
	5.8	0.69	1.61	1.00
	5.9	0.36	0.77	0.99

Step 2: Calculate weights for each index using two approaches: Entropy approach and AHP approach. Following the methods shown in Figs. C.1 and C.2, the weights were calculated and shown in Table 7.3 in Chapter 7.

Step1 Calculate normalized values of the three indexes

$$r_{ij}(x) = x_{ij} / \sum_{i=1}^{n} x_{ij} \quad \text{for } i=1, \cdots, \text{m}; \ j=1, \cdots, \text{n}$$

Step2 Calculate the entropy E_j of the data of index j.

Where K=1/ln$n$, which guarantees $0 \leqslant E_j \leqslant 1$

Step3 Calculate the degree of divergence (dj) of average intrinsic information contained by each index. c_j according to d_j=1-E_j

Step4 Calculate the weight for each index.

$$w_j = d_j / \sum_{k=1}^{m} d_k$$

Fig. C.1 Calculation method of entropy approach

Step1 Construct a pair - wise comparison matrix of indexes

$$C = \begin{bmatrix} 1 & C_{12} & C_{13} \\ C_{21} & 1 & C_{23} \\ C_{31} & C_{32} & 1 \end{bmatrix}$$

Where c_{ij} denotes the comparative importance of index i with respect to index j. In the matrix, c_{ij}=1 when $i=j$, and $c_{ij}=1/c_{ji}$.

Step2 Calculate the eigenvalue λ_{max} of comparison matrix.
The principaleigen vector w corresponding to λ_{max} of the above matrix represents the relative weights of the decision criteria is calculated.

Fig. C.2 Calculation method of AHP approach

Step 3: Calculate weighted normalized values of the three indexes.

The values calculated using different weights were presented in Tables C.2 – C.9.

Table C.2 Weighted normalized values of the three indexes using entropy approach

Settings	Cases	Criteria		
		VE	DR	EUC
H800	1.1	0.05	0.07	0.01
	1.2	0.02	0.00	0.01
	1.3	0.06	0.05	0.01
	1.4	0.17	0.13	0.01
	1.5	0.24	0.17	0.01
	1.6	0.04	0.06	0.01
	1.7	0.15	0.06	0.01
	1.8	0.06	0.04	0.01
	1.9	0.06	0.03	0.01
H1100	2.1	0.06	0.08	0.01
	2.2	0.02	0.00	0.01
	2.3	0.08	0.08	0.01
	2.4	0.08	0.11	0.01
	2.5	0.09	0.14	0.01
	2.6	0.06	0.08	0.01
	2.7	0.32	0.08	0.01
	2.8	0.08	0.07	0.01
	2.9	0.10	0.06	0.01
H1400	3.1	0.03	0.07	0.01
	3.2	0.02	0.00	0.01
	3.3	0.03	0.06	0.01
	3.4	0.01	0.03	0.00
	3.5	0.02	0.02	0.01
	3.6	0.03	0.06	0.01
	3.7	0.08	0.05	0.01
	3.8	0.04	0.04	0.01
	3.9	0.04	0.03	0.01
H1700	4.1	0.03	0.06	0.01
	4.2	0.02	0.00	0.01
	4.3	0.04	0.04	0.01
	4.4	0.02	0.02	0.01
	4.5	0.02	0.03	0.00
	4.6	0.02	0.05	0.01
	4.7	0.05	0.05	0.01
	4.8	0.03	0.03	0.01
	4.9	0.03	0.02	0.01
H2000	5.1	0.03	0.04	0.01
	5.2	0.03	0.00	0.01
	5.3	0.02	0.03	0.01
	5.4	0.02	0.01	0.01
	5.5	0.01	0.02	0.00
	5.6	0.02	0.03	0.01
	5.7	0.06	0.03	0.01
	5.8	0.01	0.02	0.01
	5.9	0.03	0.02	0.01

Table C.3 Weighted normalized values of the three indexes using AV1 preference order

Settings	Cases	Criteria		
		VE	DR	EUC
H800	1.1	0.05	0.05	0.03
	1.2	0.02	0.00	0.02
	1.3	0.06	0.04	0.03
	1.4	0.17	0.09	0.04
	1.5	0.24	0.12	0.04
	1.6	0.04	0.04	0.03
	1.7	0.15	0.04	0.03
	1.8	0.06	0.03	0.03
	1.9	0.06	0.02	0.03
H1100	2.1	0.06	0.06	0.03
	2.2	0.02	0.00	0.02
	2.3	0.08	0.06	0.03
	2.4	0.08	0.08	0.04
	2.5	0.08	0.10	0.03
	2.6	0.06	0.06	0.03
	2.7	0.32	0.06	0.03
	2.8	0.08	0.05	0.03
	2.9	0.09	0.04	0.04
H1400	3.1	0.03	0.05	0.02
	3.2	0.02	0.00	0.02
	3.3	0.03	0.04	0.02
	3.4	0.01	0.02	0.02
	3.5	0.02	0.01	0.02
	3.6	0.03	0.04	0.02
	3.7	0.08	0.04	0.02
	3.8	0.03	0.03	0.02
	3.9	0.04	0.02	0.02
H1700	4.1	0.03	0.05	0.02
	4.2	0.02	0.00	0.02
	4.3	0.04	0.03	0.02
	4.4	0.02	0.01	0.02
	4.5	0.02	0.02	0.02
	4.6	0.02	0.03	0.02
	4.7	0.05	0.03	0.02
	4.8	0.03	0.02	0.02
	4.9	0.03	0.02	0.02
H2000	5.1	0.03	0.03	0.02
	5.2	0.03	0.00	0.02
	5.3	0.02	0.02	0.02
	5.4	0.02	0.01	0.02
	5.5	0.01	0.02	0.02
	5.6	0.02	0.02	0.02
	5.7	0.06	0.02	0.02
	5.8	0.01	0.02	0.02
	5.9	0.03	0.01	0.02

Table C.4 Weighted normalized values of the three indexes using AV2 preference order

Settings	Cases	Criteria		
		VE	DR	EUC
H800	1.1	0.05	0.03	0.05
	1.2	0.02	0.00	0.03
	1.3	0.06	0.02	0.05
	1.4	0.17	0.05	0.07
	1.5	0.24	0.07	0.07
	1.6	0.04	0.02	0.05
	1.7	0.15	0.02	0.05
	1.8	0.06	0.02	0.05
	1.9	0.06	0.01	0.05
H1100	2.1	0.06	0.03	0.05
	2.2	0.02	0.00	0.03
	2.3	0.08	0.03	0.06
	2.4	0.08	0.04	0.07
	2.5	0.08	0.06	0.06
	2.6	0.06	0.03	0.06
	2.7	0.32	0.03	0.06
	2.8	0.08	0.03	0.06
	2.9	0.09	0.02	0.07
H1400	3.1	0.03	0.03	0.04
	3.2	0.02	0.00	0.03
	3.3	0.03	0.02	0.04
	3.4	0.01	0.01	0.03
	3.5	0.02	0.01	0.04
	3.6	0.03	0.02	0.04
	3.7	0.08	0.02	0.04
	3.8	0.03	0.02	0.04
	3.9	0.04	0.01	0.04
H1700	4.1	0.03	0.03	0.04
	4.2	0.02	0.00	0.03
	4.3	0.04	0.02	0.04
	4.4	0.02	0.01	0.03
	4.5	0.02	0.01	0.03
	4.6	0.02	0.02	0.04
	4.7	0.05	0.02	0.04
	4.8	0.03	0.01	0.04
	4.9	0.03	0.01	0.04
H2000	5.1	0.03	0.02	0.03
	5.2	0.03	0.00	0.03
	5.3	0.02	0.01	0.03
	5.4	0.02	0.00	0.03
	5.5	0.01	0.01	0.03
	5.6	0.02	0.01	0.03
	5.7	0.06	0.01	0.03
	5.8	0.01	0.01	0.03
	5.9	0.03	0.01	0.03

Table C.5 Weighted normalized values of the three indexes using AD1 preference order

Settings	Cases	Criteria		
		VE	DR	EUC
H800	1.1	0.03	0.09	0.03
	1.2	0.01	0.00	0.02
	1.3	0.03	0.07	0.03
	1.4	0.09	0.17	0.04
	1.5	0.13	0.22	0.04
	1.6	0.02	0.07	0.03
	1.7	0.08	0.08	0.03
	1.8	0.03	0.06	0.03
	1.9	0.03	0.04	0.03
H1100	2.1	0.03	0.11	0.03
	2.2	0.01	0.00	0.02
	2.3	0.05	0.11	0.03
	2.4	0.04	0.14	0.04
	2.5	0.05	0.18	0.03
	2.6	0.03	0.11	0.03
	2.7	0.17	0.11	0.03
	2.8	0.04	0.09	0.03
	2.9	0.05	0.08	0.04
H1400	3.1	0.02	0.09	0.02
	3.2	0.01	0.00	0.02
	3.3	0.02	0.07	0.02
	3.4	0.01	0.04	0.02
	3.5	0.01	0.03	0.02
	3.6	0.02	0.07	0.02
	3.7	0.04	0.07	0.02
	3.8	0.02	0.06	0.02
	3.9	0.02	0.04	0.02
H1700	4.1	0.02	0.08	0.02
	4.2	0.01	0.00	0.02
	4.3	0.02	0.06	0.02
	4.4	0.01	0.02	0.02
	4.5	0.01	0.04	0.02
	4.6	0.01	0.06	0.02
	4.7	0.03	0.06	0.02
	4.8	0.02	0.04	0.02
	4.9	0.02	0.03	0.02
H2000	5.1	0.02	0.05	0.02
	5.2	0.02	0.00	0.02
	5.3	0.01	0.04	0.02
	5.4	0.01	0.01	0.02
	5.5	0.01	0.03	0.02
	5.6	0.01	0.04	0.02
	5.7	0.03	0.04	0.02
	5.8	0.01	0.03	0.02
	5.9	0.01	0.02	0.02

Table C.6 Weighted normalized values of the three indexes using AD2 preference order

Settings	Cases	Criteria		
		VE	DR	EUC
H800	1.1	0.02	0.09	0.05
	1.2	0.01	0.00	0.03
	1.3	0.02	0.07	0.05
	1.4	0.05	0.17	0.07
	1.5	0.07	0.22	0.07
	1.6	0.01	0.07	0.05
	1.7	0.05	0.08	0.05
	1.8	0.02	0.06	0.05
	1.9	0.02	0.04	0.05
H1100	2.1	0.02	0.11	0.05
	2.2	0.01	0.00	0.03
	2.3	0.03	0.11	0.06
	2.4	0.02	0.14	0.07
	2.5	0.03	0.18	0.06
	2.6	0.02	0.11	0.06
	2.7	0.10	0.11	0.06
	2.8	0.02	0.09	0.06
	2.9	0.03	0.08	0.07
H1400	3.1	0.01	0.09	0.04
	3.2	0.01	0.00	0.03
	3.3	0.01	0.07	0.04
	3.4	0.00	0.04	0.03
	3.5	0.01	0.03	0.04
	3.6	0.01	0.07	0.04
	3.7	0.02	0.07	0.04
	3.8	0.01	0.06	0.04
	3.9	0.01	0.04	0.04
H1700	4.1	0.01	0.08	0.04
	4.2	0.01	0.00	0.03
	4.3	0.01	0.06	0.04
	4.4	0.01	0.02	0.03
	4.5	0.01	0.04	0.03
	4.6	0.01	0.06	0.04
	4.7	0.01	0.06	0.04
	4.8	0.01	0.04	0.04
	4.9	0.01	0.03	0.04
H2000	5.1	0.01	0.05	0.03
	5.2	0.01	0.00	0.03
	5.3	0.01	0.04	0.03
	5.4	0.00	0.01	0.03
	5.5	0.00	0.03	0.03
	5.6	0.01	0.04	0.03
	5.7	0.02	0.04	0.03
	5.8	0.00	0.03	0.03
	5.9	0.01	0.02	0.03

Table C.7 Weighted normalized values of the three indexes using AE1 preference order

Settings	Cases	Criteria		
		VE	DR	EUC
H800	1.1	0.03	0.03	0.08
	1.2	0.01	0.00	0.06
	1.3	0.03	0.02	0.09
	1.4	0.09	0.05	0.12
	1.5	0.13	0.07	0.13
	1.6	0.02	0.02	0.09
	1.7	0.08	0.02	0.09
	1.8	0.03	0.02	0.08
	1.9	0.03	0.01	0.08
H1100	2.1	0.03	0.03	0.10
	2.2	0.01	0.00	0.06
	2.3	0.05	0.03	0.10
	2.4	0.04	0.04	0.12
	2.5	0.05	0.06	0.10
	2.6	0.03	0.03	0.10
	2.7	0.17	0.03	0.10
	2.8	0.04	0.03	0.10
	2.9	0.05	0.02	0.12
H1400	3.1	0.02	0.03	0.08
	3.2	0.01	0.00	0.06
	3.3	0.02	0.02	0.08
	3.4	0.01	0.01	0.05
	3.5	0.01	0.01	0.06
	3.6	0.02	0.02	0.08
	3.7	0.04	0.02	0.08
	3.8	0.02	0.02	0.08
	3.9	0.02	0.01	0.08
H1700	4.1	0.02	0.03	0.07
	4.2	0.01	0.00	0.06
	4.3	0.02	0.02	0.07
	4.4	0.01	0.01	0.06
	4.5	0.01	0.01	0.05
	4.6	0.01	0.02	0.07
	4.7	0.03	0.02	0.07
	4.8	0.02	0.01	0.07
	4.9	0.02	0.01	0.07
H2000	5.1	0.02	0.02	0.06
	5.2	0.02	0.00	0.06
	5.3	0.01	0.01	0.06
	5.4	0.01	0.00	0.06
	5.5	0.01	0.01	0.05
	5.6	0.01	0.01	0.06
	5.7	0.03	0.01	0.06
	5.8	0.01	0.01	0.06
	5.9	0.01	0.01	0.06

Table C.8 Weighted normalized values of the three indexes using AE2 preference order

Settings	Cases	Criteria		
		VE	DR	EUC
H800	1.1	0.02	0.05	0.08
	1.2	0.01	0.00	0.06
	1.3	0.02	0.04	0.09
	1.4	0.05	0.09	0.12
	1.5	0.07	0.12	0.13
	1.6	0.01	0.04	0.09
	1.7	0.05	0.04	0.09
	1.8	0.02	0.03	0.08
	1.9	0.02	0.02	0.08
H1100	2.1	0.02	0.06	0.10
	2.2	0.01	0.00	0.06
	2.3	0.03	0.06	0.10
	2.4	0.02	0.08	0.12
	2.5	0.03	0.10	0.10
	2.6	0.02	0.06	0.10
	2.7	0.10	0.06	0.10
	2.8	0.02	0.05	0.10
	2.9	0.03	0.04	0.12
H1400	3.1	0.01	0.05	0.08
	3.2	0.01	0.00	0.06
	3.3	0.01	0.04	0.08
	3.4	0.00	0.02	0.05
	3.5	0.01	0.01	0.06
	3.6	0.01	0.04	0.08
	3.7	0.02	0.04	0.08
	3.8	0.01	0.03	0.08
	3.9	0.01	0.02	0.08
H1700	4.1	0.01	0.05	0.07
	4.2	0.01	0.00	0.06
	4.3	0.01	0.03	0.07
	4.4	0.01	0.01	0.06
	4.5	0.01	0.02	0.05
	4.6	0.01	0.03	0.07
	4.7	0.01	0.03	0.07
	4.8	0.01	0.02	0.07
	4.9	0.01	0.02	0.07
H2000	5.1	0.01	0.03	0.06
	5.2	0.01	0.00	0.06
	5.3	0.01	0.02	0.06
	5.4	0.00	0.01	0.06
	5.5	0.00	0.02	0.05
	5.6	0.01	0.02	0.06
	5.7	0.02	0.02	0.06
	5.8	0.00	0.02	0.06
	5.9	0.01	0.01	0.06

Step 4: Calculate the positive and negative ideal solutions.

Table C.9 Positive and negative ideal solutions using objective and subjective approaches

Ideal solution	Approach	VE	DR	EUC
	Entropy	0.3211	0.0004	0.0120
	AV1	0.3160	0.0003	0.0398
	AV2	0.3160	0.0002	0.0722
Positive ideal solution	AD1	0.1739	0.0005	0.0398
	AD2	0.0958	0.0005	0.0722
	AE1	0.1739	0.0002	0.1312
	AE2	0.0958	0.0003	0.1312
	Entropy	0.0106	0.1677	0.0046
	AV1	0.0104	0.1238	0.0152
	AV2	0.0104	0.0682	0.0275
Negative ideal solution	AD1	0.0057	0.2250	0.0152
	AD2	0.0032	0.2250	0.0275
	AE1	0.0057	0.0682	0.0501
	AE2	0.0032	0.1238	0.0501

Step 5: Calculate the similarities of each study case to the ideal solutions and rankings of each study case using objective and subjective approaches.

Table C.10 Similarities of study cases calculated by TOPSIS method

Settings	Study case no.	Entropy	AHP					
			AV1	AV2	AD1	AD2	AE1	AE2
H800	1.1	0.2844	0.2426	0.1870	0.4479	0.5312	0.2742	0.4443
	1.2	0.3602	0.2968	0.1897	0.5796	0.6974	0.2802	0.5190
	1.3	0.3149	0.2701	0.2099	0.4905	0.5828	0.297	0.4808
	1.4	0.4579	0.4814	0.5111	0.3605	0.3251	0.5453	0.4755
	1.5	0.5518	0.6063	0.6862	0.356	0.2655	0.6465	0.4574
	1.6	0.2873	0.2389	0.1698	0.4706	0.5688	0.2709	0.4646
	1.7	0.5001	0.4829	0.4635	0.5811	0.6201	0.4767	0.5523
	1.8	0.3337	0.2848	0.2168	0.5222	0.6243	0.3057	0.5049
	1.9	0.3491	0.2960	0.2194	0.55	0.6624	0.3154	0.5303
H1100	2.1	0.2593	0.2288	0.1952	0.3903	0.4567	0.2956	0.4266
	2.2	0.3552	0.2921	0.1859	0.5744	0.6933	0.2764	0.5153
	2.3	0.3162	0.2924	0.2690	0.4295	0.4893	0.3593	0.4748
	2.4	0.2608	0.2547	0.2583	0.3209	0.3643	0.3839	0.4499
	2.5	0.2288	0.2368	0.2508	0.2104	0.2171	0.3217	0.3265
	2.6	0.2668	0.2351	0.2014	0.4053	0.4775	0.317	0.4544
	2.7	0.7984	0.8376	0.8948	0.6516	0.5781	0.8072	0.6535
	2.8	0.3275	0.2960	0.2620	0.4681	0.5428	0.3604	0.5035
	2.9	0.3715	0.3419	0.3137	0.5152	0.5968	0.4348	0.5790
H1400	3.1	0.2537	0.2091	0.1451	0.4207	0.5056	0.2356	0.4115
	3.2	0.3576	0.2944	0.1875	0.5773	0.6967	0.2802	0.5210
	3.3	0.277	0.2268	0.1504	0.4632	0.5623	0.2421	0.4418
	3.4	0.3063	0.2487	0.1538	0.5139	0.6266	0.2324	0.4529
	3.5	0.3328	0.2726	0.1733	0.5476	0.6671	0.2626	0.4962
	3.6	0.2772	0.2268	0.1499	0.4637	0.563	0.2409	0.4411
	3.7	0.3563	0.3171	0.2668	0.5158	0.596	0.3192	0.4820
	3.8	0.3067	0.2530	0.1712	0.5051	0.614	0.2662	0.4799
	3.9	0.3307	0.2738	0.1851	0.5391	0.6562	0.2824	0.5086
H1700	4.1	0.2689	0.2205	0.1461	0.4459	0.5344	0.2164	0.4054
	4.2	0.3596	0.2964	0.1900	0.579	0.6977	0.2818	0.5216
	4.3	0.3045	0.2509	0.1673	0.5004	0.6039	0.246	0.4558
	4.4	0.334	0.2732	0.1719	0.55	0.6691	0.2587	0.4921
	4.5	0.316	0.2574	0.1609	0.5254	0.6377	0.2396	0.4610
	4.6	0.283	0.2293	0.1431	0.4791	0.5853	0.2256	0.4377
	4.7	0.3127	0.2616	0.1851	0.5016	0.5984	0.2535	0.4529
	4.8	0.3233	0.2658	0.1740	0.5311	0.645	0.2604	0.4850
	4.9	0.3383	0.2786	0.1816	0.5521	0.6708	0.272	0.5045
H2000	5.1	0.3069	0.2510	0.1614	0.5087	0.616	0.2396	0.4554
	5.2	0.3639	0.3008	0.1953	0.5826	0.7001	0.2854	0.5235
	5.3	0.3089	0.2513	0.1567	0.5168	0.631	0.2393	0.4633
	5.4	0.3408	0.2790	0.1752	0.5586	0.6777	0.2621	0.4969
	5.5	0.3211	0.2614	0.1622	0.5343	0.65	0.2425	0.4669
	5.6	0.3123	0.2542	0.1589	0.5215	0.6368	0.2427	0.4684
	5.7	0.3592	0.3054	0.2252	0.5577	0.6592	0.285	0.4891
	5.8	0.319	0.2599	0.1626	0.5317	0.651	0.2501	0.4813
	5.9	0.3426	0.2815	0.1806	0.5586	0.6767	0.2675	0.5009

Table C.11 Overall rankings of study cases based on similarities calculated by TOPSIS method

Settings	Study case no.	Entropy	AHP					
			AV1	AV2	AD1	AD2	AE1	AE2
H800	1.1	36	36	21	36	37	23	38
	1.2	7	9	19	4	3	20	8
	1.3	27	23	14	30	30	14	22
	1.4	4	4	3	42	43	3	24
	1.5	2	2	2	43	44	2	31
	1.6	35	37	32	32	32	25	28
	1.7	3	3	4	3	22	4	3
	1.8	18	16	13	20	21	13	11
	1.9	13	11	12	12	11	12	4
H1100	2.1	43	41	17	41	41	15	42
	2.2	12	15	22	7	5	22	9
	2.3	25	14	6	38	39	8	25
	2.4	42	29	9	44	42	6	37
	2.5	45	38	10	45	45	9	45
	2.6	41	39	15	40	40	11	34
	2.7	1	1	1	1	31	1	1
	2.8	21	12	8	33	35	7	13
	2.9	5	5	5	24	27	5	2
H1400	3.1	44	45	44	39	38	42	43
	3.2	10	13	20	6	4	21	7
	3.3	39	42	41	35	34	37	39
	3.4	33	35	40	25	20	43	35
	3.5	19	22	29	14	10	28	16
	3.6	38	43	42	34	33	38	40
	3.7	11	6	7	23	28	10	20
	3.8	32	31	31	27	24	27	23
	3.9	20	20	23	15	13	18	10
H1700	4.1	40	44	43	37	36	45	44
	4.2	8	10	18	5	2	19	6
	4.3	34	34	33	29	25	34	32
	4.4	17	21	30	13	9	31	17
	4.5	26	28	37	19	17	39	30
	4.6	37	40	45	31	29	44	41
	4.7	28	25	24	28	26	32	36
	4.8	22	24	28	18	16	30	19
	4.9	16	19	25	11	8	24	12
H2000	5.1	31	33	36	26	23	40	33
	5.2	6	8	16	2	1	16	5
	5.3	30	32	39	22	19	41	29
	5.4	15	18	27	8	6	29	15
	5.5	23	26	35	16	15	36	27
	5.6	29	30	38	21	18	35	26
	5.7	9	7	11	10	12	17	18
	5.8	24	27	34	17	14	33	21
	5.9	14	17	26	9	7	26	14

References

[1] ACGIH
Documentation of the Threshold Limit Values and Biological Exposure Indices, 7th Edition, American Conference of Governmental Industrial Hygienists, Inc., Cincinnati, OH 1991

[2] Akerstedt and Nilsson 2003
Akerstedt, T. and Nilsson P.M.
Sleep as restitution: an introduction. *Journal of Internal Medicine*, 2003, Vol. 254, No. 1, pp. 6-12 (2003)

[3] Amai et al. 2007
Amai, H., Tanabe, S., Akimoto, T. and Genma, T.
Thermal sensation and comfort with different task conditioning system. *Building and Environment*, 2007, Vol. 42, No. 12, pp. 3955-3964 (2007)

[4] ANSYS FLUENT User's Guide 2010
ANSYS FLUENT User's Guide. *ANSYS, Inc*. Southpointe (2010)

[5] Antony 2003
Antony, J.
Design of Experiments for Engineers and Scientists, Butterworth-Heinemann, New York, 2003.

[6] Arens et al. 1991
Arens, E.A., Bauman, F.S., Johnston, L.P. and Zhang, H.
Testing of localized ventilation systems in a new controlled environment chamber. *Indoor Air*, 1991, Vol. 1, No. 3, pp. 263-281 (1991)

[7] Argon 1994
Argon Corporation
The Argon system. Naples, FL: Argon Corporation, November (1994)

[8] Arun and Tulapurkara 2005
Arun, M. and Tulapurkara, E.G.
Computation of turbulent flow inside an enclosure with central partition. *Progress in Computational Fluid Dynamics*, 2005, Vol. 5, pp. 455-465 (2005)

[9] ASHRAE Standard 55-2013
ASHRAE
ASHRAE Standard 55-2013, Thermal Environmental Conditions for Human Occupancy (2013)

[10] ASHRAE Handbook 2013
Handbook of Fundamentals (2013)

[11] ASHRAE Standard 113-2013
ASHRAE
ASHRAE Standard 113-2013, Method of Testing for Room Air Diffusion (2009)

[12] ASHRAE Standard 62.1-2013
ASHRAE
ASHRAE Standard 62.1-2013, Ventilation for Acceptable Indoor Air Quality (2013)

[13] Bauman et al. 1993
Bauman, F.S., Zhang, H., Arens, E.A. and Benton, C.
Localized comfort control with a desktop task conditioning system: laboratory and field measurements. *ASHARE Transactions*, 1993, Vol. 99, Pt. 2, pp. 733-749 (1993)

[14] Bauman et al. 1995
Bauman, F.S., Arens, E.A., Tanabe, S., Zhang, H. and Baharlo, A.
Testing and optimizing the performance of a floor-based task conditioning system. *Energy and Buildings*, 1995, Vol. 22, No. 3, pp. 173-186 (1995)

[15] Bauman and Arens 1996
Bauman, F.S. and Arens, E.A.
Task/ambient conditioning systems: engineering and application guidelines. Research Report. Center for Environment Design Research, University of California, Berkeley (1996)

[16] Bauman et al. 1998
Bauman, F.S., Carter, T.G., Baughman, A.V. and Arens, E.A.,
Field Study of the Impact of a Desktop Task/Ambient Conditioning System in Office Buildings, *ASHRAE Transactions*, 1998, Vol. 104, No. 1, pp. 125-142 (1998)

[17] Bauman 1999
Bauman, F.S.
Giving Occupants What They Want: Guidelines for Implementing Personal Environmental Control in Your Building. *Proceedings, World Workplace 99*, 1999, pp. 447-459 (1999)

[18] Benington and Frank 2003
Benington, J.H. and Frank, M.G.
Cellular and molecular connections between sleep and synaptic plasticity. *Progress in Newrobiol*, 2003, Vol. 69 No. 2, pp. 77-101 (2003)

[19] Berthon-Jones and Sullivan 1984
Berthon-Jones, M. and Sullivan, C.E.
Ventilation and arousal responses to hypercapnia in normal sleeping humans. *Journal of applied physiology: respiratory, environmental and exercise physiology*, 1984, Vol. 57, No. 1, pp. 59-67 (1984)

[20] Bojic et al. 2002
Bojic M., Yik F., Wan K. and Burnett J.
Infuence of envelope and partition characteristics on the space cooling of high-rise residential buildings in Hong Kong. *Building and Environment*, 2002, Vol. 37, pp. 347-355 (2002)

[21] Brohus and Nielsen 1995
Brohus, H., and Nielsen, P.V.
Personal exposure to contaminant sources in uniform velocity field. *Proceedings of Healthy Buildings' 95*, 1995, No.3, pp. 1555-1560 (1995)

[22] Buguet et al. 1979
Buguet, A.G.C., Livingstone, S.D. and Reed, L.D.
Skin temperature changes in paradoxical sleep in man in the cold. *Aviation, Space, and Environmental Medicine*, 1979, Vol. 50, No. 6, pp. 567–570 (1979)

[23] Buratti et al. 2011
Buratti, C., Mariani, R. and Moretti, E.
Mean age of air in a naturally ventilated office: Experimental data and simulations. *Energy and Buildings*, 2011, Vol. 43, pp. 2021-2027 (2011)

[24] Candas et al. 1982
Candas, V., Libert, J.P. and Muzet, A.
Heating and cooling stimulations during SWS and REM sleep in man. *Journal of thermal biology*, 1982, Vol. 7, pp.155-158 (1982)

[25] CATAMA 1953
Aviation Toxicology-an Introduction to the Subject and a Handbook of Data. Committee on Aviation Toxicology, Aero Medical Association. The Blakiston Co.: New York, NY. pp. 6-9, 31-39, 52-55, 74-79, 110-115 (1953)

[26] Chao et al. 1998
Chao, N.T., Wang, W.A. and Chiang, C.M.
A study of a control strategy utilizing outdoor air to reduce the wintertime carbon dioxide levels in a typical Taiwanese bedroom. *Energy and Buildings*, 1998, Vol. 29, pp. 93-105 (1998)

[27] Chau et al. 2002
Chau, C.K., Tu, E.Y. and Chan, D.W.
Estimating the total exposure to air pollutants for different population age

groups in Hong Kong. *Environmental International*, 2002, Vol. 27, No. 8, pp. 617-630 (2002)

[28] Chen 1995
Chen, Q.
Comparison of different k-ε models for indoor airflow computations. *Numerical Heat Transfer, Part B: Fundamentals: An International Journal of Computation and Methodology*, 1995, Vol. 28, No. 3, pp. 353-369 (1995)

[29] Chen 1996
Chen, Q.
Prediction of room air motion by Reynolds-stress models. *Building and Environment*, 1996, Vol. 31, No. 3, pp. 233-244 (1996)

[30] Chen and Hwang 1992
Chen, S.J. and Hwang, C.L.
Fuzzy multiple attribute decision making: Methods and applications, Springer-Verlag, Berlin (1992)

[31] Chen and Srebric 2002
Chen, Q. and Srebric, J.
A procedure for verification, validation, and reporting of indoor environment CFD analysis. *HAVC&R Research*, 2002, Vol. 8, No. 2, pp. 201-216 (2002)

[32] Chen and Xu 1998
Chen, Q. and Xu, W.
A zero-equation turbulence model for indoor airflow simulation. *Energy and Buildings*, 1998, Vol. 28, No. 2, pp. 137-144 (1998)

[33] Chen and Zhai 2004
Chen, Q. and Zhai, Z.
The use of CFD tools for indoor environmental design. *Advanced Building Simulation*, eds, A. Malkawi, Augenbroe, G, Spon Press, 2004, Chapter 5 (2004)

[34] Chiang et al. 1998
Chiang, C.M., Chou, P.C., Lai, C.M., Wang, W.A. and Chao, N.T.
Numerical simulation of natural ventilation of a bedroom in warm climate, *ROOMVENT '98*, Vol. 2, pp. 563-568 (1998)

[35] Cho et al. 2001
Cho, S.H., Kim, W.T. and Zaheer-uddin, M.
Thermal characteristics of a personal environment module task air conditioning system: an experimental study. *Energy Conversion and Management*, 2001, Vol. 42, pp. 1023-1031 (2001)

[36] Coleman and Steele 1989

Coleman, H.W. and Steele, W.G.
Experimentation and Uncertainty Analysis for Engineers, New York, *Wiley*, 1989.

[37] Cortelli et al. 1999
Cortelli, P., Gambetti, P. and Montagna, P.
Fatal familial insomnia: clinical features and molecular genetics. *Journal of Sleep Research*, 1999, pp. 23-29 (1999)

[38] Cuellar et al. 2006
Cuellar, N.G., Ratcliffe, S.J. and Chien, D.
Effects of depression on sleep quality, fatigue, and sleepiness in persons with restless legs syndromes. *American Psychiatric Nurses Association*, 2006, Vol. 12, No. 5, pp. 262-271 (2006)

[39] Cumming et al. 2007
Cumming, G., Fidler, F. and Vaux, D. L.
Error bars in experimental biology. *The Journal of Cell Biology*, 2007, Vol. 177, pp. 7-11 (2007)

[40] Dalgaard et al. 1972
Dalgaard, J.B., Dencker, G., Fallentin, B., Hansen, P., Kaempe, B., Steensberger, J. and Wilhardt, P.
Fatal poisoning and other health hazards connected with industrial fishing. *British Journal of Industrial Medicine*, 1972, Vol. 29, pp. 307-316 (1972)

[41] David 1999,
David, F., William, J.F., Douglas, P.S. and David, P.W.
Ventilation Efficiencies of Desk-Mounted Task/Ambient Conditioning Systems. *Indoor Air*, 1999, Vol. 9, pp. 273-281 (1999)

[42] Davidson et al. 2003
Davidson, L., Nielsen, P.V. and Sveningsson, A.
Modification of the v2f model for computing the flow in a 3D wall jet. Turbulence. *Heat and Mass Transfer*, 2003, Vol. 4, pp. 577-584 (2003)

[43] de Dear and Brager 1998
de Dear, R.J. and Brager, G.S.
Developing an adaptive model of thermal comfort and preference. *ASHRAE Transactions*, 1998, Vol. 104, pp. 145–67 (1998)

[44] Dewasmes 2000
Dewasmes, G., Telliez, F. and Muzet, A.
Effects of a nocturnal environment perceived as warm on subsequent daytime sleep in humans. *Sleep*, 2000, Vol. 23, No. 3, pp. 409-413 (2000)

[45] Di Nisi et al. 1989
Di Nisi, J., Ehrhart, J., Galeou, M. and Libert, J.P.
Influence of repeated passive body heating on subsequent night sleep in humans. *European Journal of Applied Physiology*, 1989, Vol. 59, pp. 138-145 (1989)

[46] Diakoulaki et al. 1995
Diakoulaki, D., Mavrotas, G. and Papayannakis, L.
Determining objective weights in multiple indexes problems: the CRITIC method. *Computers and Operations Research*, 1995, Vol. 22, pp. 763-770 (1995)

[47] Dripps and Comroe 1947
Dripps, R.D. and Comroe, J.H.
The respiratory and circulatory response of normal man to inhalation of 7.6 and 10.4 percent carbon dioxide with a comparison of the maximal ventilation produced by severe muscular exercise, inhalation of carbon dioxide and maximal voluntary hyperventilation. *American Journal of Physiology*, 1947, Vol. 149, pp. 43-51 (1947)

[48] Emmerich 1997
Emmerich, S.J.
Use of computational fluid dynamics to analyze indoor air quality issues. Report NIS-TIR 5997, National Institute of Standards and Technology, Gaithersburg, MD (1997)

[49] Emmerich and Andrew 2001
Emmerich, S.J. and Andrew, K. P.
State-of-the-Art Review of CO_2 Demand Controlled Ventilation Technology and Application. National Technical Information Service (NTIS), Technology Administration, U.S. Department of Commerce, 2001

[50] Engle-Friedman M, 2003
Engle-Friedman, M., Riela, S., Golan, R. and Ventuneac, A.M.
The effect of sleep loss on next day effort. *Journal of Sleep Research*, 2003, Vol. 12, No. 2, pp. 113-124 (2003)

[51] Fanger 1970
Fanger, P.O.
Thermal comfort, analysis and applications in environmental engineering. McGraw-Hill, 1970

[52] Faulkner et al. 1995
Faulkner, D., Fisk, W.J. and Sullivan, D.P.,
Indoor air flow and pollutant removal in a room with floor-based task ventilation: Results of additional experiments. *Building and Environment*, 1995, Vol. 30, No. 3, pp. 323-332 (1995)

[53] Faulkner et al. 1999
Faulkner, D., Fisk W.J., Sullivan, D.P. and Wyon, D.P.
Ventilation efficiencies of desk-mounted task/ambient conditioning systems. *Indoor air*, 1999, Vol. 9, pp. 273-281 (1999)

[54] Faulkner et al. 2002
Faulkner, D., Fisk, W.J., Sullivan, D.P. and Lee, S.M.
Ventilation efficiencies of a desk-edge-mounted task ventilation system, *Proceedings of Indoor Air*, 30 June- 5 July, Monterey, CA (2002)

[55] Gagge et al. 1986
Gagge, A.P., Fobelets, A.P. and Berglund, L.G.
A standard predictive index of human response to the thermal environment. *ASHRAE Transactions*, 1986, Vol. 92, pp.709–31 (1986)

[56] Gan 1995
Gan, G.H.
Evaluation of room air distribution systems using computational fluid dynamics. *Energy and buildings*, 1995, Vol. 23, pp. 83-93 (1995)

[57] Gao and Niu 2004
Gao, N.P. and Niu, J.L.
CFD study on micro-environment around human body and personalized ventilation, *Building and Environment,* 2004, Vol. 39, pp. 795-805 (2004)

[58] Gao and Niu 2005a
Gao, N.P. and Niu, J.L.
CFD study of the thermal environment around a human body: a review. *Indoor and Built Environment*, 2005, Vol. 14, No. 1, pp. 5-16 (2005)

[59] Gao and Niu 2005b
Gao, N.P. and Niu, J.L.
Modeling the performance of personalized ventilation under different conditions of room air and personalized air. *HVAC&R Research*, 2005, Vol. 11, pp. 587-602 (2005)

[60] Gao et al. 2009
Gao, C.F., Lee, W.L. and Hua, C.
Locating room air-conditioners at floor level for energy saving in residential buildings. *Energy Conversion and Management*, 2009, Vol. 50, pp. 2009-2019 (2009)

[61] Garvin and Wilson 1998
Garvin S.L. and Wilson J.
Environmental conditions in window frames with double-glazing units, *Construction and Building Materials*, 1998, Vol. 12, pp. 289-302 (1998)

[62] Gatski and Speziale 1993
Gatski, T.B. and Speziale, C.G.
On explicit algebraic stress model for complex turbulent flows. *Journal of Fluid Mechanics*, 1993, Vol. 254, pp. 59–78 (1993)

[63] Gellhorn and Spiesman 1934
Gellhorn, E. and Spiesman, I.
Influence of variations of O2 and carbon dioxide tension in inspired air upon hearing. *Proc. Soc. Exp. Biol. Med.*, 1934, Vol.32, pp. 46-47 (1934)

[64] Germano et al. 1991
Germano, M., U. Piomelli, P. Moin, P., and W.H. Cabot.
A dynamic subgrid-scale eddy viscosity model. *Physics of Fluids A: Fluid Dynamics*, 1991, Vol. 3, pp. 1760-1765 (1991)

[65] Gibson and Launder 1978
Gibson, M.M. and Launder, B.E.
Ground Effects on Pressure Fluctuations in the Atmospheric Boundary Layer. *Journal of Fluid Mechanics*, 1978, Vol.86, pp.491-511 (1978)

[66] Gong et al. 2006
Gong, N., Tham, K.W., Melikov, A.K., Wyon, D.P., Sekhar, S.C. and Cheong, K.W.
The acceptable air velocity range for local air movement in the tropics. *HVAC&R Research*, 2006, Vol. 12, pp. 1065-1076 (2006)

[67] Zhang et al. 2010
Zhang, H., Arens, E., Kiw, D., Buchberger, E., Bauman, F. and Huizenga, C.
Comfort, perceived air quality, and work performance in a low-power task–ambient conditioning system. *Building and Environment*, 2010, Vol. 45, pp. 29-39 (2010)

[68] H´enane et al. 1977
H´enane, R., Buguet, A., Roussel, B. and Bittel, J.
Variations in evaporation and body temperatures during sleep in man. *Journal of applied physiology: respiratory, environmental and exercise physiolog*, 1977, Vol. 42, pp. 50-55 (1977)

[69] Haskell et al. 1981
Haskell, E.H., Palca, J.W., Walker, J.M., Berger, J. and Heller, H.C.
Metabolism and thermoregulation during stages of sleep in humans exposed to heat and cold. *Journal of applied physiology: respiratory, environmental and exercise physiolog*, 1981, Vol. 51, pp. 948–954 (1981)

[70] Hayashi et al. 2002
Hayashi, T., Ishizu, Y., Kato, S. and Murakami, S.

CFD analysis on characteristics of contaminated indoor air ventilation and its application in the evaluation of the effects of contaminant inhalation by a human occupant. *Building and Environment*, 2002, Vol. 37, No. 3, pp. 219-230 (2002)

[71] Hedemark and Kronenberg 1982
Hedemark, L.L. and Kronenberg, R.S.
Ventilatory and heart rate responses to hypoxia and hypercapnia during sleep in adults. *Journal of Applied Physiology*, 1982, Vol. 53, No. 2, pp. 307-312 (1982)

[72] Hobson 1995
Hobson, J.A.
Sleep. Henry Holt and Company, 1995.

[73] Holmér 2004
Holmér, I.
Thermal manikin history and application. *European Journal of Applied Physiology*, 2004, Vol. 92, No. 6, pp. 614-618 (2004)

[74] Hong Kong Energy Statistics annual report 1979–2006
Hong Kong energy statistics annual report.
Hong Kong SAR, China: Census and Statistics Department, 1979–2006. See also: /http://www.censtatd.gov.hkS.

[75] Hong Kong Energy Statistics. Annual Report 2012
Hong Kong Energy Statistics.
Census and Statistics Department, Hong Kong. Hong Kong Energy Statistics. Annual Report 2012 Edition (2012)

[76] Hong Kong monthly digest of statistics 1979–2006
Hong Kong monthly digest of statistics.
Hong Kong SAR, China: Census and Statistics Department, 1979–2006. See also: /http://www.censtatd.gov.hkS.

[77] Hoskins 2003
Hoskins, J.A.
Health effects due to indoor air pollution. *Indoor Built Environment*, 2003, Vol. 12, pp. 427-433 (2003)

[78] Hu et al. 2005
Hu, C., Kurabuchi, T. and Ohba, M.
Numerical study of cross-ventilation using two-equation rans turbulent models. *International Journal of Ventilation*, 2005, Vol. 4, pp. 123-132 (2005)

[79] Hui et al. 2007
Hui, P.S., Wong, L.T. and Mui, K.W.
An epistemic indoor air quality assessment protocol for air conditioned offices.

Indoor Built Environment, 2007, Vol. 16, No. 2, pp. 139–149 (2007)

[80] Imagawa and Mima 1991
Imagawa, N. and Mima. T.
Installation example of an all air system: Fujita headquarters building. *SHASE Journal, Special Edition: Personal Air Conditioning,* 1991, Vol. 65, No. 7. (1991) Tokyo: The Society of Heating, Air-Conditioning, and Sanitary Engineers of Japan (in Japanese)

[81] ISO Standard 7730 2005
ISO Standard 7730.
Ergonomics of the thermal environment - Analytical determination and interpretation of thermal comfort using calculation of the PMV and PPD indices and local thermal comfort criteria (2005)

[82] Jones and Launder 1973
Jones, W.P. and Launder, B.E.
The calculation of low-Reynolds-number phenomena with a two equation model of turbulence. *International Journal of Heat and Mass Transfer*, 1973, Vol. 16, pp. 1119-1130 (1973)

[83] Jones and Whittle 1992
Jones, P.J. and Whittle, G.E.
Computational fluid dynamics for building air flow prediction- Current status and capacities. *Building and Environment*, 1992, Vol. 27, No. 3, pp. 321-338 (1992)

[84] Jreijiry 2007
Jreijiry D., Husaunndee A. and Inard C.
Numerical study of a hybrid ventilation system for single family houses. *Solar Energy*, 2007, Vol. 81, pp. 227-239 (2007).

[85] Karacan et al. 1978
Karacan, I., Thornby, J.I., Anch, M., Williams, R.L. and Perkins, H.M.
Effects of high ambient temperature on sleep in young men. *Aviation, Space, and Environmental Medicine*, 1978, Vol. 49, pp. 855-860 (1978)

[86] Kendel and Schmidt-Kessen 1973
Kendel K. and Schmidt-Kessen W.
The influence of room temperature on night sleep in man (polygraphic-night sleep recordings in the climatic chamber). In: Koella, W.P. and Levin, P. (Eds.). *First European Congress on Sleep Research*. Krager, Basel, pp. 423-425 (1973)

[87] Khorshidi et al. 2013
Khorshidi, R., Hassani, A., Honarbakhsh Rauof A. and Emamy M.
Selection of an optimal refinement condition to achieve maximum tensile

properties of Al-15%Mg_2Si composite based on TOPSIS method. *Materials and Design*, 2013, Vol. 46, pp. 442-450 (2013)

[88] Kim and Chen 1989
Kim, S.W. and Chen, C.P.
A multi-time-scale turbulence model based on variable partitioning of the turbulent kinetic energy spectrum. *Numerical Heat Transfer, Part B: Fundamentals, An International Journal of Computation and Methodology*, 1989, Vol. 16, pp. 193-211 (1989)

[89] Kobayashi and Chen 2003
Kobayashi, N. and Chen, Q.
Floor-supply displacement ventilation in a small office. *Indoor and Built Environment*, 2003, Vol. 12, pp. 281-292 (2003)

[90] Kubota et al. 2009
Kubota T., Chyee D.T.H. and Ahmad S.
The effects of night ventilation technique on indoor thermal environment for residential buildings in hot-humid climate of Malaysia. *Energy and Buildings*, 2009, Vol. 41, pp. 829-839 (2009)

[91] Kuznik et al. 2007
Kuznik, F., G. Rusaouen, and J. Brau.
Experimental and numerical study of a full scale ventilated enclosure: Comparison of four two equations closure turbulence models. *Building and Environment*, 2007, Vol. 42, pp. 1043-1053 (2007)

[92] Ladeinde and Nearon 1997
Ladeinde, F. and Nearon, M.D.
CFD applications in the HVAC&R industry. *ASHRAE Journal*, 1997, Vol. 39, No. 1, pp. 44-48 (1997)

[93] Lai and Yang 1997
Lai, J.C.S. and Yang, C.Y.
Numerical simulation of turbulence suppression: Comparison of the performance of four k-ε turbulence models. *International Journal of Heat and Fluid Flow*, 1997, Vol. 18, No. 6, pp. 575-584 (1997)

[94] Lam 2001
Lam, J.C.
Residential sector air conditioning loads and electricity use in Hong Kong. *Energy Conversion & Management*, 2000, Vol. 41, pp. 1757-1768 (2000)

[95] Lam et al. 2008
Lam, J.C., Tand, H.L. and Li, H.W.
Seasonal variations in residential and commercial sector electricity consumption

in Hong Kong. *Energy*, 2008, Vol. 33, pp. 513-523 (2008)

[96] Lam and Bremhorst 1981
Lam, C.K.G. and Bremhorst, K.
A modified form of the k-ε model for predicting wall turbulence. *Journal of Fluids Engineering*, 1981, Vol. 103, No. 3, pp. 456-460 (1981)

[97] Laurence et al. 2004
Laurence, D.R., Uribe, J.C. and Utyuzhnikov, S.V.
A robost formulation of the v2-f model Flow. *Turbulence and Combustion*, 2004, Vol. 73, pp. 169-185 (2004)

[98] Lambertsen 1971
Lambertsen, C.J.
Therapeutic Gases-Oxygen, Carbon Dioxide, and Helium. *Drill's Pharmacology in Medicine*. Chapter 55, Ed. By J.R. DiPalma. McGraw-Hill Book Co.: New York, NY (1971)

[99] Lau and Chen 2007
Lau, J. and Chen, Q.Y.
Floor-supply displacement ventilation for workshops. *Building and Environment*, 2007, Vol. 42, pp. 1718-1730 (2007)

[100] Launder and Sharma 1974
Launder, B.E. and Sharma, B.I.,
Application of the energy-dissipation model of turbulence to the calculation of flow near a spinning disc. *Letters in Heat and Mass Transfer*, 1974, Vol. 1, No. 2, pp. 131-138 (1974)

[101] Launder and Spalding 1974
Launder, B.E. and Spalding, D.B.
The numerical computation of turbulent flows. *Computer Methods in Applied Mechanics and Engineering*, 1974, Vol. 3, No. 2, pp. 269-289 (1974)

[102] Lavie 1996
Lavie, P.,
The Enchanted World of Sleep. Yale University Press, New Haven and London (1996)

[103] Lee and Chang 1999
Lee, S.C. and Chang, M.
Indoor Air Quality Investigations at Five Classrooms. *Indoor Air*, 1999, Vol. 9, pp. 134-138 (1999)

[104] Lee-Chiong 2006
Lee-Chiong T.

Sleep A comprehensive handbook. Hoboken, NJ: J Wiley (2006)

[105] Lenth 1989
Lenth, R.L.
Quick and Easy Analysis of Unreplicated Factorials. *Technometrics*, 1989, Vol. 31, pp. 469-473 (1989)

[106] Li et al. 2001
Li, W.M., Lee, S.C. and Chan, L.Y.
Indoor air quality at nine shopping malls in Hong Kong. *The science of total environment*, 2001, Vol. 273, pp. 27-40 (2001)

[107] Li et al. 2014
Li H., Li X. and Qi M.
Field testing of natural ventilation in college student dormitories. *Building and Environment*, 2014, Vol. 78, pp. 36-43 (2014)

[108] Liao et al. 1991
Liao, S.S.T., Bacon, S.J. and Yoon, S.K.
Factors influencing indoor air quality in Hong Kong: measurements in offices and shops. *Environmental Technology*, 1991, Vol. 12, pp.737-745 (1991)

[109] Liddament 1991
Liddament, M.W.
A review of building air flow simulation. *AIVC Technical Not*e 33, UK (1991)

[110] Lilly 1992
Lilly, D.K.
A Proposed Modification of the Germano Subgrid-Scale Closure Model. *Physics of Fluids*, 1992, Vol. 4, pp. 633-635 (1992)

[111] Lin et al. 2005
Lin, Z., Chow, T.T., Tsang, C.F., Fong, K.F. and Chan, L.S.
CFD study on effect of the air supply location on the performance of the displacement ventilation system. *Building and Environment*, 2005, Vol. 40, pp. 1051-1067 (2005)

[112] Lin and Deng 2004
Lin, Z.P., Deng, S.M.
A study on the characteristics of nighttime bedroom cooling load in tropics and subtropics. *Building and Environment*, 2004, Vol. 39, pp. 1101-1114 (2004)

[113] Lin and Deng 2006
Lin, Z.P. and Deng, S.M.
A questionnaire survey on sleeping thermal environment and bedroom air conditioning in high-rise residences in Hong Kong. *Energy and Buildings*, 2006,

Vol. 38, pp. 1302-1307 (2006)

[114] Lin and Deng 2008a
Lin, Z.P. and Deng, S.M.
A study on the thermal comfort in sleeping environments in the subtropics—developing a thermal comfort model for sleeping environments. *Building and Environment*, 2008, Vol. 43, pp. 70-81 (2008)

[115] Lin and Deng 2008b
Lin, Z.P. and Deng, S.M.
A study on the thermal comfort in sleeping environments in the subtropics-Measuring the total insulation values for the bedding systems commonly used in the subtropics. *Building and Environment*, 2008, Vol. 43, pp. 905-916 (2008)

[116] Lin et al. 2005
Lin, Z., Chow, T.T., Fong, K.F., Tsang, C.F. and Wang, Q.W.
Comparison of performances of displacement and mixing ventilations, Part II: indoor air quality. *International Journal of Refrigeration*, 2005, Vol. 28, pp. 288-305 (2005)

[117] Liu et al. 2008
Liu, W.W., Lian, Z.W. and Yao, Y.
Optimization on indoor air diffusion of floor-standing type room air-conditioners. *Energy and Buildings*, 2008, Vol. 40, pp. 59-70 (2008)

[118] Liu et al. 2012
Liu, D., Zhao, F.Y., Wang, H.Q. and Rank, E.
Turbulent transport of airborne pollutants in a residential room with a novel air conditioning unit. *International Journal of Refrigeration*, 2012, Vol. 35, pp. 1455-1472 (2012)

[119] Macpherson 1973
Macpherson, R.K.
Thermal stress and thermal comfort. *Ergonomics*, 1973, Vol. 16, No. 5, pp. 611-622 (1973)

[120] Maroni et al. 1995
Maroni, M., Seifert, B., Lindvall, T.,
Indoor air quality a comprehensive reference book. *Amsterdam: Elsevier*, 1995.

[121] Matsunawa et al. 1995
Matsunawa, K., Lizuka, H. and Tababe, S.
Development and application of an underfloor air-conditioning system with improved outlets for a 'smart' building in Tokyo. *ASHARE Transactions*, 1995, Vol. 101, Pt. 2, pp. 887-901 (1995)

[122] McCullough 1987
McCullough, E.A., Zbikowski, P.J. and Jones, B.W.
Measurement and prediction of the insulation provided by bedding systems. *ASHRAE Transactions*, 1987, Vol. 93, pp. 1055-1068 (1987)

[123] Melikov et al. 2002
Melikov, A.K., Cermak, R. and Majer, M.
Personalized ventilation: Evaluation of different air terminal devices. *Energy and Buildings*, 2002, Vol. 34, pp. 829-836 (2002)

[124] Menter 1994
Menter, F.R.
Two-equation eddy-viscosity turbulence models for engineering applications. *AIAA Journal*, 1994, Vol. 32, pp. 1598-1605 (1994)

[125] Miyazawa 1994
Miyazawa M.
Seasonal changes of sleep environment at bedtime and on arising. *Proceedings of the 18th Symposium on Human-environment System*, Tokyo (1994) [In Japanese]

[126] Möhle et al. 2003
Möhle, G., Crump, D., Brown, V., Hunter, C., Squire, R., Mann, H. and Raw, G.J.
Development and application of a protocol for the assessment of indoor air quality. *Indoor Built Environment*, 2003, Vol. 12, pp.139-149 (2003)

[127] Molhave 1987
Molhave, L.
The sick buildings: a sub-population among problem buildings. *Proceedings of the 4th International Conference on Indoor Air Quality and Climate*, West Berlin, 1987, Vol. 2, pp. 469-473 (1987)

[128] Moser 1992
Moser, A.
Numerical simulation of room thermal convection-Review of IEA Annex 20 results. *Proceeding of International Symposium on Room Air Convection and Ventilation Effectiveness*, Tokyo, Japan, pp. 76- 96 (1992)

[129] Murakami 1998
Murakami, S.
Overview of turbulence models applied in CWE-1997. *Journal of Wind Engineering and Industrial Aerodynamics*, 1998, Vol. 74-76, pp. 1-24 (1998)

[130] Murakami et al. 1995
Murakami, S., Kato, S. and Zeng, J.

Development of a computational thermal manikin-CFD analysis of thermal environment around human body. *Tsinghua-HVAC '95*, 1995, Vol. 2, pp. 349-354 (1995)

[131] Murakami et al. 1997
Murakami, S., Kato, S. and Zeng, J.
Flow and temperature fields around human body with various room air distribution: CFD study on computational thermal manikin - Part I. *ASHRAE transactions*, 1997, Vol. 10. Pt. 1, pp. 3- 15 (1997)

[132] Murakami et al. 2000
Murakami, S., Kato, S. and Zeng, J.
Combined simulation of airflow, radiation and moisture transport for heat release from a human person. *Building and Environment*, 2000, Vol. 35, No. 6, pp. 489-500 (2000)

[133] Nakano et al. 2002
Nakano, J., Tanabe, S.I. and Kimura, K.I.
Different in perception of indoor environment between Japanese and non-Japanese workers. *Energy and Buildings*, 2002, Vol. 34, No. 6, pp. 15–21 (2002)

[134] Nelson 2000
Nelson L.
Summary of physiological effects and toxicology of CO_2 on humans. Carbon Dioxide Poisoning. *Emergency Medicine Journal*, 2000, Vol. 32, No. 5, pp. 36-38 (2000)

[135] Newsham 1997
Newsham, G.R.
A field study of office thermal comfort using questionnaire software. *ASHRAE Transactions*, 1997, Vol. 103, pp. 3–17 (1997)

[136] Nielsen 1974
Nielsen, P.V.
Flow in air-conditioned rooms: model experiments and numerical solution of the flow equation. PhD thesis, Technical University of Denmark, Copenhagen, Denmark (1974)

[137] Nielsen 1996
Nielsen, P.V.
Displacement Ventilation-Theory and Design. Department of Building Technology and Structural Engineering, Aalborg University, Aalborg, Denmark (1996)

[138] Nielsen 1998
Nielsen, P.V.

The selection of turbulence models for prediction of room airflow. *ASHRAE Transactions*, 1998, Vol. 104, Pt. 1B, pp. 1119-1127 (1998)

[139] Niu and Kooi 1992
Niu, J.L. and Kooi, J.V.D.
Grid-optimization for k-ε turbulence model simulation of natural convection in rooms. *Proceedings ROOMVENT-92: Air Distribution in Rooms-Third International Conference*, 1992, Vol. 1, pp. 207-223 (1992)

[140] Noh et al. 2005
Noh, K.C., Jang, J.S. and Oh, M.D.
Thermal comfort and indoor air quality in the lecture room with 4-way cassette air-conditioner and mixing ventilation system. *Building and Environment*, 2005, Vol. 42, pp. 689-698 (2005)

[141] OSHA 1978
Occupational health guideline for carbon dioxide 1978
Occupational health guideline for carbon dioxide. *Occupational Safety and Health Administration, U.S. Department of Labor* (1978)

[142] Okamoto-Mizuno et al. 1999
Okamoto-Mizuno, K., Mizuno, K., Michie, S., Maeda, A. and Lizuka, S.
Effects of humid heat exposure on human sleep stages and body temperature. *Sleep*, 1999, Vol. 22, No. 6, pp. 767-773 (1999)

[143] Orszag 1970
Orszag, S.A.
Analytical theories of turbulence. *Journal of Fluid Mechanics*, 1970, Vol. 41, No. 2, pp. 363-386 (1970)

[144] CCOHS 1990
OSH Answers. *Canadian Centre for Occupational Health and Safety* (CCOHS) (1990)

[145] Palca 1986
Palca, J.W.
Thermoregulation, metabolism, and stages of sleep in cold-exposed men. *Journal of Applied Physiology*, 1986, Vol. 61, No. 3, pp. 940-947 (1986)

[146] Pan et al. 2005
Pan, C.S., Chiang, H.C., Yen, M.C. and Wang, C.C.
Thermal comfort and energy saving of a personalized PFCU air-conditioning system. *Energy and Buildings*, 2005, Vol. 37, No. 5, pp. 443-449 (2005)

[147] Pan et al. 2010
Pan, D.M., Lin, Z.P. and Deng, S.M.

A mathematical model for predicting the total insulation value of a bedding system. *Building and Environment*, 2010, Vol. 45, pp. 1866-1872 (2010)

[148] Pan et al. 2011
Pan, D.M., Chan, M.Y., Deng, S.M., Xia, L. and Xu X.
Numerical studies on the microclimate around a sleeping person and the related thermal neutrality issues. *Ergonomics*, 2011, Vol. 54, No. 11, pp. 1088-1100 (2011)

[149] Pan et al. 2012
Pan, D.M., Chan, M.Y., Xia, L., Xu, X.G., and Deng, S.M.
Performance evaluation of a novel bed-based task/ambient conditioning (TAC) system. *Energy and Buildings*, 2012, Vol. 44, pp. 54-62 (2012)

[150] Persily 1997
Persily, A.K.
Evaluating building IAQ and ventilation with indoor carbon dioxide. *ASHRAE Transaction*, 1997, Vol. 103, No. 2, pp. 193-203 (1997)

[151] Priestly 2003.
Priestly, M.A.
Respiratory Acidosis. Medicine (2003)

[152] Patterson et al. 1955
Patterson, J.L., Heyman, H., Battery, L.L. and Ferguson, R.W.
Threshold of response of the cerebral vessels of man to increases in blood carbon dioxide. *J. Clin. Invest.*, 1955, Vol. 34, pp. 1857-1864 (1955)

[153] Raithby and Chui 1990
Raithby, G.D. and Chui, E.H.
A finite-volume method for predicting a radiant heat transfer in enclosures with participating media. *Journal of Heat Transfer*, 1990, Vol. 112, pp. 415-423 (1990)

[154] Rechtschaffen and Kales 1968
Rechtschaffen, A. and Kales, A.
A Manual of Standardized Terminology, Techniques and Scoring System for sleep stages of human subjects. *Psychiatry and Clinical Neurosciences*, 1968, Vol. 55, No. 3, pp. 305-310 (1968)

[155] Rodi 1991
Rodi, W.
Experience with two-layer models combining the k-ε model with a one-equation model near the wall. *29th Aerospace Sciences Meeting*, Reno, NV (1991)

[156] Rohles 1983

Rohles, F.H.
New directions in comfort research. *ASHRAE Transactions*, 1983, V.89, Pt.2B, pp. 634-645 (1983)

[157] Saaty 1980
Saaty, T.L.
The analytic hierarchy process. McGraw-Hill, New York (1980)

[158] Sayar et al. 2002
Sayar, K., Arikan, M. and Yontem, T.
Sleep quality in chronic pain patients. *Canadian Journal of Psychiatry*, 2002, Vol. 47, No. 9, pp. 844-848 (2002)

[159] Schiller 1990
Schiller, G.E.
A comparison of measured and predicted comfort in office buildings. *ASHRAE Transactions*, 1990, Vol. 96, pp. 609–22 (1990)

[160] Schulte 1964
Schulte, J.H.
Sealed environments in relation to health and disease. *Archives of Environmental Health*, 1964, Vol. 8, pp. 438-452 (1964)

[161] Screbric 2008
Screbric, J., Vukovic, V., He, G.Q. and Yang, X.D.
CFD boundary conditions for contaminant dispersion heat transfer and airflow simulations around human occupants in indoor environments, *Building and Environment*, 2008, Vol. 43, pp. 294-303 (2008)

[162] Sechzer et al. 1960
Sechzer, P.H., Egbert, L.D., Linde, H.W., Cooper, D.Y., Dripps, R.D. and Price, H.L.
Effect of CO_2 inhalation on arterial pressure, ECG and plasma catecholamines and 17-OH corticosteroids in normal man. *J. Appl. Physiol*. 1960, Vol. 15, No. 3, pp. 454-458 (1960)

[163] Seppänen et al. 1999
Seppänen, O.A., Fisk, W.J. and Mendell, M.J.
Association of ventilation rates and CO2 concentrations with health and other responses in commercial and institutional buildings. *Indoor Air*, 1999, Vol. 9, pp. 226-252 (1999)

[164] Sevilgen and Kilic 2011
Sevilgen, G. and Kilic, M.
Numerical analysis of air flow, heat transfer, moisture transport and thermal comfort in a room heated by two-panel radiators. *Energy and Buildings*, 2011, Vol. 43, pp. 137-146 (2011)

[165] Sewitch et al. 1986
Sewitch, D.E., Kittrell, E.M.W., Kupfer, D.J. and Reynolds, C.F.
Body temperature and sleep architecture in response to a mild cold stress in women. *Physiology & Behavior*, 1986, Vol. 36, pp. 951-957 (1986)

[166] Schaefer 1958
Schaefer, K.E.
Environmental effects on consciousness. *International symposium on submarine and space medicine*, 1st, New London, 1958

[167] Shannon and Weaver 1947
Shannon, C.E. and Weaver W.
The mathematical theory of communication. Urbana: The University of Illinios Press (1947).

[168] Sharma et al. 2008
Sharma, M.J., Ilkyeong, M. and Hyerim, B.
Analytic hierarchy process to assess and optimize distribution network. *Applied Mathmatics and Computation*, 2008, Vol. 202, pp. 256–265 (2008)

[169] Shaw et al. 2002
Shaw, P.J., Tononi, G., Greenspan, R.J. and Robinson, D.F.
Stress response genes protect against lethal effects of sleep deprivation in Drosophila. *Nature*, 2002, Vol. 417, pp. 287-291 (2002)

[170] Shih et al. 1995
Shih, T., Liou, W., Shabbir, A., Yang, Z., and Zhu, J.
A new k-ε eddy viscosity model for high reynolds number turbulent flows. *Journal Computer Fluids*, 1995, Vol. 24, pp. 227-238 (1995)

[171] Shute 1992
Shute, R.W.
Integrating access floor plenums for HVAC air distribution. *ASHRAE Journal*, 1992, Vol. 34, No. 10, pp. 46-51 (1992)

[172] Shute 1995
Shute, R.W.
Integrated access floor HVAC: lessons learned. *ASHRAE Transactions*, 1995, Vol. 101, Pt. 2, pp. 877-886 (1995)

[173] Silva and Coelho 2002
Silva, M.C.G. and Coelho, J.A.
Convection coefficients for the human body parts determined with a thermal mannequin. *Proceedings of ROOMVENT 2002*, Copenhagen, Denmark, pp. 277-280 (2002)

[174] Sleep in America Poll 2014
Sleep in America Poll 2014: Sleep in the Modern Family. 2014

[175] Smagorinsky 1963
Smagorinsky, J.
General circulation experiments with the primitive equations I: the basic experiment. *Monthly Weather Review,* 1993, Vol. 91, pp. 99-164 (1963)

[176] Sodec 1984
Sodec, F.
Air distribution systems. Report No. 3554A, Aachen, West Germany: Krantz GmbH & Co., September (1984)

[177] Sodec and Craig 1991
Sodec, F. and Craig, R.
Underfloor air supply system: guidelines for the mechanical engineer. Report No. 3787A, Aachen, West Germany: Krantz GmbH & Co., January (1991)

[178] Sørensen 2002
Sørensen, D.N.
Radiation between segments of the seated human body. *Roomvent*, 2002, Vol. 1, pp. 317-320 (2002)

[179] Sørensen and Voigt 2003
SØrensen, D.N. and Voigt, L.K.
Modeling flow and heat transfer around a seated human body by computational dynamics. *Building and Environment*, 2003, Vol. 38, No. 6, pp. 753-762 (2003)

[180] Spengler and Chen 2000
Spengler, J.D. and Chen, Q.
Indoor air quality factors in designing a healthy building. *Annual Review of Energy and the Environment*, 2000, Vol. 25, pp. 567-600 (2000)

[181] Spoormaker 1990
Spoormaker, H.J.
Low-pressure underfloor HVAC system. *ASHRAE Transactions*, 1990, Vol. 96, Pt. 2, pp. 670-677 (1990)

[182] Srebric and Chen 2002
Srebric, J. and Chen Q.Y.
Simplified numerical models for complex air supply diffusers. *HVAC&R Research*, 2002, Vol. 8, pp. 277-294 (2002)

[183] Stamou and Katsiris 2006
Stamou, A. and Katsiris, I.

Verification of a CFD model for indoor airflow and heat transfer. *Building and Environment*, 2006, Vol. 41, No. 9, pp. 1171-1181 (2006)

[184] Stickgold et al. 2001
Stickgold, R., Hobson, J.A., Fosse, R. and Fosse, M.
Sleep, learning and dreams: off-line memory reprocessing. *Science*, 2001, Vol. 294, pp. 1052-1057 (2001).

[185] Tamblyn 1995
Tamblyn, R.T.
Toward zero complaint for office conditioning system. *Heating, Piping and Air Conditioning*, 1995, Vol. 120, pp. 67-72 (1995)

[186] Tanabe 1995
Tanabe, S.
Task/ambient conditioning systems in Japan. *Proceedings: Workshop on task/ambient conditioning systems in commercial buildings*, San Francisco, CA (1995)

[187] Teofilo 2005
Teofilo, L.L.C.
Sleep Medicine Essentials. Wiley-Blackwell (2005)

[188] Tham et al. 2004
Tham, K.W., Sekhar, S.C., Cheong, D.K.W. and Gong, N.
A case study of quantitative energy efficiency of personalized ventilation in the tropics. *Proceedings of ROOMVENT*, 2004, Portugal, pp. 5-8 (2004)

[189] Trung and Kumar 2005
Trung, D.N. and Kumar, S.
Resource use and waste management in Vietnam hotel industry. *Journal of Clearner Productio*n, 2005, Vol. 13, 109-116 (2005)

[190] Tso and Yau 2003
Tso, K.F. and Yau, K.W.
A study of domestic energy usage patterns in Hong Kong. *Energy*, 2003, Vol. 28, pp. 1671-1682 (2003)

[191] Tsuzuki et al. 1999
Tsuzuki, K., Arens, E.A., Bauman, F.S. and Wyon, D.P.
Individual thermal comfort control with desk-mounted and floor-mounted task/ambient conditioning (TAC) system. *Proceddings of Indoor Air'99*, Edinburgh, Scotland, pp. 8-13 (1999)

[192] Tsuzuki et al. 2008
Tsuzuki, K., Okamoto-Mizuno. K., Mizuno, K. and Iwaki, T.

Effects of airflow on body temperatures and sleep stages in a warm humid climate. *International Journal of Biometeorology*, 2008, Vol. 52, No. 4, pp. 261-270 (2008)

[193] Parmeggiani and Velluti 2005
Parmeggiani, P.L. and Velluti, R.A.
The Physiologic Nature of Sleep. Imperial College Press (2005)

[194] Voigt 2001
Voigt, L.K.
Navier–Stokes simulations of airflow in rooms and around a human body. PhD thesis, Technical University of Denmark (2001)

[195] Walsh and Leong 2004
Walsh, P.C. and Leong, W.H.
Effectiveness of several turbulence models in natural convection. *International Journal of Numerical Methods for Heat & Fluid Flow*, 2004, Vol. 14, No. 5, pp. 633-648 (2004)

[196] Wan and Yik 2004
Wan, K.S.Y. and Yik, F.W.H.
Building design and energy end-use characteristics of high-rise residential buildings in Hong Kong. *Applied Energy*, 2004, Vol. 78, pp. 19–36 (2004)

[197] Wang and Wong 2007
Wang L.P. and Wong N.H.
The impacts of ventilation strategies and facade on indoor thermal environment for naturally ventilated residential buildings in Singapore. *Building and Environment*, 2007, Vol. 42, pp. 4006-4015 (2007)

[198] Wang 2012
Wang, J.C.
A study on the energy performance of hotel buildings in Taiwan. *Energy and Buildings*, 2012, Vol. 49, pp. 268-275 (2012)

[199] Webster et al. 2002
Webster, T., Bauman, F. and Ring, E.,
Supply fan energy use in pressurized underfloor air distribution system. In: CBE Summary Report, Berkeley (2002)

[200] Wilcox 1988
Wilcox, D.C.
Reassessment of the Scale-Determining Equation for Advanced Turbulence Models. *AIAA Journal*, 1988, Vol. 26, No. 11, pp. 1299-1310 (1988)

[201] Wilcox 1994

Wilcox, D.C.
Simulation of Transition with a Two-Equation Turbulence Model. *AIAA J.*, 1994, Vol. 32, pp. 247-254 (1994)

[202] Wong 1992
Wong, KL.
Carbon Dioxide. Internal Report, Johnson Space Center Toxicology Group. National Aeronautics and Space Administration, Houston, TX.

[203] Wringt and Eason 1999
Wringt, N.G. and Eason, G.J.
Comparison of several computational turbulence models with full-scale measurements of flow around a building. *Wind and Structures*, 1999, Vol. 2, No. 4, pp. 305-323 (1999)

[204] Wyon 1995
Wyon, D.
Thermal manikin experiments on Climadesk. *Proceedings: Workshop on task/ambient conditioning systems in commercial buildings*, San Francisco, CA (1995)

[205] Yakhot and Orszag 1986
Yakhot, V. and Orszag, S.A., Renormalization group analysis of turbulence. *Journal of Scientific Computing*, 1986, Vol. 1, No. 1, pp. 3-51 (1986)

[206] Yakhot et al. 1992
Yakhot, V., Orszag, S.A., Thangam, S., Gatski, T.B. and Speziale, C.G.
Development of turbulence models for shear flows by a double expansion technique. *Physics of Fluids*, 1992, Vol. 4, No. 7, pp. 1510-1520 (1992)

[207] Yang et al. 2002
Yang, JH., Kato, S., Hayashi, T. and Murakami, S.
Measurement of local convective heat transfer coefficients of the human body in outdoor and indoor environments. *Proceedings of ROOMVENT* 2002, Copenhagen, Denmark, pp. 281-284 (2002)

[208] Yang et al. 2008
Yang, B., Sekhar, S.C. and Melikov, A.K.
Cooling effect of ceiling mounted personalized ventilation system. *Proceedings of Indoor Air 2008*, Copenhagen, Denmark, August (2008)

[209] Yang et al. 2009
Yang, B., Sekhar, S.C. and Melikov, A.K.
Performance evaluation of ceiling mounted personalized ventilation system. *ASHARE Transactions*, 2009, Vol. 115, Pt. 2, pp. 395-406 (2009)

[210] Yang et al. 2010
Yang, B., Sekhar, S.C. and Melikov, A.K.
Ceiling-mounted personalized ventilation system integrated with a secondary air distribution system - a human response study in hot and humid climate. *Indoor air*, 2010, Vol. 20, No. 4, pp. 309-319 (2010)

[211] Yoon and Hwang 1995
Yoon, K.P. and Hwang, C.L.
Multiple attribute decision making, Sage Publication, Thousand Oaks CA, 1995.

[212] Yu et al. 2011
Yu, K.C., Yu, J.M. and Lai, S.M.
Numerical simulation and construction of using indoor plants to improve indoor air quality. *International Journal of the Physical Sciences*, 2011, Vol. 6, No. 33, pp. 7604-7613 (2011)

[213] Zhai 2006
Zhai, Z.
Applications of CFD in building designing: Aspects and trends. *Indoor and Built Environment*, 2006, Vol. 15, No. 4, pp. 305-313 (2006)

[214] Zhai et al. 2005
Zhai, Z.Q., Zhang, Z., Zhang, W. and Chen, Q.Y.
Evaluation of various turbulence models in predicting airflow and turbulence in enclosed environments by CFD: Part-1: summary of prevalent turbulence models. *HVAC&R Research*, 2005, Vol. 13, pp. 853-870 (2005)

[215] Zhang et al. 2007
Zhang, Z., Zhang, W., Zhai, Z. and Chen, Q.
Evaluation of various turbulence models in predicting airflow and turbulence in enclosed environments by CFD: Part 2- Comparison with experimental data from literature. *HVAC&R Research*, 2007, Vol. 13, No. 6, pp. 871-886 (2007)

[216] Zhang et al. 2010
Zhang, H., Arens, E., Kiw, D., Buchberger, E., Bauman, F. and Huizenga, C.
Comfort, perceived air quality, and work performance in a low-power task–ambient conditioning system. *Building and Environment*, 2010, Vol. 45, pp. 29-39 (2010)

[217] Zhen et al. 2009
Zhen, G.Z., Jing, Y.Y. and Huang, H.X.
Thermal comfort and indoor air quality of task ambient air conditioning in modern office buildings. *International Conference on information management, innovation management and industrial engineering*, 2009, Xi’an, China (2009)

[218] Zhou 2010

Zhou, J.Q.
Numerical investigation of indoor CO_2 concentration distribution in an apartment, *SHB 2010-3rd International Symposium on Sustainable Healthy Buildings*, 2010, Seoul, Korea, 27 May, (2010)

[219] Zhou et al. 2013
Zhou, X., Lian, Z.W. and Lan, L.
Experimental study on a bedside personalized ventilation system for improving sleep comfort and quality. *Indoor and Built Environment*, 2013, pp. 1-11 (2013)